

THE ROLE OF CALCINEURIN/NFAT SIGNALING IN FIBROBLAST HOMEOSTASIS AND  
ACTIVATION

Allyson Lieberman

A DISSERTATION

in

Cell and Molecular Biology

Presented to the Faculties of the University of Pennsylvania

in

Partial Fulfillment of the Requirements for the

Degree of Doctor of Philosophy

2019

Supervisor of Dissertation

Co-Supervisor of Dissertation

---

Dr. Sandra Ryeom

---

Dr. Ellen Puré

Associate Professor, Cancer Biology

Professor and Chair, Biomedical Sciences

Graduate Group Chairperson

---

Dr. Daniel Kessler, Associate Professor, Cell and Developmental Biology

Dissertation Committee

Dr. Craig Bassing, Associate Professor, Pathology and Laboratory Medicine

Dr. Costas Koumenis, Richard H. Chamberlain Professor of Research Oncology, Radiation Oncology

Dr. Susan Volk, Associate Professor, Small Animal Surgery, School of Veterinary Medicine

Dr. Eric Witze, Associate Professor, Cancer Biology

*Dedication page*

To my parents, Dr. Julie Kovach and Dr. Richard Lieberman, for your unending,  
unconditional support, love, and guidance.

## ACKNOWLEDGMENTS

I would not have made it to the end of my degree without all the support, mentorship, and encouragement I received from my mentors, thesis committee, labmates, friends, and most importantly, family. Individually naming people is a sure-fire way to forget someone important – so I am acknowledging everyone who touched my life, big or small, over the past 5 years. Thank you for your unconditional love and support.

That having been said, I would like to thank my mentors, Dr. Ellen Puré and Dr. Sandra Ryeom, for your mentorship, guidance, advocacy, and patience throughout the course of my PhD. You are such incredible role models, and I'm very lucky to have had the opportunity to study and work in your laboratories.

Thanks also go to Diana Avery, James Monslow, and Priya Govindaraju of the Puré lab and Keri Schadler, Alice Zhou, and Jacob Till of the Ryeom lab for their assistance with experimental design, technique, and protocol, with special thanks to Diana Avery for laying down the groundwork regarding fibroblast activation, substratum stiffness, and TGF- $\beta$ , assisting me with multiple technical aspects, and providing the conceptual basis for a large number of my experiments. I acknowledge all my thesis committee members, past and present, for their invaluable expertise and faith in me as a student and scientist.

Thank you to the University of Pennsylvania MSTP, including Dr. Skip Brass and Maggie Krall, for the opportunity to pursue this degree and research project, as well as the support necessary to navigate each of the difficult transition points in this program.

Finally, I would like to acknowledge and thank my funding from the F30 fellowship through the National Cancer Institute, as well as the Patel family for their financial support via the Patel Scholar Award.

## ABSTRACT

### THE ROLE OF CALCINEURIN/NFAT SIGNALING IN FIBROBLAST HOMEOSTASIS AND ACTIVATION

Allyson Lieberman

Dr. Ellen Puré and Dr. Sandra Ryeom

Fibroblast activation is a crucial step in tumor growth and metastatic progression; activated fibroblasts remodel extracellular matrix (ECM) in primary tumor and metastatic microenvironments, exerting both pro- and anti-tumorigenic effects. However, the intrinsic mechanisms that regulate the activation of fibroblasts are not well defined. The signaling axis comprising the calcium-activated Ser/Thr phosphatase calcineurin (CN), and its downstream target nuclear factor of activated T cells (NFAT), has been shown to play important roles in endothelial and immune cell activation, but its role in fibroblasts is not known. We have shown that deletion of CN in fibroblasts in vitro results in alterations in fibroblast morphology and function consistent with an activated phenotype relative to wild-type fibroblasts. CN-null fibroblasts have greater migratory capacity, demonstrate increased collagen secretion and remodeling, and promote more robust endothelial cell activation in vitro. ECM generated by CN-null fibroblasts contain more collagen with greater alignment of fibrillar collagen compared to wild-type fibroblast-derived matrix. These differences in matrix composition and organization impose distinct changes in morphology and cytoskeletal architecture of both fibroblasts and tumor cells that may represent changes in their biological function, e.g. activation or epithelial-mesenchymal transition. However, while they are more activated at baseline, *Cn*<sup>-/-</sup> fibroblasts cannot

functionally respond to TGF- $\beta$  stimulation in multiple activation assays. They are also unable to upregulate FAP on soft, fibronectin-coated substrates to the same extent as WT fibroblasts. Consistent with this *in vitro* phenotype, we show that mice with stromal CN deletion exhibit a greater incidence and larger lung metastases. Our data suggest that CN/NFAT signaling contributes to the maintenance of fibroblast homeostasis and that loss of CN/NFAT signaling is sufficient to promote fibroblast activation, leading to the outgrowth of lung metastases. With a better understanding of how CN affects fibroblast homeostasis, new therapeutic targets may be identified that prevent the priming of the metastatic niche.

## TABLE OF CONTENTS

<b>Acknowledgments.....</b>	<b>iii</b>
<b>Abstract .....</b>	<b>iv</b>
<b>List of Figures/Tables .....</b>	<b>vii</b>
<b>Chapter 1: General Introduction.....</b>	<b>1</b>
<b>Chapter 2: Deletion of calcineurin promotes a pro-tumorigenic fibroblast phenotype.....</b>	<b>25</b>
<b>Chapter 3: Calcineurin-null fibroblasts do not respond to TGF-<math>\beta</math> stimulation <i>in vitro</i>.....</b>	<b>46</b>
<b>Chapter 4: The effects of stromal calcineurin deletion in various <i>in vivo</i> models.....</b>	<b>60</b>
<b>Conclusions and Future Directions.....</b>	<b>70</b>
<b>Materials and Methods.....</b>	<b>84</b>
<b>References .....</b>	<b>99</b>

## LIST OF FIGURES/TABLES

### Chapter 1

<b>Figure 1.1:</b> Overview of the three major compartments of the tumor microenvironment and their roles in tumor growth and progression.....	2
<b>Table 1.1:</b> Common components present in interstitial extracellular matrix.....	10
<b>Figure 1.2:</b> Tumor-associated collagen signals (TACS) during tumor progression.....	12
<b>Figure 1.3:</b> Schematic of the activation and function of fibroblasts in pathologic and physiologic states.....	14
<b>Figure 1.4:</b> Simplified diagram of the calcineurin/NFAT signaling axis.....	21
<b>Figure 1.5:</b> The proliferative response to calcineurin signaling in endothelial cells follows a U-shaped curve.....	2c

### Chapter 2

<b>Figure 2.1:</b> Calcineurin deletion promotes fibroblast migration but inhibits invasion.....	29
<b>Figure 2.2:</b> Calcineurin-null fibroblasts exhibit increased collagen contractility and matrix remodeling.....	31
<b>Figure 2.3:</b> Calcineurin deletion leads to alterations in collagen processing consistent with a CAF-like state.....	33
<b>Figure 2.4:</b> Calcineurin-null fibroblast-derived matrices induce cytoskeletal reorganization.....	35
<b>Figure 2.5:</b> <i>Cn</i> <sup>-/-</sup> fibroblasts promote endothelial cell tube formation.....	37
<b>Figure 2.6:</b> Stromal deletion of calcineurin increases the incidence and size of lung metastases.....	38
<b>Figure 2.7:</b> Constitutively active NFAT partially rescues CN deletion.....	40

### Chapter 3

<b>Figure 3.1:</b> Phase-contrast imaging of fibroblasts cultured on soft type I collagen gels in the presence or absence of TGF- $\beta$ .....	50
<b>Figure 3.2:</b> Cytokine antibody array analysis of WT and <i>Cn</i> <sup>-/-</sup> fibroblasts cultured on type I collagen gels with and without 2 ng/ml TGF- $\beta$ .....	51
<b>Figure 3.3:</b> Collagen contraction assays of free-floating type I collagen gels with and without 2 ng/ml TGF- $\beta$ .....	52

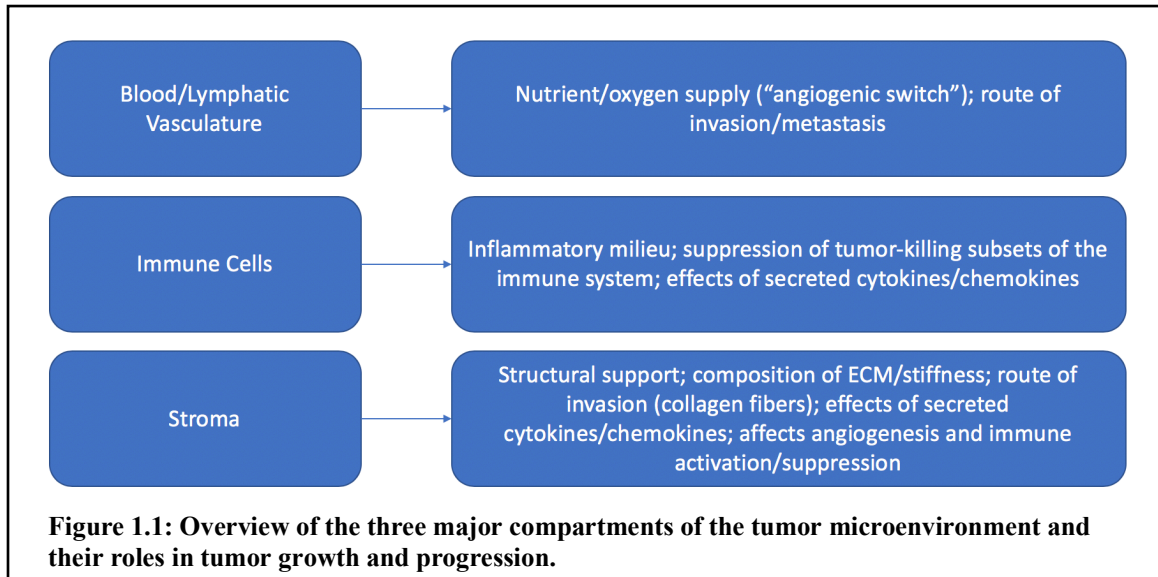
<b>Figure 3.4:</b> CN deletion paradoxically reduces fibroblast motility.....	<b>54</b>
<b>Figure 3.5:</b> Quantitative sandwich ELISA of total and active TGF- $\beta$ in unwounded and wounded WT and $Cn^{-/-}$ fibroblast monolayers.....	<b>55</b>
<b>Figure 3.6:</b> Western blot with densitometric analysis of Smad2 phosphorylation in fibroblasts 1 and 12h following TGF- $\beta$ treatment.....	<b>56</b>
 <b><u>Chapter 4</u></b>	
<b>Figure 4.1:</b> Imaging and flow cytometric analysis of WT and $Cn^{-/-}$ fibroblasts cultured on fibronectin-coated hydrogels.....	<b>61</b>
<b>Figure 4.2:</b> Summary of intravenous injection experiments of YFP <sup>+</sup> sarcoma cells in WT and stromal CN-null mice.....	<b>63</b>
<b>Figure 4.3:</b> Col1a1-Cre; $CnB^{fl/fl}$ mice accumulate more collagen in the lung at baseline.....	<b>64</b>
<b>Figure 4.4:</b> Stromal CN deletion does not alter the kinetics of dermal wound closure.....	<b>65</b>
 <b><u>Chapter 5</u></b>	
<b>Figure 5.1:</b> Schematic describing the role of calcineurin in maintaining fibroblast homeostasis.....	<b>70</b>

## CHAPTER 1: GENERAL INTRODUCTION

Metastatic disease is responsible for 90% of total cancer deaths<sup>1</sup>; despite significant advances in cancer treatment over the past few decades, the 5-year survival rate of patients whose tumors have metastasized to distant organ sites is still much lower than that of patients whose tumors have not spread<sup>2</sup>. Given that most cancers have likely already spread at the time of diagnosis<sup>3</sup>, it is of utmost importance that metastatic disease be further investigated, and new targets identified.

There have been many efforts to identify specific factors or signaling pathways in tumor cells in order to better target tumor cells and successfully prevent and/or treat metastases. However, these modalities are often complicated by the fact that the increased proliferation and mutation rates of cancer cells facilitate the development of resistance to targeted therapies<sup>4</sup>. Thus, the tumor microenvironment (TME) has become an increasingly appealing target of study. The concept that the surrounding microenvironment might affect a tumor cell's ability to colonize and grow in a certain tissue has existed since 1889, when the surgeon Dr. Stephen Paget hypothesized that metastatic growth in a specific organ requires both the “seed,” the tumor cell, as well as the “soil,” a permissive microenvironment<sup>5</sup>. It is increasingly clear, too, that the microenvironment of the distant site is “primed” for metastasis prior to metastatic colonization<sup>6</sup>. Since Dr. Paget's original hypothesis, numerous studies have characterized the role of different cellular compartments of the microenvironment – the blood and lymphatic vasculature, the immune system, and the stroma – in tumor growth and progression (**Figure 1.1**). These findings

have led to the development of a number of therapies targeting the microenvironment with varying degrees of success.



## The microenvironment is crucial to tumor growth and progression

### *The endothelium, angiogenesis and tumor growth*

Blood and lymphatic vessels are crucial in tumor formation, as tumor cells are rapidly growing and highly metabolically active, requiring a large amount of oxygen and nutrients to support their growth. As they grow, the metabolic demand of tumors quickly outstrips their vascular supply, which leads to intratumoral hypoxia and acidosis. These changes in turn trigger blood vessel formation via the activation of hypoxia inducible factors (HIF); this induction of angiogenesis is often referred to as the “angiogenic switch<sup>7</sup>.” However, the constant, pathologic activation of angiogenic pathways without a resolution phase leads to the formation of abnormal blood vessels; tumor vasculature is

often characterized by its increased vascular permeability (i.e. leakiness) and irregular architecture when compared to normal vasculature<sup>8</sup>. This increased, abnormal angiogenesis originally made it an appealing target for cancer drug development.

Some anti-angiogenic therapies have shown efficacy in specific cancer types, but by and large, efforts to target tumor vasculature have not been as successful as initially hoped. Anti-VEGF antibodies have been approved for use as a first-line therapy in only a small number of cancers, including glioblastoma multiforme, colon cancer, and renal carcinoma. Although anti-angiogenic therapies often lead to an increase in progression-free survival, their effects on overall survival are significantly more modest or nonexistent, and discontinuation of the drug may lead to “rebound vascularization” and subsequent worsening of tumor growth<sup>9,10</sup>. The use of anti-VEGF therapy is also complicated by significant adverse effects, including gastrointestinal perforation, thrombosis, and hypertension<sup>11</sup>.

### *The immune system and immune surveillance*

Equally important, and a current topic of particular interest in cancer therapeutics, is the immune system. In order for tumors to grow, they must evade immune surveillance despite an overall increase in inflammation, inflammatory cytokines, and tumor infiltrating lymphocytes. This is accomplished through a variety of mechanisms. First, they can downregulate the antigens they process and present, thus avoiding detection by immune cells. Tumors can also induce the recruitment of suppressive immune cells such as regulatory T cells (T<sub>reg</sub>) and myeloid derived suppressor cells (MDSC) by secreting anti-

inflammatory cytokines, or by expressing inhibitory ligands that suppress T cell activation<sup>12</sup>.

Two main strategies are currently being investigated to take advantage of the immune system in cancer therapy: immune checkpoint inhibitors and engineered T cells. The use of immune checkpoint blockade *via* CTLA-4, PD-1, or PD-L1 inhibitors seeks to re-activate tumor cell-reactive T cells by blocking their regulatory signals<sup>13</sup>. Checkpoint inhibitors have recently been approved for use in metastatic melanoma, prostate, lung, and pancreatic cancers, among others and have shown efficacy; their use in other cancer types is currently being investigated<sup>12</sup>. The second immune therapy currently under extensive development is the use of chimeric antigen receptor-expressing T cells (CAR-T cells), in which a patient's T cells are virally transduced with a chimeric antigen receptor that directs cell killing to an antigen of interest, then re-introduced to the patient. Currently, CD19-specific CAR-T cell therapy is in use for patients with B cell malignancies (leukemia and lymphoma), with many patients achieving complete and durable remission<sup>14</sup>. However, clinical trials utilizing a wide variety of tumor antigens are underway, with varying degrees of success and side effect profiles based on the tumor antigen used<sup>15</sup>. While CAR-T cells appear to be a promising and powerful tool in cancer treatment, they are limited to cancers with a targetable, surface-expressed tumor antigen that is broadly expressed across tumor cells while being specific enough to prevent significant off-target effects.

#### *The tumor-associated stroma*

The third main component of the microenvironment, and the focus of my thesis project, is the stroma, a term that encompasses the structural component of an organ or

tissue broadly consisting of extracellular matrix (ECM), the blood vessels/nerves supplying the organ, and several cell types such as fibroblasts, pericytes, and certain immune cells. The stroma is of particular interest as it undergoes marked changes upon tumor initiation and progression that can be both pro- and anti-tumorigenic<sup>16</sup>. These will be discussed in further detail in later sections; tumor-associated stroma is generally characterized by increases in and re-organization of ECM, an increase in cell density consisting primarily of fibroblasts and immune cells, and an overall pro-inflammatory milieu.

The stroma supports tumor cell growth and invasion, but it also participates in significant crosstalk with the immune and endothelial compartments of the microenvironment. Cancer-associated fibroblasts have been shown to alter the immune system in ways that both promote and suppress tumor growth, through both direct interactions with immune cells as well as secretion of a number of pro- and anti-inflammatory cytokines<sup>17</sup>. Depletion of  $\alpha$ SMA<sup>+</sup> myofibroblasts in a mouse model of pancreatic cancer decreased immune surveillance by increasing the number of intratumoral regulatory T cells, ultimately resulting in greater invasiveness and mortality<sup>18</sup>. Recent work in breast cancer identified four distinct subsets of CAFs with opposing effects on tumor immunity and demonstrated differential accumulation of each of these populations in different subtypes of breast cancer<sup>19</sup>.

Similarly, fibroblasts have been shown to enhance angiogenesis in both *in vitro* co-culture assays as well as in murine models of tumor growth<sup>20,21</sup>. Fibroblasts can support angiogenesis via a number of mechanisms, including upregulation of pro-angiogenic factors such as HGF or VEGF<sup>22,23</sup>, downregulation of anti-angiogenic factors such as

thrombospondin-1<sup>24,25</sup>, and deposition/remodeling of extracellular matrix<sup>26,27</sup>. While tumor-associated, proliferative fibroblasts are considered to be pro-angiogenic, some evidence suggests that fibroblasts may switch to an anti-angiogenic secretory phenotype as they become quiescent in the setting of serum depletion<sup>28</sup>.

These interactions with other components of the microenvironment have important implications for cancer therapeutics. For example, targeted deletion of FAP<sup>+</sup> activated fibroblasts has been shown to potentiate the response to anti-PD-L1 immunotherapy in pancreatic cancer in a CXCL-12-dependent manner, suggesting that the stroma is partially responsible for resistance to these therapies<sup>29</sup>. The stroma has also been implicated in resistance to anti-angiogenic therapy, both via the secretion of pro-angiogenic factors as well as deposition of matrix proteins such as periostin<sup>30,31</sup>.

Currently, clinically approved treatments exist that target or co-opt the endothelium and immune system. However, drugs targeting the stroma are less well developed, though several clinical trials are in progress. Thus far, attempts to target cancer-associated fibroblasts (CAFs) have fallen into two categories: inhibiting their enzymatic function and eliminating them entirely. Unfortunately, however, inhibitors targeting several markers of activated fibroblasts, including fibroblast activation protein (FAP) and matrix metalloproteinases (MMPs), have shown little to no clinical efficacy despite promising results in mouse models<sup>32,33</sup>. Depleting tumors of cancer-associated fibroblasts has shown some promise in preclinical studies and is currently being tested clinically. We and others have designed CAR-T cells specific for CAF surface markers such as FAP, and studies in mouse models of pancreatic cancer show that depletion of activated fibroblasts disrupts the desmoplastic response and can improve chemotherapeutic efficacy<sup>34</sup>. However, the

heterogeneity of cancer-associated fibroblasts means that not all CAFs will be eliminated; identifying the most influential subpopulation of fibroblasts in a particular cancer will be crucial to the success of this treatment modality.

Additionally, activated fibroblasts play a key role in the maintenance of normal tissues, and targeting CAFs may have significant side effects. One method of reducing off-target toxicity is to select an activated fibroblast marker such as FAP that is minimally expressed in normal tissues in order to minimize effects on normal tissue<sup>35,36</sup>. Our lab has shown that targeting FAP<sup>+</sup> cells using CAR-T cells causes only minimal off-tumor toxicity<sup>37</sup>. That having been said, one study in mice demonstrated that depletion of FAP<sup>+</sup> stromal cells in mice led to significant cachexia and anemia due to the prevalence of these cells in normal skeletal muscle and bone marrow<sup>38</sup>. Even if normal tissues at baseline are relatively unaffected by these therapies, targeting activated stroma may lead to an inability for tissues to respond to external stressors. While activated fibroblasts play an important role in pathologic processes such as tumor growth and fibrosis, they are also crucial to physiologic processes such as wound healing and normal tissue remodeling<sup>39,40</sup>. In diseases such as cancer, which can be managed both surgically and medically, targeting of activated fibroblasts may lead to increased surgical morbidity due to alterations in inflammation and wound healing.

There is also interest in targeting the ECM itself; current studies have focused on pancreatic cancer, a cancer type known for its significant desmoplasia. Excessive amounts of hyaluronic acid lead to high interstitial fluid pressure within the tumor, in turn limiting chemotherapeutic accessibility. Consequently, treatment of *in vivo* mouse models of cancer with a pegylated form of hyaluronidase (PEGPH20) increases the efficacy of chemotherapy

and improves tumor response<sup>41</sup>. Clinical trials of PEGPH20 in patients with advanced hyaluronan-high pancreatic cancer are currently underway and show promise in terms of response rate and progression-free survival<sup>42</sup>. However, this treatment will only have significant effects in hyaluronan-dense tumors, meaning that it will be ineffective in a large number of cancers.

Targeting the stroma is an attractive target because of the potential to be widely applicable across multiple cancer types; however, much research still needs to be done for these targeted therapies to be effective. One of the reasons that stroma-targeting therapies have only been partially successful thus far is because the mechanisms informing the activation and formation of tumor-associated stroma are not well understood in comparison to the endothelium and immune system. While many activating stimuli have been identified, and the changes in activated stroma characterized, the molecular mechanisms causing stromal activation are largely unknown. Thus, previous therapeutic efforts have focused primarily on targeting specific surface markers or extracellular matrix components as opposed to blocking or reversing the activation of the stroma itself. To deprogram activated, cancer-associated stroma effectively requires a better understanding of how it is activated in the first place. I will next briefly review and discuss what is known regarding the two major components of the stroma: the extracellular matrix and the fibroblasts that secrete and remodel it.

### **The extracellular matrix**

The extracellular matrix is a hydrogel that consists of a variety of matrix proteins, proteoglycans, and polysaccharides organized in a way that lends structure to the organ or

tissue it supports (**Table 1.1**). Two main types of ECM exist in tissues: the basement membrane, which largely consists of type IV collagen and serves as a barrier and basal layer for epithelial cells, and the interstitial ECM, which provides a supportive medium between cells in a tissue<sup>43</sup>. Together, these form a scaffold and provide anchoring points for the numerous cell types and structures within an organ.

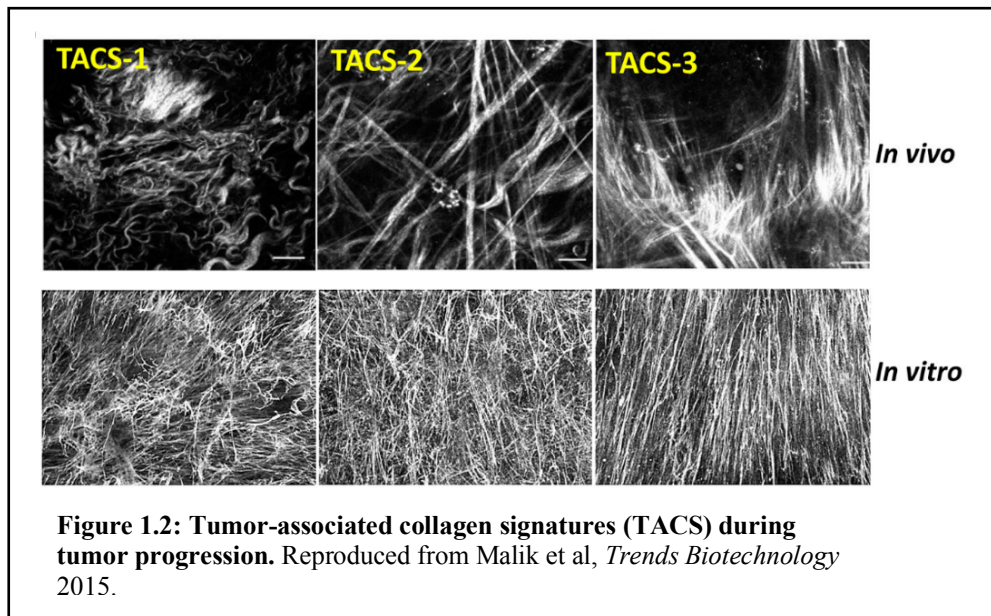
One of the most abundant components of the interstitial ECM is collagen, specifically the fibrillar collagens such as types I, II, III, and VI<sup>44</sup>. Collagen is secreted in an immature form and must undergo multiple proteolytic processing steps and post-translational modifications in order to form mature collagen fibrils<sup>44,45</sup>. Crosslinking of collagen fibrils is crucial to the overall architecture of collagen; large amounts of crosslinks lead to the linearization of collagen fibers, a process that is often mediated by proteins such as lysyl oxidase (LOX)<sup>44</sup>. Once mature fibrils have been established, they can be proteolytically processed by the collagenase family of matrix metalloproteinases such as MMP1 and MMP8, whereas denatured collagen is processed by the gelatinases such as MMP2 and MMP9; this processing can degrade collagen, release bioactive fragments, or help to change its architecture and re-orientation<sup>46</sup>. We have also shown that FAP is capable of cleaving fibrillar collagen, but only after it has been processed into  $\frac{1}{4}$  and  $\frac{3}{4}$  fragments by collagenases such as MMP1<sup>47</sup>. Apart from collagen, other abundant macromolecules in the interstitial ECM include fibronectin, tenascin C, hyaluronic acid and other glycosaminoglycans, and periostin<sup>43</sup>. There are significant interactions between different matrix proteins; for example, collagen binds to fibronectin and increases its rigidity, thus improving the affinity of fibronectin for its receptors<sup>44</sup>.

<b>Components of Interstitial ECM</b>
Fibrillar collagens (I, II, III, V, VI, XI, XXIV, XXVII)
Fibronectin
Elastin
Laminin
Hyaluronic acid
Tenascin C
Periostin
Proteoglycans (heparan, chondroitin, keratan sulfate)
Fibrin

**Table 1.1: Common components present in interstitial extracellular matrix.**

Apart from its roles in tissue integrity and architecture, the ECM is crucial to cellular function within a tissue by transducing signals through several methods. First, the organization and composition of the matrix informs its mechanical stiffness, and this stiffness in turn can activate signaling pathways such as FAK and YAP/TAZ in a number of cell types, including fibroblasts<sup>48</sup>. The matrix proteins themselves can engage cell surface receptors, most notably integrins. The binding of matrix components to integrins can differ depending on the size of the matrix fragment or its conformation; one major example is the increased affinity of integrin  $\alpha_1\beta_1$  to monomeric over mature fibrillar type I collagen, implicating its role in early collagen fibrillogenesis<sup>49</sup>. This allows the ECM to inform cell signaling based on its structural properties<sup>44,50</sup>. Finally, the ECM can be a source of growth factors, cytokines, and chemokines. Matrix proteins can sequester certain growth factors by binding to them; these growth factors can then be released upon proteolysis of the matrix<sup>51</sup>. Further, proteolytic processing of the matrix can release bioactive fragments of the matrix itself. One such example is endostatin, which is a C terminal fragment of type XVIII collagen with substantial anti-angiogenic properties<sup>52</sup>.

The ECM plays many crucial roles in disease processes such as fibrosis and cancer. In most solid tumors, the matrix undergoes several changes over the course of tumor progression, transitioning from a fibrin- and fibronectin-rich “provisional matrix” to a desmoplastic, fibrillar collagen-rich environment<sup>53</sup>. One of the ways this progressive remodeling of ECM can be identified is via tumor-associated collagen signatures (TACS), which were first defined in mammary tumor progression (**Figure 1.2**). TACS-1, corresponding to pre-malignant lesions, represents an increase in total collagen signal. TACS-2, seen in early tumor growth, occurs when these collagen fibers begin to linearize, oriented parallel to the tumor boundary and constraining the edges of the tumor, due to a combination of proteolytic processing, crosslinking, and contractile forces exerted by tumor-associated fibroblasts. Finally, TACS-3, observed in invasive cancers, occurs when these linear collagen fibers become re-oriented in a perpendicular fashion to the tumor boundary<sup>54</sup>. These alterations in collagen architecture have been shown to have both pro- and anti-tumorigenic properties. TACS-3-like collagen signatures are thought to specifically promote invasion: in tumor tissues, these linear, perpendicular collagen fibers serve as a scaffold along which invasive tumor cells can escape and enter the interstitium<sup>55</sup>.



**Fibroblasts are a key component of the stroma and are activated in both physiologic and pathologic states**

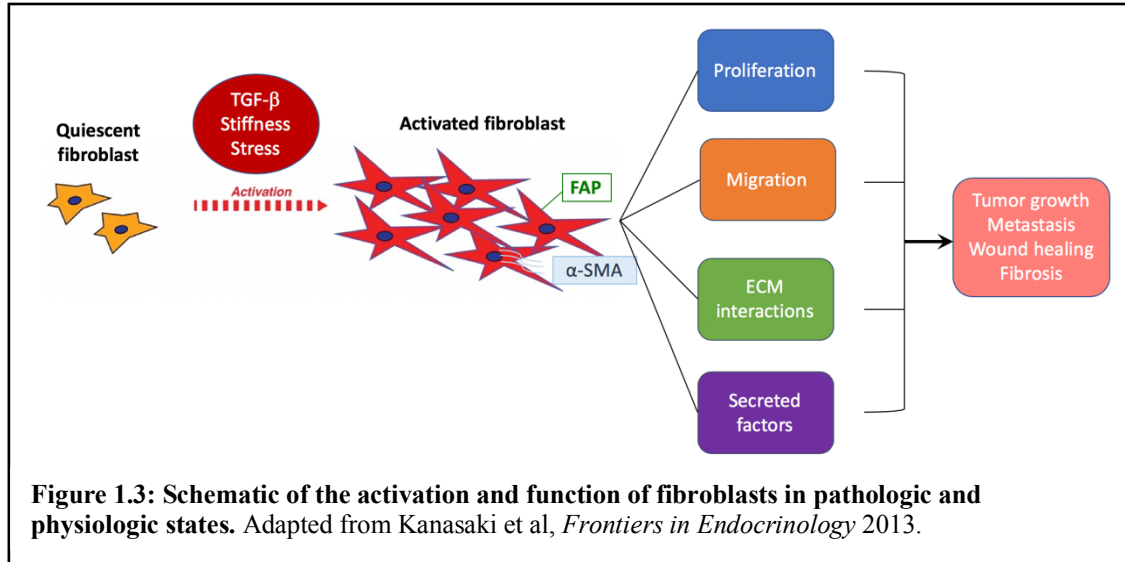
Fibroblasts are the cell type in the microenvironment that is primarily responsible for secreting and remodeling ECM in both normal and diseased tissues. They have been identified as key mediators of many of the phenotypes present in tumor-associated stroma, specifically via their activation. Fibroblasts are cells of mesenchymal origin; one difficulty inherent in their study is the fact that no one universal and specific marker defining the fibroblast population has yet been identified, unlike, for example, CD31 in endothelial cells. Fibroblasts are known to express vimentin due to their mesenchymal origin, as well as CD90/Thy1; however, neither of these markers is specific to fibroblasts and must be used in combination with other markers such as CD45 as well as contextual clues, i.e. their location in a specific tissue. Despite its name, the expression of fibroblast-specific protein 1 (FSP1)/S100A4 is not limited to fibroblasts, as it has been observed to be expressed in a

variety of cell types, including hematopoietic cells, endothelial cells, and vascular smooth muscle cells<sup>56</sup>. On the other hand, markers such as fibroblast activation protein (FAP) and alpha-smooth muscle actin ( $\alpha$ SMA) are generally expressed only by activated fibroblasts, which omits a large percentage of fibroblasts in tissue. Due to the lack of a universal fibroblast marker, the isolation of fibroblasts is generally performed through a functional property, by selection for adherent cells, and are characterized by their spindle-shaped morphology in combination with one or more of the markers described above<sup>57</sup>.

The majority of tissue-resident fibroblasts are quiescent and un-activated, with the exception of dermal fibroblasts, which express a small amount of FAP at baseline. Tissue-resident fibroblasts generally have very low proliferation rates and may contribute to a small amount of baseline ECM secretion and remodeling, but they are otherwise relatively mitotically and transcriptionally inactive<sup>57</sup>. When these quiescent fibroblasts are exposed to disease-related stimuli, however, they undergo a process of activation that leads to drastic changes in their function. Before describing the phenotypes associated with fibroblast activation, it is important to note that activated fibroblasts represent a heterogeneous population. Some of this may be due to the fact that they have multiple cells/tissues of origin<sup>58</sup>. In addition, gene expression-related profiling often reveals a large number of distinct, yet overlapping, cell populations that fall under the category of activated fibroblasts<sup>59</sup>. Cancer-associated fibroblasts have proven to be a particularly heterogeneous population, with studies revealing many distinct subpopulations of fibroblasts in a variety of cancers<sup>60-63</sup>. Thus, when considering activated fibroblasts, it is

important to profile a variety of their functions to determine the specific functional phenotypes they represent.

Fibroblast activation is functionally defined by several changes (**Figure 1.3**). Given their heterogeneity, activated fibroblasts can exhibit one or many of these changes, and specific subpopulations often select for a specific subset of these functions. They can increase their proliferation, thus at least partially accounting for the increased number of fibroblasts seen in diseased tissues. They undergo cytoskeletal reorganization and a change in morphology; their migratory capacity increases dramatically. They deposit large amounts of ECM, especially collagen, and remodel existing matrix, leading to re-orientation of collagen fibers. Finally, they secrete a wide variety of cytokines, chemokines, and other molecules that can have effects on immune, endothelial, and tumor cells as well as having autocrine effects to amplify fibroblast activation<sup>57,64,65</sup>.



Fibroblast activation plays a critical role in a variety of both physiologic and pathologic processes. In normal wound healing, dermal fibroblasts transdifferentiate into myofibroblasts in order to assist in wound closure and remodel the matrix in the developing

scar<sup>66</sup>. When this process is deregulated, it can lead to the development of keloid scars, benign hyperproliferative lesions that are difficult to treat, have a high recurrence rate, and can significantly negatively affect quality of life. Histologic analysis of keloid scar tissue demonstrates an increase in fibroblast proliferation, extracellular matrix production, and invasion into surrounding healthy tissue compared to normal wound healing. Further, evidence suggests that FAP may be crucial to the development of keloids by promoting invasiveness in keloid fibroblasts<sup>67</sup>. Apart from their role in dermatologic processes, activated fibroblasts also play an important role in the initiation and progression of fibrotic disease in a variety of organs, including the lung, liver, and kidneys. Activated fibroblasts in the tumor microenvironment, often called cancer-associated fibroblasts (CAFs) in this setting, are major contributors to tumor progression and metastasis. Tumors have often been described as “wounds that do not heal” due to the fact that much of the tumor stroma closely resembles that of healing wounds that, unlike normal wound healing, do not resolve over time<sup>53</sup>. In the setting of cancer and metastasis, activated fibroblasts are generally considered to be pro-tumorigenic; conversely, normal fibroblasts can be tumor-preventative, thus making fibroblast activation a requirement for tumor progression<sup>68,69</sup>.

A wide variety of fibroblast-activating stimuli have been identified. These can be separated into several sub-groups: mechanical forces such as elastic stretching or changes in substratum stiffness; secreted factors and cytokines such as TGF- $\beta$ , PDGF, and IL-6; ECM composition and contents of the substratum; and cellular stress/damage such as reactive oxygen species (ROS)<sup>57</sup>. Of note, different stimuli may also select for specific sub-populations of activated fibroblasts. Our lab has previously shown that the levels of FAP

and  $\alpha$ SMA differ greatly depending on which growth factors and/or chemokines are added; furthermore, alterations in the content and/or stiffness of the ECM are sufficient to direct pulmonary fibroblasts toward either a FAP<sup>+</sup>, secretory fibroblast state, or an  $\alpha$ SMA<sup>+</sup>, myofibroblast state<sup>60</sup>.

Though the activating stimuli of fibroblasts have been well-profiled, the molecular mechanisms that underlie fibroblast activation are less well known. A number of signaling pathways, especially those downstream of the ligands Notch and Sonic hedgehog (Shh), have been of particular recent interest in the modulation of the CAF phenotype<sup>57</sup>. Loss- and gain-of-function studies have identified the epithelial-to-mesenchymal transition marker Twist1 as crucial to the function of pancreatic cancer-associated fibroblasts<sup>70</sup>. While many of these signaling pathways have been shown to be sufficient to induce a CAF-like state, it is unclear which of these mechanisms are specifically required for fibroblast activation.

### **Fibroblast quiescence: how the un-activated state is maintained**

Current understanding of cell quiescence argues that it is not a dormant or default state but rather an active cell state that requires maintenance. As opposed to irreversible dormant states, quiescence must be quickly reversible, which requires that the cell be primed for re-entry into a more transcriptionally active and/or proliferative state. Homeostasis often involves the maintenance of a specific biologic value (e.g. gene expression levels) within a certain range and not necessarily at a fixed point, a process requiring the constant expression and function of molecular sensors<sup>71</sup>. Furthermore, in order for cells to exit the homeostatic steady state, they must achieve a certain “activation

energy” that allows them to enter an unstable transition state prior to activation, differentiation, and/or proliferation<sup>72</sup>. Cellular homeostasis and quiescence have been studied extensively in stem cells, a cell type in which the maintenance of the quiescent, undifferentiated state is crucial to proper tissue renewal. The loss of homeostatic regulators of hematopoietic stem cells, such as folliculin, leads to bone marrow failure due to uncontrolled differentiation and lack of self-renewal, suggesting that the “energy barrier” to differentiation maintained by this regulator is removed<sup>73</sup>.

Compared to many other cell types, fibroblasts exhibit significant phenotypic plasticity and are able to tightly regulate the transition between multiple cellular states throughout disease progression<sup>74</sup>. This plasticity suggests that the “quiescent state” of tissue resident fibroblasts may in fact represent a steady state of constant, dynamic changes in gene expression, contractility, and motility. One study examining the forces exerted by spreading fibroblasts on a fibronectin substrate demonstrated that fibroblasts have the ability to maintain tensional homeostasis within a specific range via “tensional buffering,” a process in which fibroblasts exert variable forces on the substrate in order to maintain steady state tension<sup>75</sup>. Quiescent fibroblasts exhibit significant levels of metabolic activity despite their relatively low transcriptional activity, suggesting that fibroblast quiescence is actively maintained<sup>76</sup>. Interestingly, some evidence suggests that quiescent fibroblasts may be more capable of promoting inflammation, as measured by greater levels of cyclooxygenase-2 expression in response to IL-1 $\beta$  stimulation, compared to proliferating fibroblasts<sup>77</sup>.

The mechanisms that maintain the quiescent, un-activated state in tissue-resident fibroblasts are still largely unknown. Few markers that specifically delineate the quiescent fibroblast state versus the activated fibroblast have been identified; an un-activated fibroblast is most frequently defined by its *lack* of activated fibroblast-associated markers and functions. A 2016 review of the role of fibroblasts in cancer suggested that FSP1 is a specific marker of quiescent fibroblasts<sup>57</sup>; however, there is little to no literature evidence to support this claim. One recent study used cell-surface phenotyping to identify CD36 and CD97 as markers of quiescent lung fibroblasts; they showed that its expression in primary lung fibroblasts was attenuated with TGF $\beta$ -induced myofibroblast differentiation and did not overlap with  $\alpha$ SMA expression<sup>78</sup>.

There is some evidence that specific factors are capable of either maintaining quiescence and/or blocking fibroblast activation. Prostaglandin E<sub>2</sub> (PGE<sub>2</sub>) has several anti-fibrotic effects mediated by the multiple signaling pathways downstream of the E-prostanoid 2 receptor<sup>79-81</sup>. Additionally, secreted protein acidic and rich in cysteine (SPARC) modulates myofibroblast differentiation and ECM secretion in response to TGF- $\beta$ , though its specific role in fibrotic disease is complex, encompassing both pro- and anti-fibrotic effects<sup>82-84</sup>. Alterations in substratum stiffness have also been shown to be sufficient to “deprogram” myofibroblasts, transitioning from a more activated to a less activated state. One group utilized polyacrylamide hydrogels whose stiffness could be decreased by ultraviolet light-induced depolymerization. Valvular fibroblasts cultured on stiff (32 kPa) hydrogels express  $\alpha$ SMA and otherwise display a myofibroblast phenotype; when these stiff hydrogels are softened via depolymerization, the fibroblasts cultured on

them lose their  $\alpha$ SMA expression and myofibroblast phenotype<sup>85</sup>. Notably, however, we have shown that fibroblasts initially cultured on 20-25 kPa (stiff) polyacrylamide hydrogels and passaged onto 2-5 kPa (soft) hydrogels switch from an  $\alpha$ SMA<sup>hi</sup> to a FAP<sup>hi</sup> phenotype, suggesting that a decrease in mechanical stiffness to a less pathologic but still supraphysiologic value alters the phenotype of fibroblasts to a non-myofibroblast but still functionally activated state. This suggests that the loss of myofibroblast markers observed upon UV-induced depolymerization may not represent complete deprogramming but instead a shift in their activated fibroblast phenotype. Finally, several studies have identified small molecule inhibitors capable of preventing fibroblast activation. Nintedanib, a multikinase inhibitor that has been approved for use in non-small cell lung adenocarcinoma, is capable of blocking TGF- $\beta$ 1-induced myofibroblast differentiation and pro-tumorigenic function in tumor-associated fibroblasts<sup>86,87</sup>. The drug Minnelide has also been shown to inhibit fibroblast activation in the setting of PDAC through mechanisms that are currently incompletely defined<sup>88</sup>.

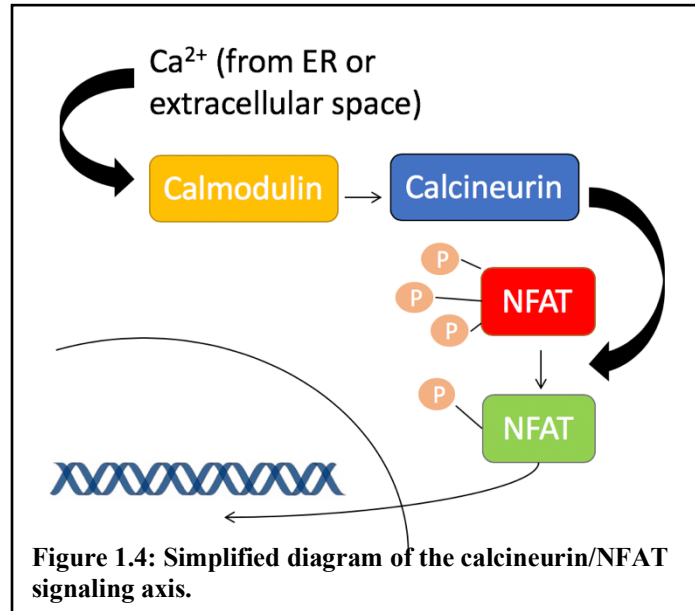
While anti-fibrotic factors and drugs have been identified, little is known about the molecular mechanisms that maintain the quiescent fibroblast phenotype. It is clear that the quiescent fibroblast state consists of more than a simple arrest in proliferation, and the fibroblast-intrinsic processes that actively maintain their quiescence in terms of functional activation are not well defined. The tumor suppressor p53 has been shown to play an important role in the tumor suppressive effects of normal fibroblasts; however, p53-regulated transcription is drastically changed in cancer-associated fibroblasts, instead supporting the CAF phenotype<sup>89</sup>. Some signaling pathways have been found to be

downregulated in CAFs in certain cancers; the Notch effector CBF1, Suppressor of Hairless, Lag-1 (CSL) has been shown to regulate fibroblast homeostasis through direct interactions with p53<sup>90</sup>. In many dermatologic malignancies, CSL activity, and subsequently fibroblast quiescence, is reduced via the downregulation of androgen receptor, which interacts with CSL in order to restrain the activation of CAFs through transcriptional repression<sup>91</sup>. Cellular quiescence in fibroblasts may also rely on paracrine signaling from other compartments of the microenvironment, particularly normal epithelium<sup>92</sup>.

**Calcineurin/NFAT: a signaling axis responsible for both activation and quiescence in a number of cell types**

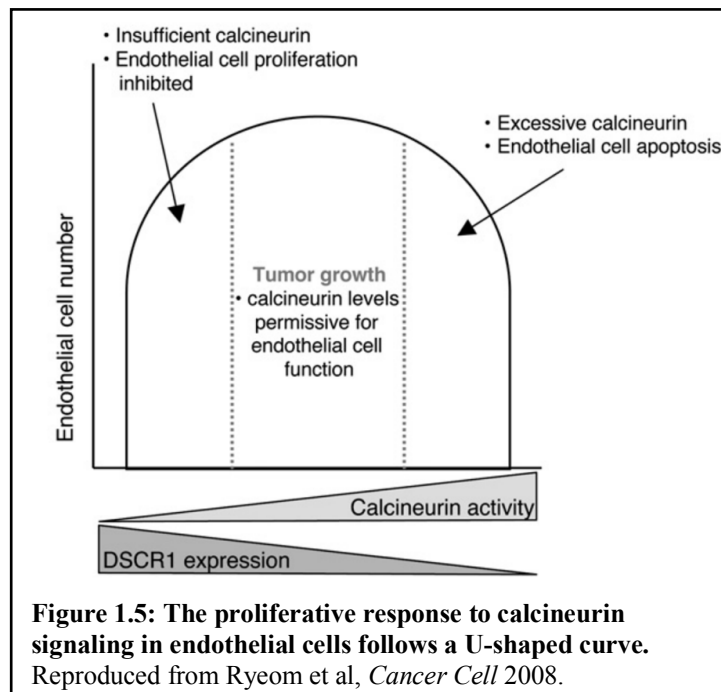
One signaling pathway that has been implicated in several cell types in the tumor microenvironment is the axis consisting of calcineurin (CN) and its canonical targets, the nuclear factor of activated T cells (NFAT) family of transcription factors (**Figure 1.4**). CN/NFAT was first identified as a regulator of T cell activation but has since been shown to play a role in a variety of cell types. CN is a calcium-regulated serine-threonine phosphatase that consists of two subunits: a catalytic (calcineurin A) and a regulatory subunit (calcineurin B)<sup>93</sup>. Upon increased calcium flux into the cytoplasm, calcineurin is activated through a conformational change, exposing its catalytic site. The best-known substrates of CN are the NFAT family of transcription factors, which translocate to the nucleus upon their dephosphorylation by CN and transactivate tissue-specific genes. NFAT exists in 4 canonical isoforms, known as NFAT1-4 or NFATc1-4. NFAT5 shares homology with the other NFAT isoforms but is not activated by calcineurin. All NFAT

isoforms alone display weak DNA-binding capabilities; thus, they require a more strongly DNA-binding transcriptional co-activator or co-repressor for effective signal transduction<sup>94</sup>.



CN signaling has been shown to play a crucial role in both tumor cells and their microenvironment. Interestingly, individuals with Down syndrome, who due to trisomy 21 have 3 copies of the endogenous CN inhibitor Down syndrome critical region 1 (DSCR1), have a lower incidence of solid tumors than the general population, though they have a higher incidence of leukemias<sup>95-97</sup>. This is thought to be due to decreased angiogenesis secondary to an increase in inhibition of the calcineurin-mediated response to VEGF signaling, as well as increased inhibition of calcineurin leading to impaired cell cycle progression and, consequently, tumorigenesis<sup>98-100</sup>. On the other hand, transplant patients receiving cyclosporine A (CsA) or other calcineurin inhibitors such as tacrolimus have an increased risk of malignancy; conversely, this is generally thought to be due to a decrease in tumor immune surveillance<sup>101</sup>. These clinical findings have led to a large amount of

research ultimately demonstrating that CN/NFAT signaling plays a crucial role not only in tumor cells themselves<sup>100,102,103</sup> (most likely in an NFAT isoform-specific manner<sup>99</sup>), but in many cell types in the microenvironment as well<sup>94</sup>. Our lab has previously shown that activation of CN/NFAT in the endothelium is a crucial step in the priming of the lung as a distant metastatic site<sup>104</sup>. At the same time, we have shown that genetic deletion of *Dscr1* suppresses tumor growth due to dysregulation of apoptotic ligands and subsequent endothelial apoptosis, suggesting that excessive calcineurin signaling can instead limit tumor growth (**Figure 1.5**)<sup>105</sup>.



While calcineurin's role in tumor cells, immune cells, and the endothelium are fairly well-characterized, little work has been done to study the effect of CN/NFAT specifically in cancer-associated fibroblasts. Previous studies examining the role of CN/NFAT in fibroblasts have identified both pro- and anti-fibrotic effects of CN signaling.

Long-term treatment of transplant patients with the calcineurin inhibitors cyclosporin A (CsA) and/or tacrolimus is often complicated by acute and chronic nephrotoxicity, of which tubulointerstitial fibrosis is a hallmark<sup>106–108</sup>. Further, CsA has been shown to have direct fibrogenic effects on renal tubulointerstitial cells and fibroblasts<sup>109</sup>, and deletion of the  $\alpha$  isoform of CnA is sufficient to cause renal fibrosis and increased fibronectin and TGF $\beta$  expression in renal fibroblasts<sup>110</sup>. However, other studies have shown that downregulation of CN/NFAT signaling via pharmacologic inhibition or genetic deletion leads to a decrease in fibrosis-associated phenotypes in cardiac<sup>111,112</sup>, dermal<sup>113</sup>, and lung<sup>114</sup> fibroblasts. Additionally, many of these studies utilized CsA to inhibit CN, and we and others have shown that CsA has a number of calcineurin-independent targets and effects<sup>115,116</sup>. For example, CsA has been shown to attenuate disease progression in a bleomycin model of murine lung fibrosis; however, this effect was demonstrated to be independent of calcineurin signaling, as administration of tacrolimus did not recapitulate this phenotype<sup>117</sup>.

In summary, fibroblast activation is a crucial process in both physiologic and pathologic states, but the molecular mechanisms mediating their activation are not fully defined, and very little is known regarding the mechanisms maintaining their quiescence. There is some previous evidence that CN/NFAT signaling may play a role in fibroblast activation, but the current data is conflicting, and results are often confounded by the significant off-target effects of pharmacologic inhibition of CN. Therefore, the goal of my thesis project was to fully investigate the role of CN/NFAT signaling in fibroblast activation in the setting of the lung. By studying the phenotype of the CN-null pulmonary fibroblast *in vitro* and *in vivo*, we identified how CN specifically mediates the homeostasis

and activation of fibroblasts, and how this phenotype may affect disease states such as cancer.

## CHAPTER 2: DELETION OF CALCINEURIN PROMOTES A PRO-TUMORIGENIC FIBROBLAST PHENOTYPE.

### Introduction

The tumor microenvironment (TME) consists of multiple cell types, including endothelial, immune, and stromal cells<sup>118</sup>. It is instrumental in the development of both primary tumors and distant metastases, making it an appealing potential therapeutic target. Fibroblasts, a key component of the stroma, are cells of mesenchymal origin that play a number of roles in both normal and diseased tissues. Resident fibroblasts can orchestrate and maintain the architecture of extracellular matrix (ECM) in normal tissues, but activation of fibroblasts is crucial to dynamically remodel the matrix in both physiologic processes such as wound healing as well as pathologic processes such as fibrosis and cancer<sup>119</sup>. Studies have indicated that normal tissues are resistant to tumor cell colonization and growth due in part to fibroblast homeostasis, and that fibroblast activation is required for both primary tumor progression and metastatic colonization<sup>119,120</sup>. While multiple stimuli that contribute to the activation of fibroblasts have been identified, the cell-intrinsic molecular mechanisms underlying the transition from quiescent to activated fibroblasts, or the “stromagenic switch,” are less well understood.

The most widely used markers of activated fibroblasts currently include fibroblast activation protein (FAP)<sup>121,122</sup> and the myofibroblast marker alpha-smooth muscle actin ( $\alpha$ SMA)<sup>123</sup>. Expression of these and other markers indicate they represent heterogeneous populations with unique gene expression profiles dependent on both context and tissue of origin<sup>124</sup>. However, collectively, activated fibroblasts can increase their migration and

contractility, secrete and remodel extracellular matrix, including collagen, and produce cytokines and growth factors that affect other cellular compartments in the microenvironment such as the immune system and the endothelium. A variety of stimuli are responsible for fibroblast activation, including changes in substratum mechanical stiffness, composition and architecture of the ECM, growth factors such as TGF $\beta$  or PDGF, cytokines and chemokines, and sources of cellular stress such as hypoxia or ROS<sup>125</sup>.

While many of the activating stimuli of fibroblasts and their downstream mediators of activation have been well-defined, less is known about cell-intrinsic pathways required to maintain the homeostatic state of resident un-activated fibroblasts. It is increasingly evident that quiescence is not simply a default state but rather requires active maintenance; however, little is known about the intracellular signaling pathways responsible for maintaining homeostasis<sup>71</sup>. The calcineurin (CN)/nuclear factor of activated T cells (NFAT) signaling pathway was originally identified as critical for T cell activation and has since been shown by us and others to also play key roles in numerous other cell types, including endothelial cell activation and tumor angiogenesis<sup>95,104,105</sup>. CN is a calcium-regulated serine-threonine phosphatase that consists of two subunits: a catalytic (calcineurin A) and a regulatory subunit (calcineurin B)<sup>93</sup>. Upon increased calcium flux into the cytoplasm, calcineurin is activated through a conformational change, exposing its catalytic site. Its best-known substrates are the NFAT family of transcription factors, which translocate to the nucleus upon their dephosphorylation by CN and transactivate tissue-specific genes. We previously demonstrated that the CN/NFAT pathway plays a key role in mediating endothelial cell activation downstream of VEGF, and that pharmacologic or genetic deregulation of CN signaling affects both primary tumor growth and metastatic

progression<sup>95,104,105</sup>. Prior studies by others have shown contrasting effects of the CN pathway in activated fibroblasts, with reports of both pro- and anti-fibrotic effects of CN *in vitro* and *in vivo*<sup>37-45</sup>. Moreover, to our knowledge, the role of CN/NFAT in fibroblasts in the TME has not yet been investigated.

As the CN/NFAT pathway has been implicated in regulating the function of multiple cell types in the TME<sup>94</sup>, as well as in fibroblast activation in wound healing and fibrosis, we hypothesized that CN/NFAT may play a role in regulating the function of fibroblasts in the TME. To test this hypothesis, we examined the role of CN signaling in lung fibroblasts and assessed the impact of fibroblast-specific deletion of CN on lung metastasis. Here we demonstrate that acute deletion of calcineurin in lung fibroblasts leads to increased proliferation, migration, and contractility compared to wild-type fibroblasts, changes consistent with activation. Furthermore, we found that extracellular matrix derived from *Cn*<sup>-/-</sup> fibroblasts contains greater amounts and more linearly aligned fibrillar collagen, and that *Cn*<sup>-/-</sup> fibroblasts support more robust endothelial cell tube formation *in vitro*. Consistent with our *in vitro* findings, we found that stromal cell specific *Cn* deletion in mice leads to a higher incidence and increased size of lung metastases in a spontaneous lung metastasis model with two different tumor cell lines. Our findings implicate CN in maintaining fibroblast homeostasis in normal, unstimulated states, and in attenuating the pro-tumorigenic activity of fibroblasts in the metastatic niche.

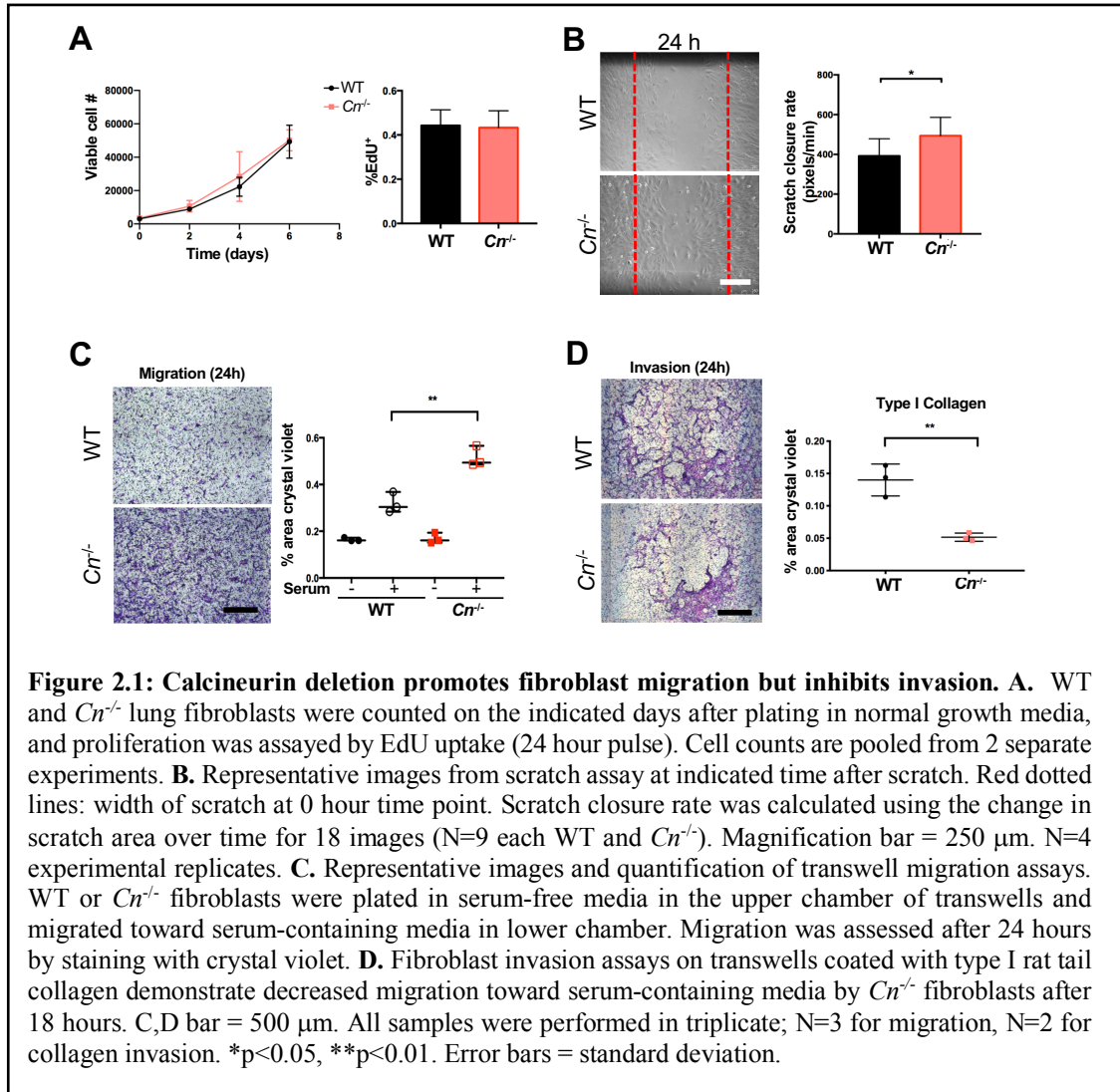
## **Results**

### *Calcineurin deletion in vitro promotes fibroblast migration*

To analyze the role of calcineurin in fibroblast activation *in vitro*, we treated primary lung fibroblasts derived from calcineurin B (*CnB*) floxed mice with adenoviral Cre recombinase. Deletion of *CnB* destabilizes and promotes proteolytic degradation of the calcineurin A subunit<sup>126</sup>. Benign and malignant diseases, including wound healing, fibrosis, and cancer, all feature increased numbers of fibroblasts that can be attributed to a combination of fibroblast proliferation, migration of nearby resident fibroblasts to lesions, and recruitment of mesenchymal precursors from the bone marrow. Thus, we first examined whether acute deletion of CN altered fibroblast proliferation. We observed no difference in cell proliferation between WT and *Cn*<sup>-/-</sup> fibroblasts (**Figure 2.1A**). However, in scratch assays of confluent monolayers, *Cn*<sup>-/-</sup> fibroblasts exhibited enhanced closure at 24 hours post-wounding (**Figure 2.1B**), and live-cell imaging over the first 24 hours post-scratch revealed that *Cn*<sup>-/-</sup> fibroblasts exhibited accelerated and markedly different migratory phenotypes compared to WT fibroblasts. Specifically, *Cn*<sup>-/-</sup> fibroblasts migrated oriented perpendicularly to the leading edge of the wound as compared to WT fibroblasts, which exhibited more stochastic motion throughout wound closure (**Supplemental Video 1**).

The accelerated wound closure by *Cn*<sup>-/-</sup> fibroblasts in scratch assays suggested that deletion of calcineurin might increase the migratory ability of fibroblasts. Indeed, we found that in uncoated transwell migration assays, *Cn*<sup>-/-</sup> fibroblasts exhibited greater migration compared to wild-type fibroblasts after 24 hours (**Figure 2.1C**). However, *Cn*<sup>-/-</sup> fibroblasts exhibited impaired migration compared to WT controls on transwells coated with type I collagen (**Figure 2.1D**), implicating an inability of calcineurin-null fibroblasts to invade and migrate through a collagen matrix. Collectively, these data indicate that while CN

deletion increased fibroblast migration, it inhibited collagen invasion and had no effect on fibroblast proliferation.



*Calcineurin-null fibroblasts exhibit increased collagen contractility and matrix remodeling*

As another key function of activated fibroblasts is to process and remodel collagen, we plated fibroblasts onto thick type I collagen gels. In the absence of fibroblasts, these collagen gels contain very little fibrillar collagen as visualized by 2-photon second harmonic generation (SHG) imaging; once fibroblasts are added, they remodel and exert

tension on the collagen substratum, leading to the formation of a network of collagen fibers visible by SHG. *Cn*<sup>-/-</sup> fibroblasts remodeled type I collagen gels to a greater extent than WT fibroblasts, leading to increased SHG signal (**Figure 2.2A**).

To further investigate the effects of CN deletion on collagen remodeling, we utilized a collagen contraction assay, in which fibroblasts were embedded in a type I collagen gel that was then detached and allowed to float freely in culture medium. When the solidified collagen gels are detached, a combination of collagen remodeling and fibroblast contractility exerts forces on the gel, causing it to contract<sup>127</sup>. CN deletion significantly increased the rate of collagen gel contraction at 6 and 12 hours post-detachment with maximal contraction by 12 hours. In contrast, WT fibroblasts required almost 20 hours post-detachment for maximal contraction (**Figure 2.2B**).

We assessed the ability of *Cn*<sup>-/-</sup> fibroblasts to deposit, accumulate and remodel collagen by comparing fibroblast-derived matrices (FDMs) from WT and *Cn*<sup>-/-</sup> fibroblasts<sup>128</sup>. We found that CN deletion led to significant increases in the accumulation of fibrillar collagen and alignment of collagen fibrils as observed by SHG imaging (**Figure 2.2C**). Extracellular matrix can be remodeled through multiple mechanisms, including the production of collagenases by fibroblasts, so we compared the collagenase activity associated with CN-null and WT fibroblasts by overlaying DQ<sup>TM</sup> type I collagen on fibroblasts cultured on collagen gels. DQ collagen is saturated with quenched fluorescein molecules, and digestion by collagenases releases fluorescent fragments of collagen that are visible by fluorescence microscopy. *Cn*<sup>-/-</sup> fibroblasts plated on either gelatin-coated chamber slides or a collagen substratum exhibited greater collagenase activity than WT fibroblasts (**Figure 2.2D-E**).

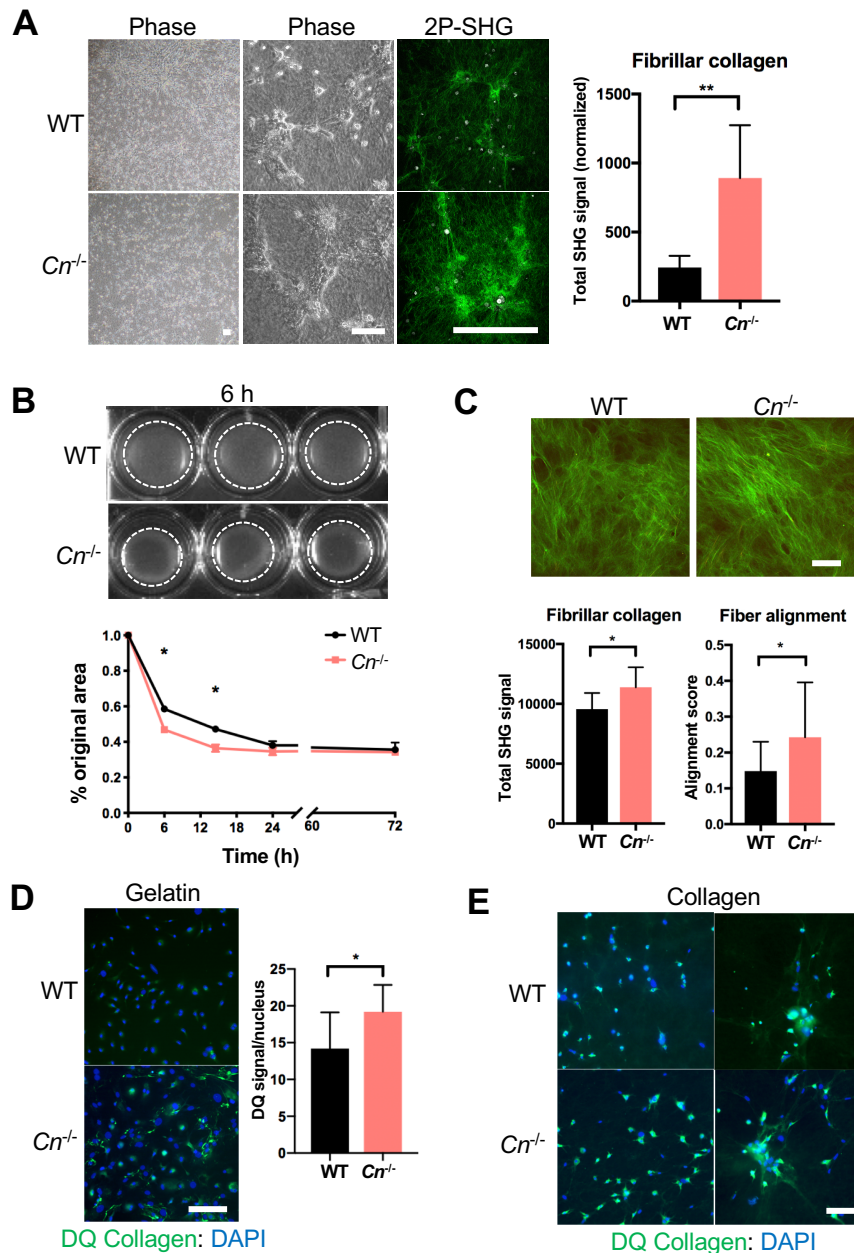


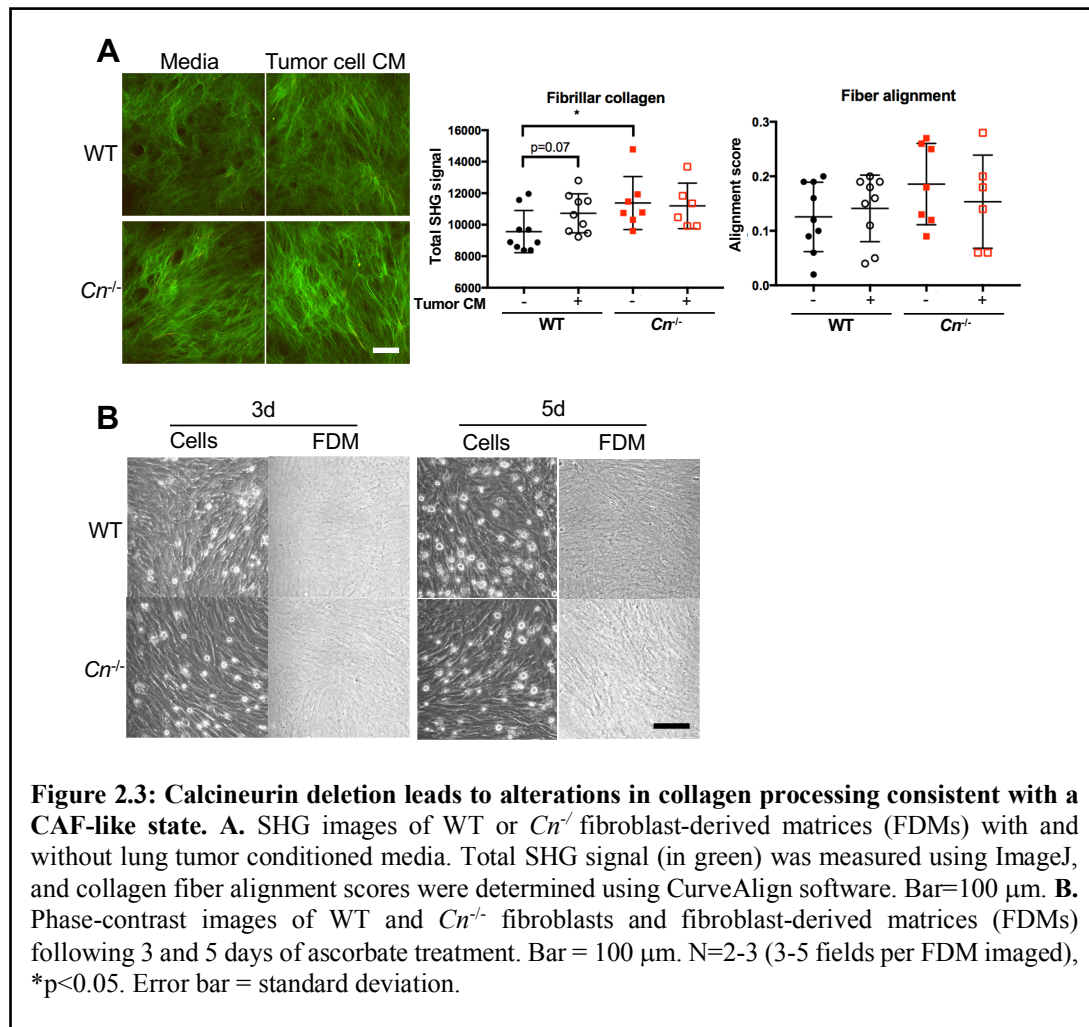
**Figure 2.2: Calcineurin-null fibroblasts exhibit increased collagen contractility and matrix remodeling.** **A.** Phase-contrast and 2-photon second harmonic generation (2P-SHG) images of WT and *Cnr*<sup>-/-</sup> fibroblasts cultured on collagen gels in serum-containing media for 48 hours. Total SHG signal (green) was quantified using ImageJ and normalized to cell count as measured by autofluorescent signal (white). Magnification bar = 250  $\mu$ m. **B.** Representative images (after 6 hours) and quantification of collagen contraction by WT and *Cnr*<sup>-/-</sup> fibroblasts at indicated times. White dotted lines denote collagen gel circumference. **C.** Representative 2P-SHG images of fibroblast-derived matrices. Total SHG signal (green) was quantified using ImageJ, and collagen fiber alignment scores were determined using CurveAlign software. Bar = 100  $\mu$ m. **D.** Images from DQ collagen assay on gelatin-coated glass and quantification of average DQ signal per nucleus using ImageJ. **E.** Images from DQ collagen assay on type I collagen gels. Collagenase-digested DQ<sup>TM</sup> collagen signal is green and nuclei (DAPI stain) are blue. Bar = 250  $\mu$ m. All samples were assayed in triplicate, N=2-5. \*p<0.05, \*\*p<0.01. Error bars = standard deviation.

This effect was specific for collagenase activity, as we observed no difference in gelatinase activity under either culture condition (data not shown). Taken together, our data indicate that CN deletion leads to an increase in collagen accumulation, remodeling, and contractility in the absence of exogenous activating stimuli, suggesting that the calcineurin pathway may be important for fibroblast homeostasis.

*Calcineurin deletion leads to alterations in collagen processing consistent with a CAF-like state*

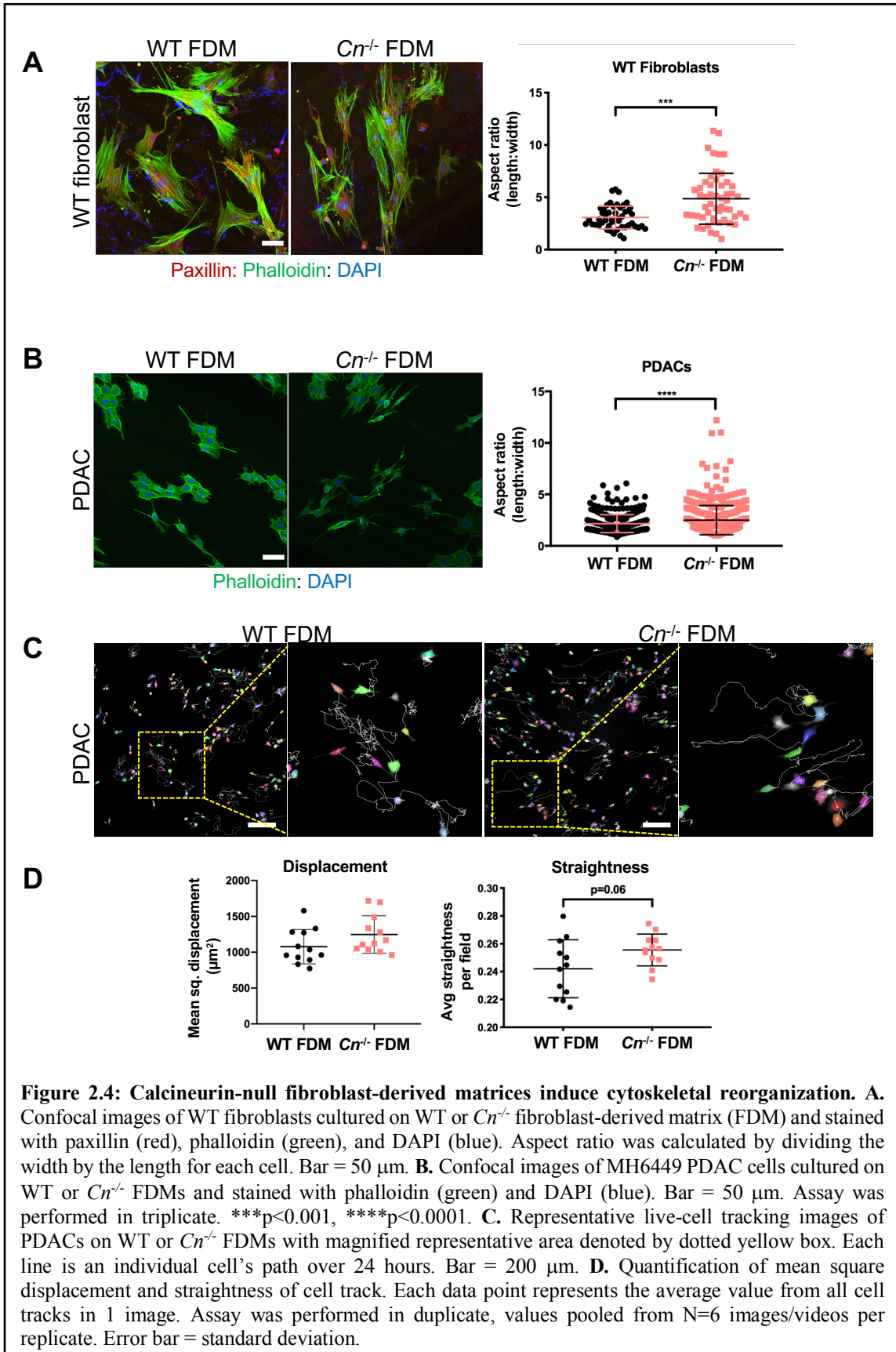
Given that higher fiber density and greater fiber alignment are characteristic of FDMs derived from cancer-associated fibroblasts, we compared WT and *Cn*<sup>-/-</sup> fibroblast-derived matrices generated in the presence of normal media or cancer cell conditioned media (CM) from SR0144 cells, a murine lung adenocarcinoma cell line driven by loss of *Tp53* and expression of oncogenic *Kras*. As expected, when WT fibroblasts were cultured with tumor CM, we observed a greater accumulation of fibrillar collagen in the generated matrix as measured by SHG signal than in matrix generated by WT cells in normal media. We also observed foci of more highly aligned collagen in FDMs generated by WT cells in the presence of tumor CM. Interestingly, we found that FDMs generated by *Cn*<sup>-/-</sup> fibroblasts in the presence of normal media also exhibited increased accumulation of fibrillar collagen similar to that seen in WT FDMs generated in tumor CM (**Figure 2.3A**). These data suggest *Cn*<sup>-/-</sup> fibroblasts are phenotypically similar to tumor cell CM-treated WT fibroblasts and do not respond to further stimulation by tumor CM.

We decellularized and examined  $Cn^{-/-}$  and WT FDMs at earlier timepoints to determine differences in matrix deposition and remodeling. After 3 days, there were noticeable differences in both fibroblast and matrix alignment in CN-null fibroblasts as determined by phase contrast imaging, which were further enhanced after 5 days (**Figure 2.3B**). Consistent with the increase in linear alignment of collagen fibrils in FDMs derived from  $Cn^{-/-}$  fibroblasts, the cells themselves were also more linearly aligned and elongated.



*Cytoskeletal reorganization in fibroblasts is regulated by calcineurin*

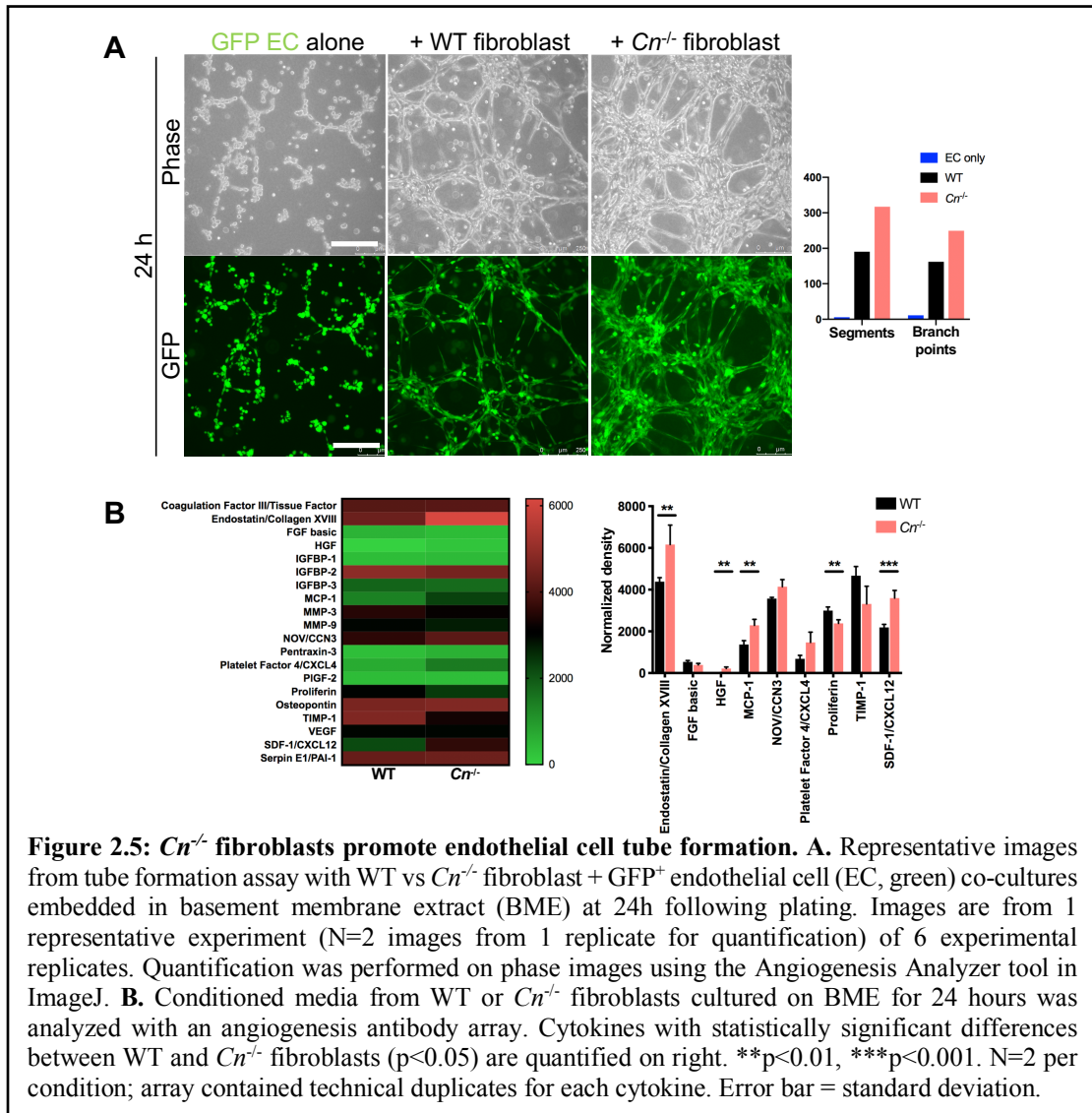
Our data show that calcineurin regulates fibroblast-mediated matrix remodeling, and it is well-established that alterations in matrix organization drive cytoskeletal reorganization as well as cell size and shape. Thus, we compared how FDMs derived from WT and CN-deleted fibroblasts affected reorganization of the actin cytoskeleton in fibroblasts and/or tumor cells. When WT fibroblasts were plated on *Cn*<sup>-/-</sup> FDMs and stained for phalloidin and the focal adhesion complex protein paxillin, they extended long, thin cytoplasmic processes and demonstrated an elongated morphology compared to their behavior on WT FDMs (**Figure 2.4A**). We also plated murine YFP-expressing pancreatic ductal adenocarcinoma cells (PDAC) onto FDMs generated from WT and *Cn*<sup>-/-</sup> fibroblasts and analyzed their cytoskeletal architecture via phalloidin staining and confocal microscopy. Similar to the fibroblasts, PDACs cultured on FDMs derived from *Cn*<sup>-/-</sup> fibroblasts were also elongated (**Figure 2.4B**), and live-cell imaging of PDACs on these FDMs revealed greater displacement and more linear movement on *Cn*<sup>-/-</sup> FDMs as compared to WT FDMs (**Figure 2.4C-D, Supplemental Video 2**). Therefore, the matrix generated by *Cn*<sup>-/-</sup> fibroblasts is sufficient to significantly alter the cytoskeletal architecture of both tumor cells and fibroblasts as compared to matrix derived from WT fibroblasts.



*Loss of calcineurin in fibroblasts promotes EC tube formation*

Activated fibroblasts and their associated matrix play a crucial role in angiogenesis, both by providing structural support and by secreting pro-angiogenic factors. We utilized a co-culture model of EC tube formation in which primary lung ECs were mixed with WT or *Cn*<sup>-/-</sup> fibroblasts on basement membrane extract (BME), and 2D tube formation was quantified. *Cn*<sup>-/-</sup> fibroblasts supported more robust EC tube formation measured by number of tube segments and branch points as compared to WT fibroblasts (**Figure 2.5A**).

Therefore, we examined the secretome of WT and *Cn*<sup>-/-</sup> fibroblasts during tube formation. We generated conditioned media from WT and *Cn*<sup>-/-</sup> fibroblasts cultured on BME and probed for angiogenesis-related proteins. Deletion of CN led to significant upregulation of multiple cytokines and growth factors, including SDF-1, a chemokine that has been shown to promote angiogenesis as well as the myofibroblast phenotype in both cancer and fibrotic disease<sup>129-132</sup> (**Figure 2.5B**). Thus, the differences observed in our *in vitro* tubulogenesis assays may be at least partially mediated by differences in angiogenic secreted factors of CN-null fibroblasts.



### *Loss of calcineurin in fibroblasts promotes metastasis*

Our data suggest that CN deletion in fibroblasts leads to an activated phenotype in fibroblasts that may be pro-tumorigenic. To investigate tumor growth and metastases in mice with fibroblast specific deletion of calcineurin, we cross-bred calcineurin B floxed mice with transgenic mice expressing tamoxifen-inducible Cre driven by a fragment of the type I collagen alpha-1 chain promoter (*Coll1a1-Cre-ER(T)*)<sup>133,134</sup> to delete CN from the stroma *in vivo*. While previous literature suggested that the 2.3kb fragment of the *Coll1a1*

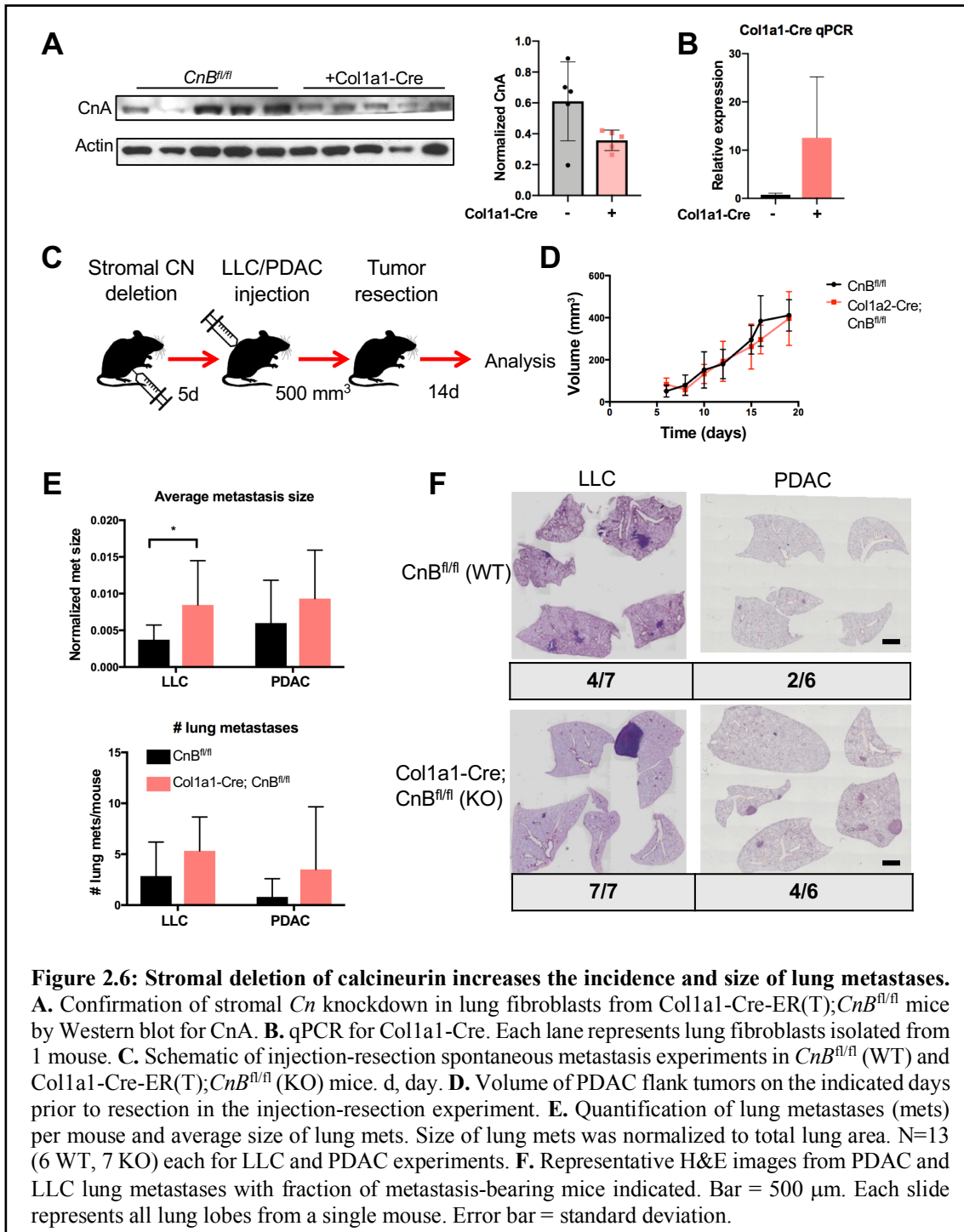


**Figure 2.6: Stromal deletion of calcineurin increases the incidence and size of lung metastases.**

**A.** Confirmation of stromal *Cn* knockdown in lung fibroblasts from *Col1a1-Cre-ER(T);CnB<sup>fl/fl</sup>* mice by Western blot for CnA. **B.** qPCR for *Col1a1-Cre*. Each lane represents lung fibroblasts isolated from 1 mouse. **C.** Schematic of injection-resection spontaneous metastasis experiments in *CnB<sup>fl/fl</sup>* (WT) and *Col1a1-Cre-ER(T);CnB<sup>fl/fl</sup>* (KO) mice. d, day. **D.** Volume of PDAC flank tumors on the indicated days prior to resection in the injection-resection experiment. **E.** Quantification of lung metastases (mets) per mouse and average size of lung mets. Size of lung mets was normalized to total lung area. N=13 (6 WT, 7 KO) each for LLC and PDAC experiments. **F.** Representative H&E images from PDAC and LLC lung metastases with fraction of metastasis-bearing mice indicated. Bar = 500  $\mu$ m. Each slide represents all lung lobes from a single mouse. Error bar = standard deviation.

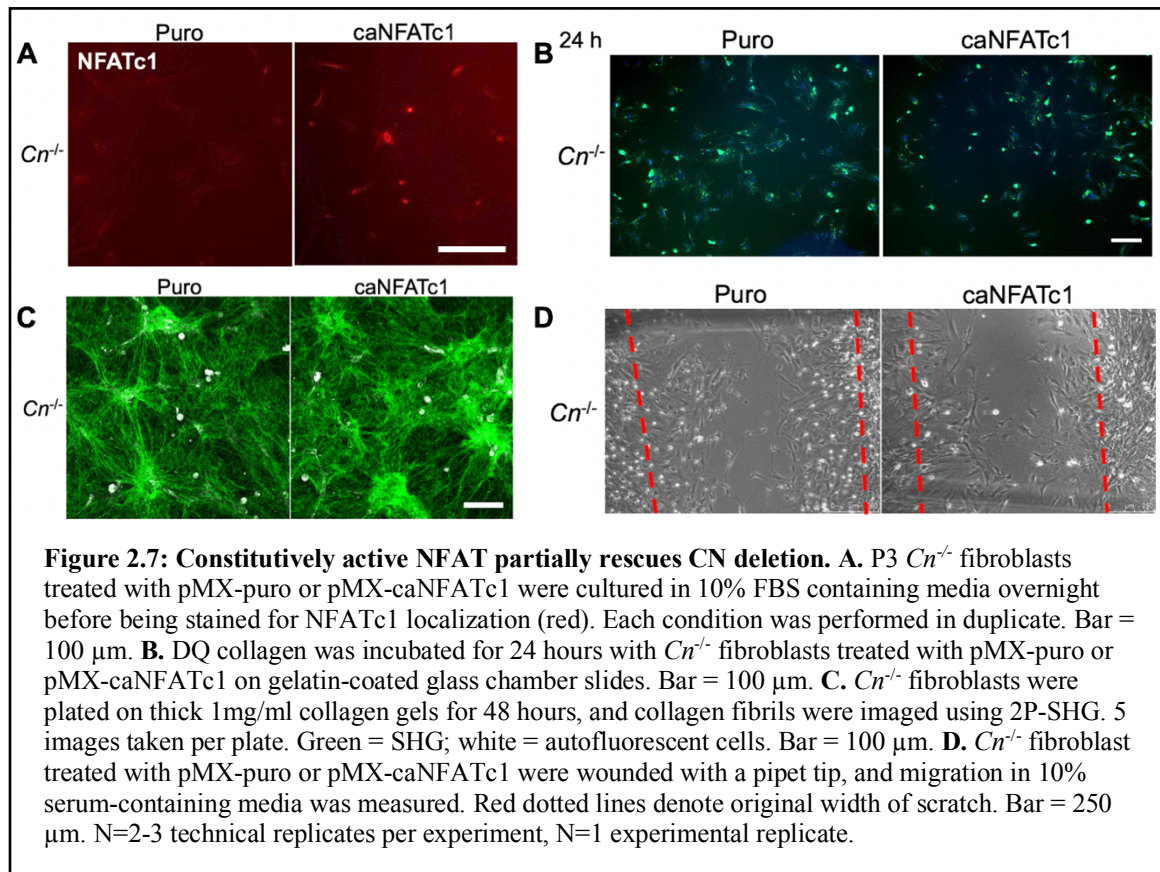
promoter is solely expressed in dermal fibroblasts (along with osteoblasts and osteoclasts), we demonstrated Cre expression as well as a significant decrease in CN expression in lung fibroblasts after 1 week of tamoxifen administration (**Figure 2.6A**).

To examine both primary tumor growth and metastases, we utilized an injection-resection experimental model of spontaneous lung metastasis using two separate tumor cell lines: Lewis lung carcinoma and the MH6449 PDAC cell line. Following tamoxifen injection to delete CN from fibroblasts, subcutaneous tumors were established and allowed to grow to 400-600 mm<sup>3</sup> before resection; 14 days following resection, mice were sacrificed and lungs analyzed for metastases (**Figure 2.6B**). There was no significant difference in primary tumor growth between *Cn<sup>fl/fl</sup>* (WT) and *Colla1-Cre;Cn<sup>ΔΔ</sup>* mice (**Figure 2.6C**). However, there was an increase in the size of LLC lung mets and a trend towards larger PDAC lung metastases in *Colla1-Cre;Cn<sup>ΔΔ</sup>* mice (**Figure 2.6D**). Additionally, 6/6 of stromal *Cn<sup>ΔΔ</sup>* vs 4/6 WT mice in the LLC and 4/6 vs 2/6 in the PDAC model developed visible lung metastases, indicating an increase in the development of lung metastases upon CN deletion in lung fibroblasts (**Figure 2.6E**). These data suggest that stromal deletion of CN specifically increases both the colonization and outgrowth of lung metastases.

*Expression of constitutively active NFAT signaling partially rescues CN deletion*

To determine whether restoration of NFAT activation could rescue the phenotype of *Cn<sup>-/-</sup>* fibroblasts and limit fibroblast activation, we transduced *Cn<sup>-/-</sup>* fibroblasts with a constitutively nuclear form of NFATc1 (caNFATc1) (**Figure 2.7A**) and assayed its effects on collagen remodeling and migration. Expression of caNFATc1 partially reversed the increase in collagenase activity of *Cn<sup>-/-</sup>* fibroblasts in DQ type I collagen assays as compared to *Cn<sup>-/-</sup>* fibroblasts (**Figure 2.7B**). However, scratch assays on *Cn<sup>-/-</sup>* fibroblasts with caNFATc1 expression showed similar increased migration and a flattened fibroblast morphology similar to *Cn<sup>-/-</sup>* fibroblasts (**Figure 2.7D**) and had a nominal effect on fibrillar

collagen remodeling in fibroblasts cultured on type I collagen gels (**Figure 2.7C**). These data suggest that restoration of NFAT signaling leads to a decrease in collagenase activity by CN-null fibroblasts similar to WT fibroblasts but does not significantly affect fibroblast migration and fibrillar collagen remodeling.



## Discussion

In this study, we characterized the effect of CN deletion in fibroblasts *in vitro* and *in vivo*. Our data show that calcineurin deletion in fibroblasts *in vitro* leads to a number of functional alterations consistent with an activated, pro-tumorigenic fibroblast phenotype. This suggests CN may play a crucial role in the maintenance of fibroblast homeostasis or the “un-activated” state. We demonstrate that  $Cn^{-/-}$  fibroblasts exhibited greater migratory capacity during scratch assays and transwell migration assays; however, they do not invade

through type I collagen gels to the same extent as WT. Our studies identified a role for CN in the deposition and remodeling of extracellular matrix, particularly collagen, with  $Cn^{-/-}$  fibroblasts exhibiting increased collagenase activity and collagen remodeling. CN deletion leads to an increase in fibrillar collagen in  $Cn^{-/-}$  fibroblast-derived matrices and when  $Cn^{-/-}$  fibroblasts are cultured on type I collagen gels. These differences in matrix direct the cytoskeletal reorganization of both fibroblasts and tumor cells, and tumor cells exhibit more linearly directed movement when cultured on  $Cn^{-/-}$  matrix. Finally, our *in vitro* studies show that CN-null fibroblasts promote endothelial cell tube formation and increase their production of angiogenesis-related proteins. Fibroblast-specific deletion of CN *in vivo* increased the incidence and size of lung metastases in an experimental model of spontaneous metastasis. Our data suggest that CN deletion leads to an activated fibroblast phenotype in the absence of activating stimuli, phenocopying cancer-associated, pro-tumorigenic fibroblasts.

We show that CN deletion leads to an increase in fibroblast migratory capacity, but a decrease in invasion through type I collagen. Given that  $Cn^{-/-}$  fibroblasts demonstrated increased collagenase activity in other assays, it is unlikely that this phenotype is caused by a decrease in collagen proteolysis. It is possible that the increased collagenase activity as observed in the DQ collagen assays revealed a greater number of cryptic binding sites to which the  $Cn^{-/-}$  fibroblasts can bind via engagement of their integrins, or that the increase in fibrillar collagen as observed by SHG imaging of  $Cn^{-/-}$  fibroblasts on type I collagen gels encouraged engagement of integrins with specificity for collagen in its triple helical fibril structure, such as integrins  $\alpha 1\beta 1$  and  $\alpha 2\beta 1$ <sup>50</sup>. This pro-remodeling phenotype may promote interactivity with the collagen substratum instead of invasion through it.

Our work also identifies a role for CN in the secretion and remodeling of extracellular matrix, specifically in collagen.  $Cn^{-/-}$  fibroblasts are capable of both remodeling and exerting contractile forces on existing collagen substrates as well as secreting and remodeling new ECM *de novo* to a greater extent than WT fibroblasts. However, we observed no difference in gelatinase activity, suggesting that calcineurin specifically regulates the processing of fibrillar collagen and not its denatured form, possibly through differential expression of collagenases but not gelatinases. Fibroblast-derived matrices generated using  $Cn^{-/-}$  fibroblasts have a greater amount of fibrillar collagen that is more linearly aligned, findings that are consistent with FDMs generated from cancer-associated fibroblasts compared to normal fibroblasts<sup>135</sup>. In support of this hypothesis, WT FDMs generated in the presence of tumor-conditioned media resemble  $Cn^{-/-}$  FDMs generated in normal growth media, and  $Cn^{-/-}$  FDMs do not undergo further changes when generated in the presence of tumor-conditioned media.

We then demonstrated that the matrix derived from  $Cn^{-/-}$  fibroblasts is sufficient to direct the cytoskeletal architecture of both WT fibroblasts and PDAC tumor cells, causing their aspect ratio to increase. The elongation of PDACs on  $Cn^{-/-}$  FDMs as measured by cell aspect ratio may be an indicator that these cells are undergoing epithelial-to-mesenchymal transition (EMT) at a higher rate than PDACs cultured on WT FDMs. The increased straightness of tumor cell migration paths on  $Cn^{-/-}$  FDMs, as well as the right-skewing of the mean square displacement distribution of PDACs on  $Cn^{-/-}$  FDMs, corresponds to their increased migration along the more linearly aligned collagen fibrils, a phenomenon that is frequently observed in tumor growth and invasion *in vivo*<sup>136</sup>.

We propose that the alterations in collagen fiber architecture we observed *in vitro* may inform the increase in the incidence and size of metastases in stromal CN-null mice in an experimental model of spontaneous metastasis. We did not observe gross differences in collagen fiber morphology or density, or in microvessel density in the PDAC primary tumors from the injection-resection experiments (data not shown); however, at the time of resection, these tumors were very large (~500 mm<sup>3</sup>), well past the size at which the angiogenic and stromagenic switch occur<sup>7,119</sup>. It may be that differences in ECM architecture and angiogenesis at earlier time points may enhance the intravasation of tumor cells, and analyzing tumors at the time of resection masks any differences that may be more apparent earlier, despite no difference in the rate of primary tumor growth.

Our work identifies calcineurin as one of the necessary signaling pathways through which fibroblast homeostasis is regulated, as deletion of calcineurin leads to activation in the absence of exogenous activating stimuli such as TGF- $\beta$ . While our work is the first to identify a role for CN specifically in fibroblast homeostasis, CN deletion has been shown to disrupt homeostasis in many other cell types and disease models<sup>137-140</sup>. The current literature examining the role of CN/NFAT signaling in fibroblast activation, however, is complex. Evidence exists for both pro- and anti-fibrotic effects of CN/NFAT signaling in fibroblasts isolated from a variety of tissues<sup>106-114</sup>. However, it is important to note that some of this work was conducted using pharmacologic inhibition of CN via CsA; we and others have shown that CsA has a significant number of calcineurin-independent targets and effects<sup>115,116</sup>, and the anti-fibrotic effects of CsA observed in one study were not recapitulated when tacrolimus, a CN inhibitor with a different mechanism of action, was

utilized<sup>117</sup>. Therefore, it is possible that many of the anti-fibrotic effects of CsA administration that have been previously observed are due to its off-target effects.

We must consider whether the activated phenotype of *Cn*<sup>-/-</sup> fibroblasts is dependent on NFAT signaling, as CN has been shown to dephosphorylate a number of other targets outside of NFAT<sup>93,141</sup>. Previous evidence suggests that NFAT is activated in response to activating stimuli such as mechanical stretching or TGF- $\beta$  treatment<sup>111,142</sup>; however, constitutively active NFAT can instead suppress myofibroblast transdifferentiation<sup>143</sup>. One possible NFAT target that may be at least partially responsible for the phenotype we observed is SDF-1/CXCL12, a pro-fibrotic and pro-angiogenic chemokine that was upregulated in *Cn*<sup>-/-</sup> fibroblasts in our angiogenic secretome array as well as in cytokine/chemokine secretome arrays generated from fibroblasts cultured on both type I collagen gels and fibronectin-coated hydrogels (data not shown). Some evidence exists for the negative regulation of SDF-1 by NFAT in osteoblasts<sup>144</sup> and cytotrophoblast cells<sup>145</sup>. Thus, one potential mechanism by which calcineurin deletion leads to a pro-tumorigenic phenotype in fibroblasts may be via this increase in autocrine SDF-1 expression.

Collectively, our data demonstrate a role for calcineurin signaling in fibroblast homeostasis by showing that calcineurin deletion leads to a pro-tumorigenic, activated phenotype in primary lung fibroblasts, and that stromal deletion of CN *in vivo* leads to an increase in the incidence and size of lung metastases. Though the increased incidence of tumors in transplant patients receiving calcineurin inhibitors has often been attributed to the desired immune suppressive effects of these drugs, our work demonstrates that the effects of calcineurin inhibition on the stroma may also play a part in this phenomenon. Further elucidation of the specific transcriptional targets of NFAT in lung fibroblasts may

identify specific signaling cascades through which this homeostasis is maintained as well as potential pathways to pharmacologically target the stroma.

## CHAPTER 3: CALCINEURIN-NULL FIBROBLASTS DO NOT RESPOND TO TGF- $\beta$ STIMULATION *IN VITRO*.

### Introduction

We have shown in **Chapter 2** that deletion of calcineurin in primary lung fibroblasts leads to an activated, pro-tumorigenic phenotype in the absence of exogenous activating stimuli. Next, we wished to determine how *Cn*<sup>-/-</sup> fibroblasts would respond when activating stimuli were added. Previously, we showed that the content and alignment of WT fibroblast derived matrices are significantly altered upon the addition of tumor conditioned media, whereas *Cn*<sup>-/-</sup> FDMs are not. This suggests that despite their baseline activation, *Cn*<sup>-/-</sup> fibroblasts may be unable to respond to certain activating stimuli to the same extent as WT. TGF- $\beta$ 1 is one of the main cytokines responsible for fibroblast activation in wound healing, fibrotic disease, and cancer; thus, we elected to specifically investigate the role of CN signaling in the functional response to TGF- $\beta$  stimulation in fibroblasts.

The TGF- $\beta$  superfamily of growth factors consists of a large group of proteins that are similar in their dimeric protein structure, often featuring disulfide bonding between the two monomers<sup>146</sup>. They can be divided into several subgroups: the transforming growth factors (TGF), bone morphogenic proteins (BMP), activins and inhibins, growth differentiation factors (GDF), and other factors such as Müllerian inhibiting substance (MIS). TGF family members are only expressed in vertebrates and play a significant role in normal development. Additionally, dysregulation of TGF signaling is implicated in a variety of disease states<sup>146</sup>: many tumor cells secrete increased levels of TGF- $\beta$ 1, leading

to widespread inflammatory and pro-fibrotic changes, and TGF- $\beta$ 1 is often implicated as one of the major inflammatory cytokines responsible for fibrotic disease<sup>147</sup>.

Given its important role in many developmental and physiologic processes, TGF signaling is a highly regulated and controlled process. TGF- $\beta$  is initially secreted in a latent, inactive form; an N-terminal latency-associated protein (LAP) is disulfide bonded to the active C-terminal TGF domain, and this bond must be disrupted in order for active TGF- $\beta$  to be released<sup>148</sup>. Active TGF- $\beta$  binds the TGF- $\beta$  receptor, a heterodimer consisting of one type I and one type II receptor; these heterodimers themselves dimerize, forming an active intracellular kinase complex<sup>147</sup>. The canonical TGF- $\beta$  signaling pathway following engagement and dimerization of the TGF- $\beta$  receptor occurs when the dimerized TGF- $\beta$  receptor phosphorylates regulatory Smad (R-Smad) proteins such as Smad2 and Smad3. These R-Smads form heterodimers with Smad4, and this heterodimer translocates to the nucleus and regulates the expression of a wide variety of genes. Control of TGF- $\beta$  signaling is mediated by a variety of endogenous inhibitory factors. The expression of inhibitory Smads (I-Smads) is stimulated by TGF- $\beta$  signaling, thus forming a negative feedback loop. The effects of TGF stimulation are often concentration-dependent, with opposing effects on cellular function and gene expression at low versus high concentrations of TGF<sup>149–151</sup>. In many cell types, such as podocytes, TGF- $\beta$  signaling is pro-proliferative at low concentrations and becomes pro-apoptotic above a critical threshold concentration, often in a Smad3-dependent manner<sup>152</sup>.

TGF- $\beta$  signaling also varies significantly based on cellular context, as evidenced by the many often contradictory roles TGF- $\beta$  plays in different cell types and disease settings<sup>153</sup>. Specifically, in fibroblasts, TGF- $\beta$ 1 signaling has been associated with

differentiation into the myofibroblast phenotype in wound healing, fibrosis, and cancer. TGF- $\beta$  stimulation of fibroblasts leads to the upregulation of a number of pro-fibrotic genes, including ECM proteins such as the  $\alpha$ -1 chain of type I collagen (COL1A1) and the EDA variant of fibronectin (EDA-FN), matrix metalloproteinases (MMPs), and other collagen remodeling enzymes such as lysyl oxidase (LOX). It also directly regulates the expression of the myofibroblast marker  $\alpha$ SMA and can lead to an increase in contractility in collagen contraction assays.

Previous studies suggest that calcineurin may play an important role in the response to TGF- $\beta$  in fibroblasts. First, TGF- $\beta$  is known to lead to calcium influx and calcineurin activity in many cell types, including renal fibroblasts<sup>142</sup>. Davis et al. then demonstrated that the expression of the calcium channel TRPC6 independently stimulate myofibroblast differentiation in a manner very similar to TGF- $\beta$  treatment; further, deletion of TRPC6 rendered cardiac and dermal fibroblasts unable to differentiate into myofibroblasts in response to TGF- $\beta$ , a phenotype that could be replicated. Notably, they identified that TRPC6 expression was induced by TGF- $\beta$  through non-canonical signaling via p38 and SRF<sup>66</sup>. These findings demonstrating direct effects of TGF- $\beta$  on calcium influx suggest that TGF- $\beta$  signaling results in activation of calcineurin. Finally, there is also some evidence that CN and TGF- $\beta$  signaling pathways can affect one another; in T cells, it has been shown that NFAT may act as a co-transcription factor with Smad2 and Smad3 to promote the expression of specific genes<sup>154,155</sup>.

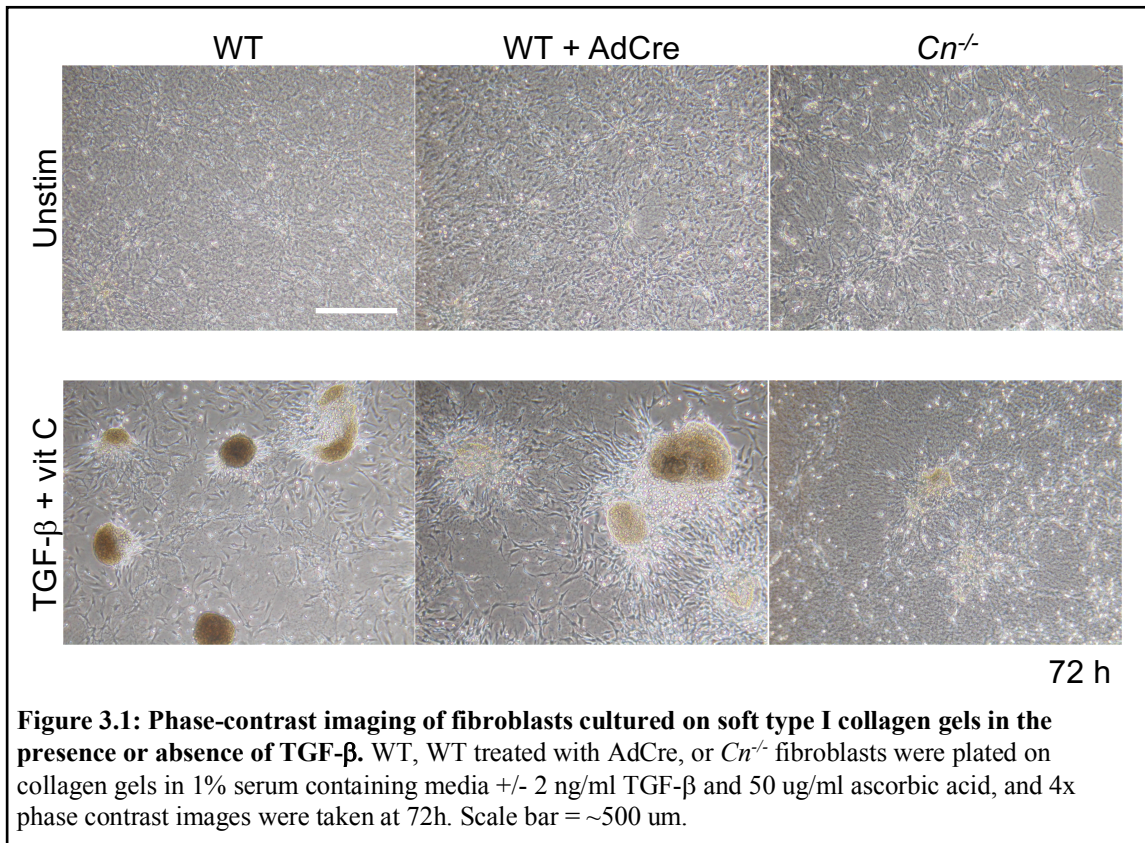
In summary, fibroblast activation in both cancer and fibrotic disease is often mediated by TGF- $\beta$ , and calcineurin may at least partially regulate the fibroblast response to TGF- $\beta$  stimulation. Therefore, we hypothesized that calcineurin deletion in fibroblasts

would abrogate their ability to respond functionally to TGF- $\beta$  stimulation. Thus, we sought to examine the functional response of WT and *Cn*<sup>-/-</sup> lung fibroblasts to TGF- $\beta$  treatment *in vitro* using many of the functional assays described in **Chapter 2**.

## **Results**

### *Calcineurin deletion attenuates phenotypic changes in fibroblasts on collagen gels in response to TGF- $\beta$*

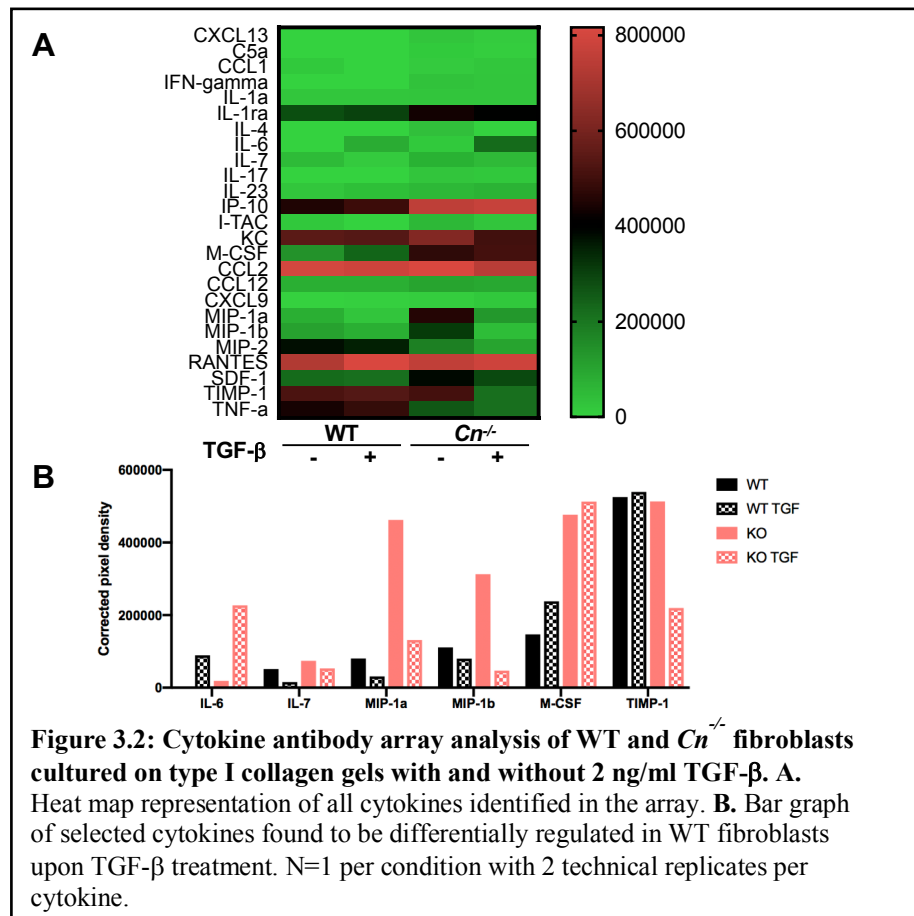
To determine the effects of calcineurin deletion on TGF- $\beta$ -induced activation, fibroblasts were grown on soft 1 mg/ml type I collagen gels and treated with and without 2ng/ml TGF- $\beta$  + 50  $\mu$ g/ml ascorbic acid. Ascorbic acid was added to TGF- $\beta$  treatment, as we have previously shown that the addition of ascorbate to TGF- $\beta$  treatment can amplify FAP expression<sup>60</sup>. When WT fibroblasts are treated with TGF- $\beta$ , they undergo a dramatic change in phenotype: the cells form large, globular clumps with cytoplasmic processes extending radially from them. Viability dye analysis reveals that these clumps of cells consist of a largely necrotic center surrounded by a surface of viable cells (data not shown). Notably, these TGF- $\beta$ -induced phenotypic changes occurred to a much lesser extent in *Cn*<sup>-/-</sup> fibroblasts (**Figure 3.1**). There was no difference in phenotype when WT fibroblasts were treated with AdCre, suggesting that this effect is not due to off-target effects of either adenovirus or Cre. Treating with TGF- $\beta$  alone in the absence of ascorbic acid gave nearly identical results; thus, we performed the rest of our assays using TGF- $\beta$  treatment alone in order to specifically isolate the role of CN in TGF- $\beta$ -induced activation.



### *Calcineurin deletion alters TGF- $\beta$ -stimulated changes in cytokine secretome*

One crucial function of activated fibroblasts is their ability to secrete a variety of cytokines, chemokines, and growth factors that act in both autocrine and paracrine manners. It has previously been established that TGF- $\beta$  treatment leads to alterations in the cytokine secretome in WT fibroblasts. Thus, we sought to determine which, if any, of these TGF- $\beta$ -mediated changes in cytokine secretion might require CN signaling. Conditioned media collected from WT and  $Cn^{-/-}$  fibroblasts cultured on soft type I collagen gels was analyzed for the expression of 40 cytokines using an antibody array (**Figure 3.2A**). We elected to focus on those specific cytokines whose secretion was differentially regulated (either increased or decreased) in WT fibroblasts upon TGF- $\beta$  treatment: IL-6, IL-7, MIP-1a, MIP-1b, and M-CSF (**Figure 3.2B**). Of these cytokines, MIP-1a, MIP-1b, and M-CSF

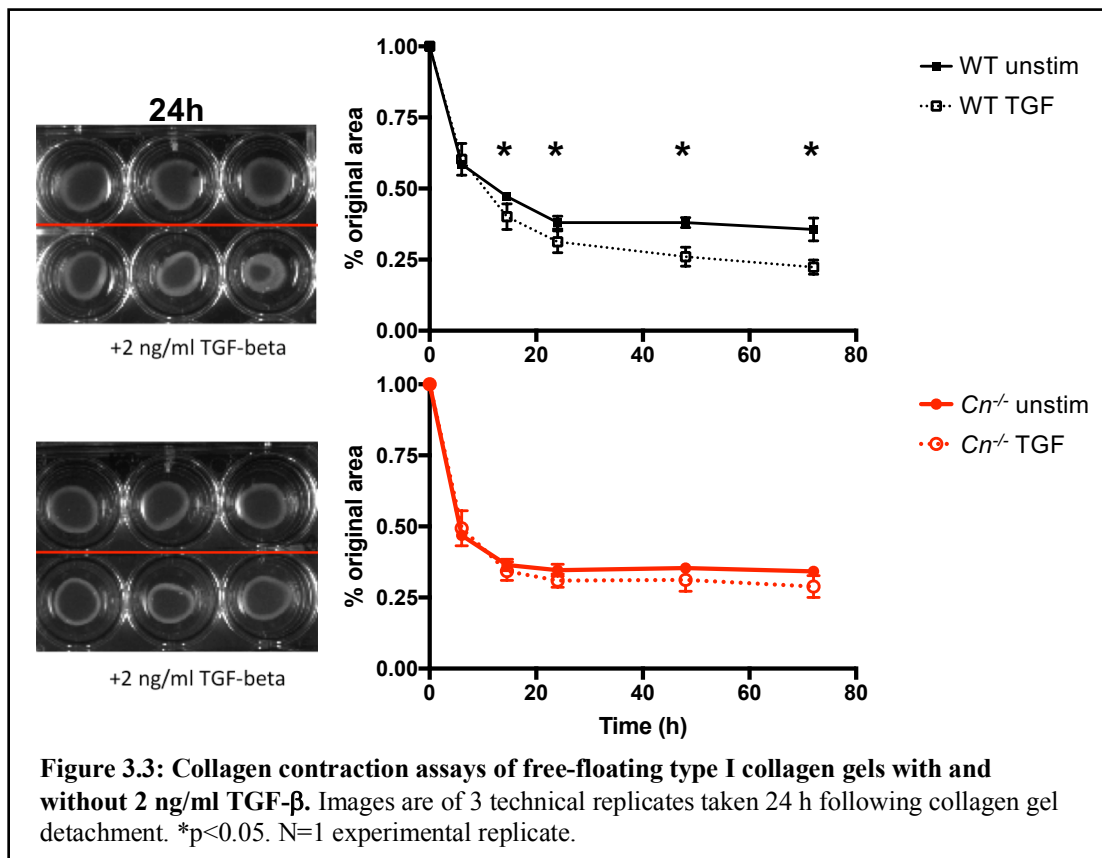
were expressed at higher levels at baseline in *Cn*<sup>-/-</sup> fibroblasts. TGF-β treatment either increased or decreased levels of IL-6, MIP-1a, and MIP-1b in *Cn*<sup>-/-</sup> fibroblasts in a similar manner to WT. However, IL-7 and M-CSF levels were unaffected in *Cn*<sup>-/-</sup> fibroblasts upon TGF-β treatment, whereas they decreased in WT TGF-treated fibroblasts. Additionally, while TGF-β treatment did not alter TIMP-1 expression in WT fibroblasts, levels of TIMP-1 decreased significantly in *Cn*<sup>-/-</sup> fibroblasts upon TGF-β stimulation. Taken together, this



suggests that TGF-β-mediated regulation of IL-7 and M-CSF secretion are dependent on calcineurin signaling, and that CN may regulate TIMP-1 levels in the presence of TGF-β.

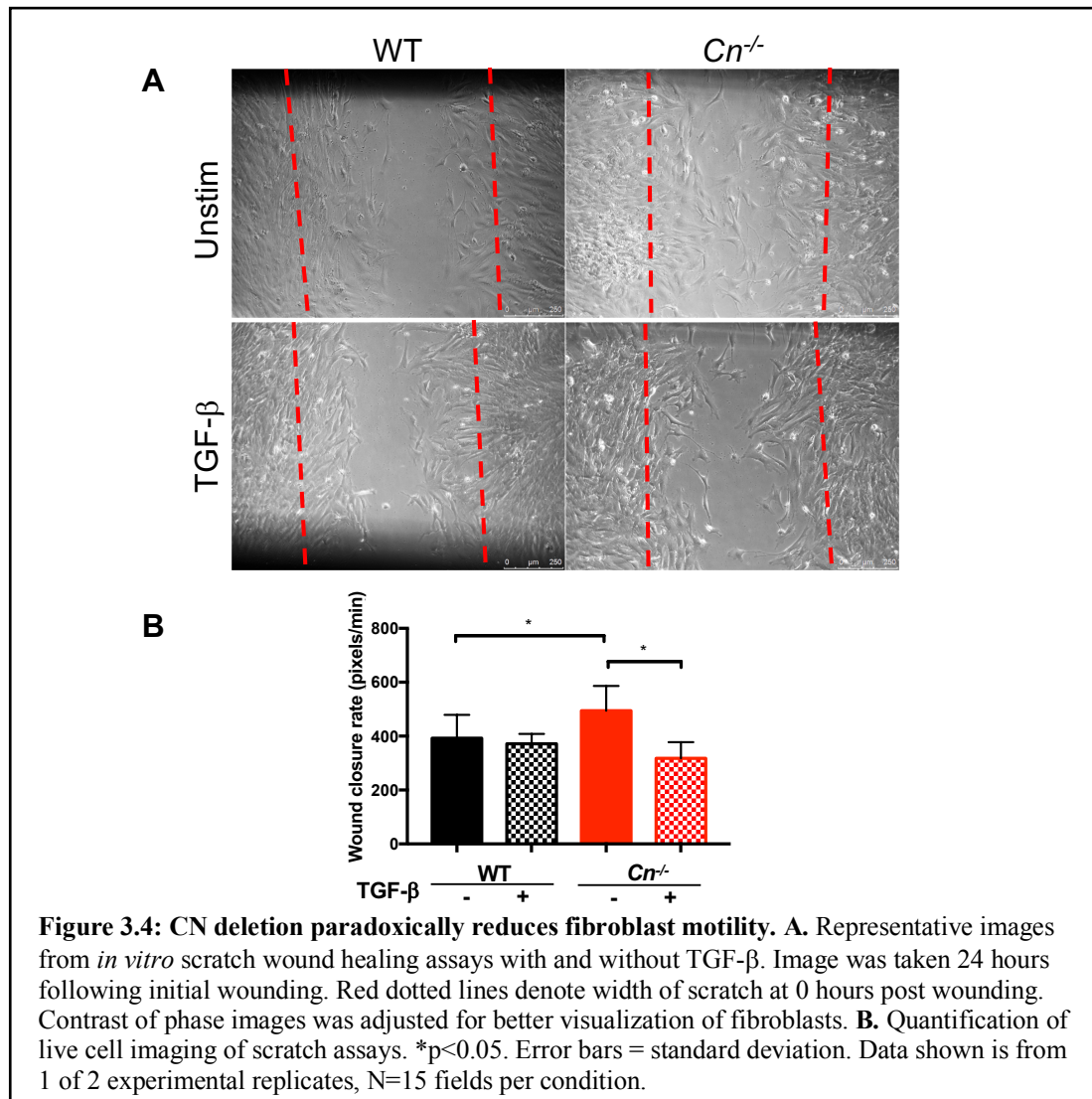
*TGF- $\beta$  stimulation does not affect collagen contraction by calcineurin-null fibroblasts*

We showed that calcineurin-null fibroblasts exhibit greater collagen remodeling and contraction when embedded in free-floating collagen gels; in these assays, we also treated free-floating collagen gels with TGF- $\beta$ . As expected, when WT fibroblasts are treated with TGF- $\beta$ , they increase their contractility and remodeling compared to unstimulated conditions; this difference persists for at least 72 hours following detachment of collagen gels (**Figure 3.3**, upper panel). However, TGF- $\beta$  treatment does not affect contractility in *Cn*<sup>-/-</sup> fibroblasts, suggesting that calcineurin is required for TGF- $\beta$ -mediated changes in collagen remodeling and contractility in fibroblasts (**Figure 3.3**, lower panel).



*Calcineurin-null fibroblast migration is paradoxically inhibited by TGF- $\beta$  in in vitro wound healing assays*

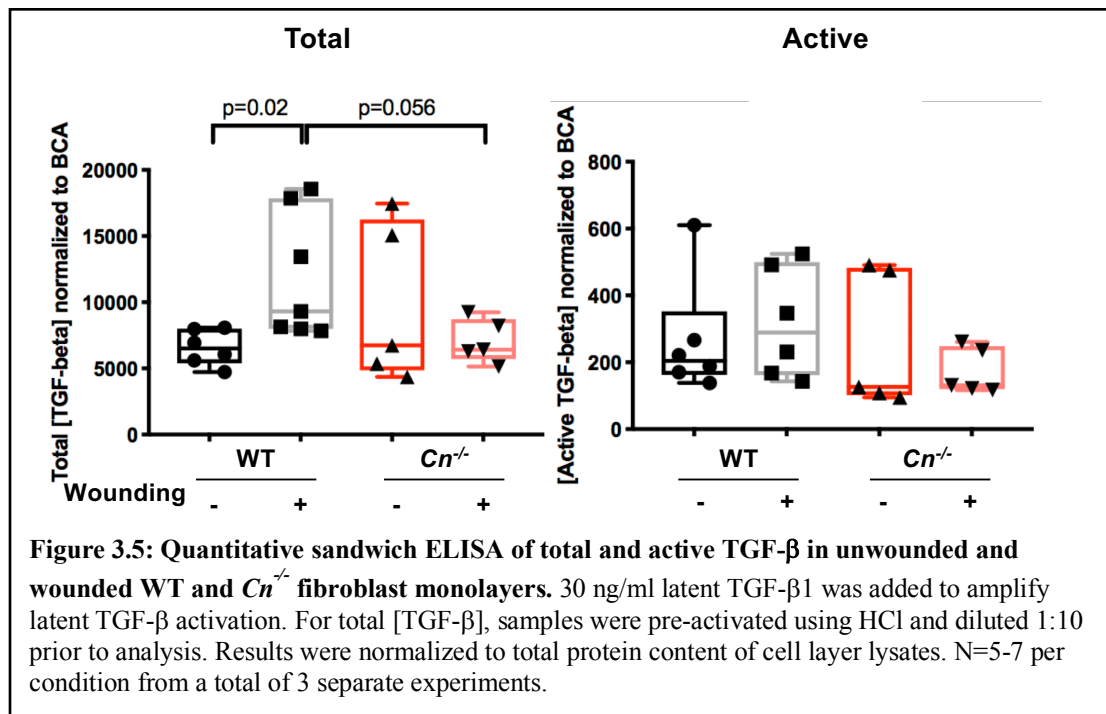
We previously demonstrated that *Cn*<sup>-/-</sup> fibroblasts exhibit greater wound closure in *in vitro* scratch wound healing assays compared to WT. We have previously shown that TGF- $\beta$  activation is crucial in inducing fibroblast migration in scratch assays<sup>156</sup>, so we also assessed wound closure of WT vs *Cn*<sup>-/-</sup> fibroblasts in the presence and absence of TGF- $\beta$ . Phase contrast imaging revealed that TGF- $\beta$  treatment caused WT fibroblasts to extend more cytoplasmic processes and orient themselves parallel to the scratch wound (**Figure 3.4A**). However, TGF- $\beta$  treatment did not significantly alter fibroblast orientation or morphology in *Cn*<sup>-/-</sup> fibroblasts, and fibroblast migration across the scratch wound appeared to be impaired in the presence of TGF. While TGF- $\beta$  treatment did not significantly affect the rate of wound closure in WT fibroblasts as measured by decrease in wound area over time, live cell imaging showed significant differences in fibroblast motility, with greater fibroblast movement parallel to the wounded area and more individual fibroblasts migrating along the scratch wound. Conversely, there was little difference in morphology or motility of wounded *Cn*<sup>-/-</sup> fibroblast monolayers in the presence of TGF- $\beta$ ; in fact, wound closure rates were slower in *Cn*<sup>-/-</sup> fibroblasts when treated with TGF- $\beta$  (**Figure 3.4B**). These findings demonstrate that unlike in WT fibroblasts, *Cn*<sup>-/-</sup> fibroblast motility may actually be hindered by the addition of TGF- $\beta$  to scratch wound assays.



*Calcineurin-null fibroblasts do not secrete or activate TGF- $\beta$  in response to scratch wounding*

Previous studies from our lab have shown that scratch wounding of WT cell monolayers leads to an increase in both total TGF- $\beta$  secretion as well as latent TGF- $\beta$  activation in a CD44-dependent manner<sup>156</sup>. Thus, we compared the amount of TGF- $\beta$  in unwounded vs. wounded cell layers in WT and Cn<sup>-/-</sup> fibroblasts to determine whether the increased migration observed in Cn<sup>-/-</sup> fibroblasts is mediated by TGF- $\beta$  secretion and/or activation. In order to better assess and amplify any differences in the activation of latent

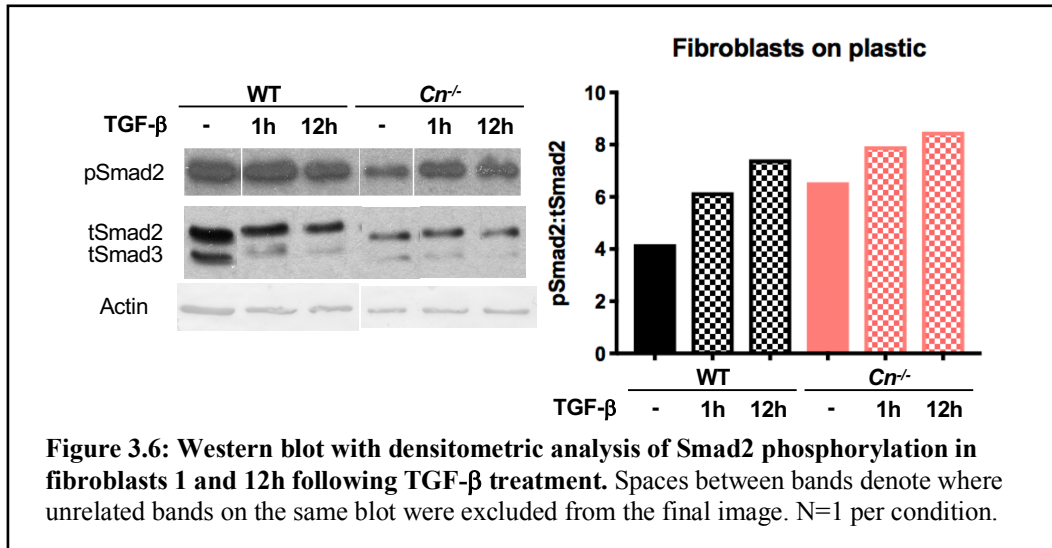
TGF- $\beta$ , we added 30 ng/ml latent TGF- $\beta$ 1 at the time of wounding to all samples. Upon scratch wounding, the concentration of total TGF- $\beta$  in the culture media increased in WT but not  $Cn^{-/-}$  fibroblasts (**Figure 3.5**, left). However, while there was a trend toward increased levels of active TGF- $\beta$  in wounded WT fibroblast layers, there were no such differences when  $Cn^{-/-}$  fibroblast layers were wounded (**Figure 3.5**, right). Therefore,  $Cn^{-/-}$  fibroblasts are unable to increase levels of either total or active TGF- $\beta$  in response to scratch wounding.



### *Smad phosphorylation in response to TGF- $\beta$ is intact in calcineurin-null fibroblasts*

Given the lack of functional response of  $Cn^{-/-}$  fibroblasts to TGF- $\beta$  stimulation, we wished to determine where specifically in the TGF- $\beta$  signaling cascade signal transduction was impaired. Fibroblasts cultured on plastic were treated with 2 ng/ml TGF- $\beta$  for 1 or 12h and analyzed via Western blot for Smad2 phosphorylation. In both WT and  $Cn^{-/-}$

fibroblasts, Smad2 phosphorylation was induced following both 1 and 12 hours of TGF- $\beta$  treatment, suggesting that calcineurin is not required for TGF- $\beta$ -induced Smad2 phosphorylation (**Figure 3.6**).



## Discussion

These data suggest that while calcineurin-null fibroblasts are activated at baseline, they are unable to respond functionally in response to TGF- $\beta$  treatment. We demonstrate that CN is required for several phenotypic and functional changes induced by TGF- $\beta$  in WT fibroblasts. The significance of the cell clumping phenomenon when WT fibroblasts are cultured on collagen gels and treated with TGF is still somewhat unclear; there is significant collagen remodeling as shown by both phase contrast and 2P-SHG imaging, suggesting that this alteration in morphology is directly related to fibrillar collagen re-orientation. The clumping of cells could represent an increase in motility and/or proliferation. Given that proliferation assays have shown that treatment with TGF- $\beta$  impairs fibroblast proliferation, it is more likely that the clumping observed is a result of

alterations in fibroblast motility and aggregation. Regardless of their functional significance, these changes do not occur in *Cn*<sup>-/-</sup> fibroblasts.

Similar to the angiogenesis array performed on WT and *Cn*<sup>-/-</sup> fibroblasts cultured on BME, secretome array analysis of cells cultured on soft type I collagen gels revealed global changes in the cytokine secretome of *Cn*<sup>-/-</sup> fibroblasts at baseline compared to WT. Our findings in WT fibroblasts are consistent with previous literature evidence regarding the effects of TGF- $\beta$  on the fibroblast secretome; TGF- $\beta$  has been shown to upregulate IL-6 in human lung fibroblasts<sup>157</sup>, and there is evidence in macrophages that it can downregulate MIP-1 $\alpha$  expression<sup>158</sup>. Further, the decrease in IL-7 and increase in M-CSF secretion induced in WT fibroblasts by TGF- $\beta$  treatment may be dependent on CN signaling, as these changes were effectively abrogated in *Cn*<sup>-/-</sup> fibroblasts. Just as importantly, calcineurin does not appear to be required for TGF- $\beta$ -mediated stimulation of IL-6, a pro-inflammatory and pro-fibrotic cytokine that has been implicated in the pathogenesis of pulmonary fibrosis<sup>159</sup>.

Finally, we demonstrated that TGF- $\beta$  treatment increased contractility in WT fibroblasts in collagen contraction assays, consistent with data from our and others' prior studies. However, TGF- $\beta$  did not affect contractility and/or remodeling of *Cn*<sup>-/-</sup> fibroblasts on type I collagen. Taken together, these three experiments show that CN deletion in fibroblasts renders them unable to respond to TGF- $\beta$  stimulation when cultured on soft type I collagen.

Further, we show that the increase in wound closure and alterations in cell morphology and orientation in *Cn*<sup>-/-</sup> fibroblasts compared to WT are not due to differences in TGF- $\beta$  signaling. Since we had previously showed that scratch wounding led to

increased secretion and activation of TGF- $\beta$ , and that *Cn*<sup>-/-</sup> fibroblast motility and morphology in scratch assays resembled WT TGF-treated fibroblasts, we hypothesized that *Cn*<sup>-/-</sup> fibroblasts might secrete or activate more TGF- $\beta$  in scratch assays. However, levels of TGF in wounded *Cn*<sup>-/-</sup> fibroblast-conditioned media did not differ from WT, and wounding *Cn*<sup>-/-</sup> fibroblast monolayers did not lead to an increase in secretion or activation of TGF. Of note, in our assays, there was not a significant difference in TGF- $\beta$  activation upon scratch wounding in WT fibroblasts, whereas previous studies have observed an increase in TGF- $\beta$  activation in response to wounding. However, it is likely that ELISA-based assay we utilized was less sensitive to small changes in active TGF- $\beta$  compared to the reporter assay that was previously used.

Finally, we show that *Cn*<sup>-/-</sup> fibroblasts are capable of phosphorylating Smad2 in response to TGF- $\beta$  treatment. This suggests that the block in TGF- $\beta$  signaling in *Cn*<sup>-/-</sup> fibroblasts occurs either downstream or independently of Smad2 phosphorylation. These findings are consistent with previous literature, which has shown that calcineurin activation occurs via non-canonical TGF- $\beta$  signaling. However, our results are complicated by the fact that these fibroblasts were cultured on tissue culture plastic, a substrate thousands of times stiffer than physiologic conditions. Due to this increase in substratum stiffness, the fibroblasts were already in an activated state and thus had a significant baseline amount of TGF- $\beta$  secretion and Smad phosphorylation, possibly masking any further increases in response to TGF- $\beta$  treatment. Future studies should investigate the mechanisms of Smad phosphorylation and other downstream aspects of TGF signaling on softer substrates such as collagen gels or polyacrylamide hydrogels as well as on fibroblast-derived matrices.

There are two main possibilities as to why *Cn*<sup>-/-</sup> fibroblasts may be unable to respond to TGF-β stimulus. First, calcineurin may be required for the signaling mechanisms downstream of TGF-β engagement with its receptor. The introduction to this chapter outlines specific literature evidence that TGF-β directly leads to calcium influx. Another possibility is that activation-related transcriptional programs are already active in *Cn*<sup>-/-</sup> fibroblasts due to dysregulation of fibroblast homeostasis. Thus, further treatment with an activating stimulus such as TGF-β would have no effect since these pathways have already been activated. At the same time, given the heterogeneity of activated fibroblasts, it is unlikely that a single transcriptional program is responsible for the entirety of the activated fibroblast phenotype. It is important to note, though, that these hypotheses are not mutually exclusive, and the lack of response to activating stimulus may be due to both decreased TGF-β-mediated calcium influx and increased transduction of activation-related signaling pathways in *Cn*<sup>-/-</sup> fibroblasts.

These experiments merely represent preliminary investigations into the role of CN signaling in the TGF-β response, and much remains to be investigated. First, it is crucial to determine specifically which parts of the TGF-β signaling pathway in fibroblasts are affected by calcineurin signaling. One way of achieving this is to further define which functional and transcriptional aspects of TGF-β-mediated activation require calcineurin signaling. Further understanding of alterations in NFAT targets upon TGF-β treatment would help determine how specifically calcineurin deletion leads to a functional inability to respond to TGF stimulation.

## CHAPTER 4: THE EFFECTS OF STROMAL CALCINEURIN DELETION IN VARIOUS *IN VIVO* MODELS.

### Introduction

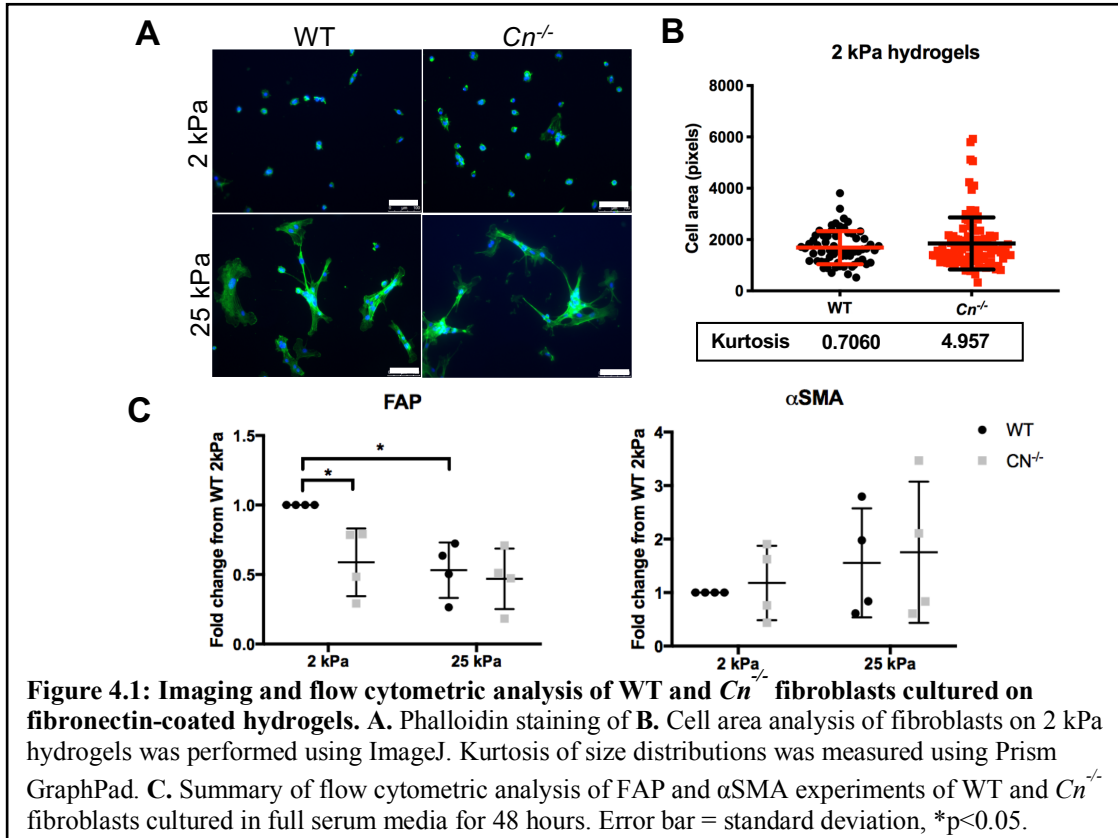
The *in vivo* data presented in **Chapter 2** suggest that the phenotypic changes observed in lung fibroblasts *in vitro* are relevant to *in vivo* models of metastasis, as the pro-tumorigenic changes observed in functional studies correlate with an increase in metastatic outgrowth in mouse models. However, it is also important to more broadly characterize the role of calcineurin signaling in fibroblasts *in vivo*, as fibroblasts play key roles in a large number of physiologic and pathologic processes. While few studies have been performed examining the role of CN in cancer-associated stroma *in vivo*, as discussed in **Chapter 1**, prior data suggest that stromal CN plays a role in a variety of other *in vivo* models, including fibrosis, wound healing, and cardiac remodeling. This chapter describes our efforts to define the effects of stromal CN deletion in several *in vivo* models, encompassing both physiologic and disease processes.

### **Results**

#### *Calcineurin is required for stiffness-dependent regulation of FAP but not $\alpha$ SMA expression*

To assess how fibroblast activation is affected when CN is deleted from fibroblasts *in vivo*, we investigated fibroblast activation and activation marker expression *in vitro* on a substratum that mimicked *in vivo* conditions. We utilized a tunable polyacrylamide hydrogel system in order to replicate the stiffness of soft/less fibrotic (2 kPa) and stiff/more fibrotic (20-25 kPa) lung tissue *in vitro*<sup>160</sup>. When *Cn*<sup>-/-</sup> fibroblasts are grown on 2 kPa

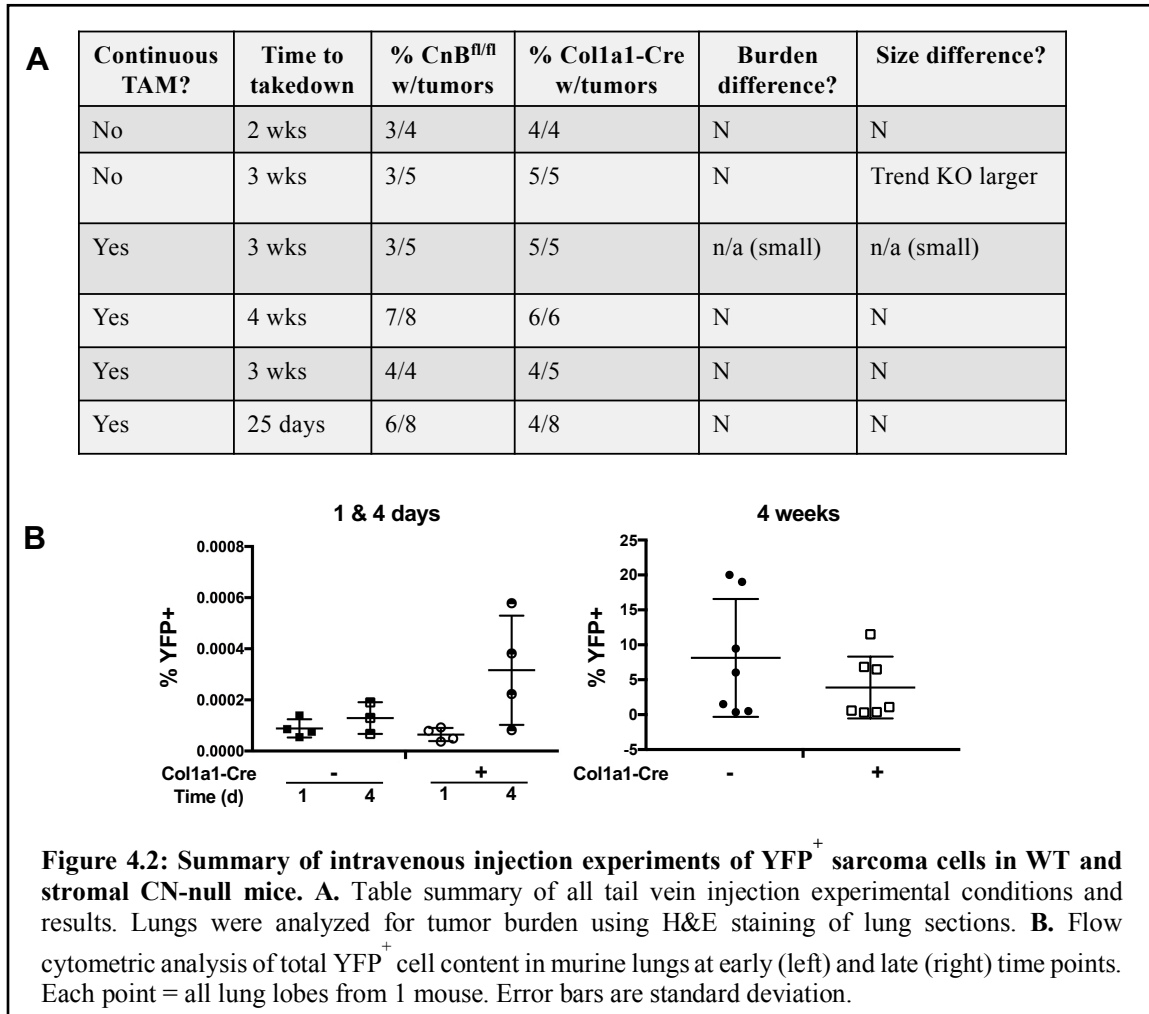
fibronectin-coated hydrogels, they spread to a greater extent (**Figure 4.1A**). While the average cell size was the same in both groups, the distribution of cellular size of  $Cn^{-/-}$  fibroblasts was shifted further to the right and had more weight in the right tail of the distribution (as measured by kurtosis) compared to WT fibroblasts, implying that  $Cn^{-/-}$  fibroblasts had a higher proportion of large, spread cells when cultured on soft hydrogels (**Figure 4.1B**). Unlike on soft substrates, there were no noticeable differences in morphology between WT and  $Cn^{-/-}$  fibroblasts when cultured on 25 kPa hydrogels. We have previously observed that 2 kPa fibronectin-coated hydrogels select for a FAP<sup>hi</sup> population in WT fibroblasts, whereas stiffer substrates shift the fibroblast phenotype to one that is  $\alpha$ SMA<sup>hi</sup> and more myofibroblastic<sup>60</sup>. FAP and  $\alpha$ SMA expression by WT and  $Cn^{-/-}$  fibroblasts on hydrogels was assessed by flow cytometry and revealed that  $Cn^{-/-}$  fibroblasts are unable to upregulate FAP on soft substrates, while  $\alpha$ SMA expression is



comparable to that of WT fibroblasts. These data suggest that CN deletion alters both cytoskeletal morphology and FAP expression of fibroblasts on soft, but not stiff, substrates.

*Loss of CN in fibroblasts does not affect tumor cell colonization of the lung*

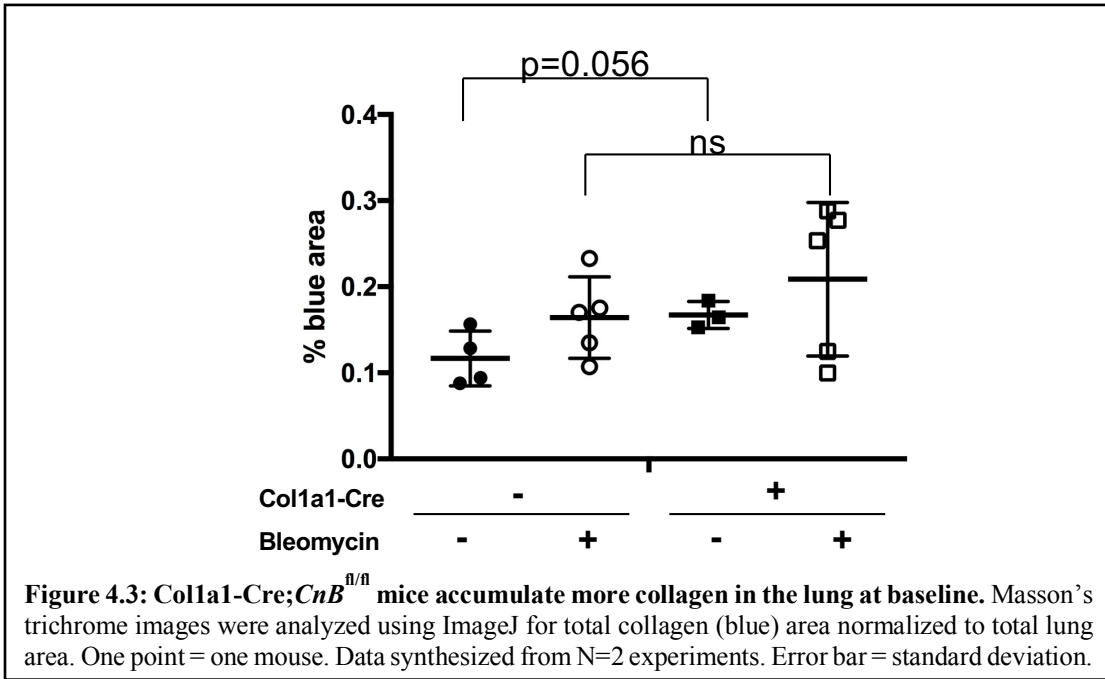
While the injection-resection model of metastasis we utilized is a physiologically relevant model of spontaneous metastasis, it cannot specifically identify which aspect of metastasis is altered by stromal calcineurin deletion, such as extravasation, intravasation, or colonization. We investigated the role of stromal calcineurin deletion in tumor cell migration, lung colonization, and micrometastatic formation using intravenous tumor cell injection. We injected WT and stromal CN-null mice (Col1a1-Cre) intravenously into the lateral tail vein with SKPY42.1 cells, a YFP-expressing clonal cell line isolated from a model of undifferentiated pleomorphic sarcoma featuring oncogenic Kras and p53 deletion<sup>161</sup>. We observed no significant difference in lung colonization between the WT and Col1a1-Cre mice as measured by H&E staining at multiple time points (**Figure 4.2A**). Flow cytometry of murine lungs for YFP<sup>+</sup> tumor cells revealed an increase in cell number at 4 days in Col1a1-Cre mice following tumor cell injection; however, this difference was highly variable and not statistically significant (**Figure 4.2B**). Quantification of YFP<sup>+</sup> tumor cells in the lung at later timepoints by flow cytometry also did not reveal any differences between WT and stromal CN-null mice. Taken together, these data show that colonization of the lung by sarcoma cells is not affected by stromal CN deletion.



*Stromal calcineurin deletion alters collagen content in the lung at baseline*

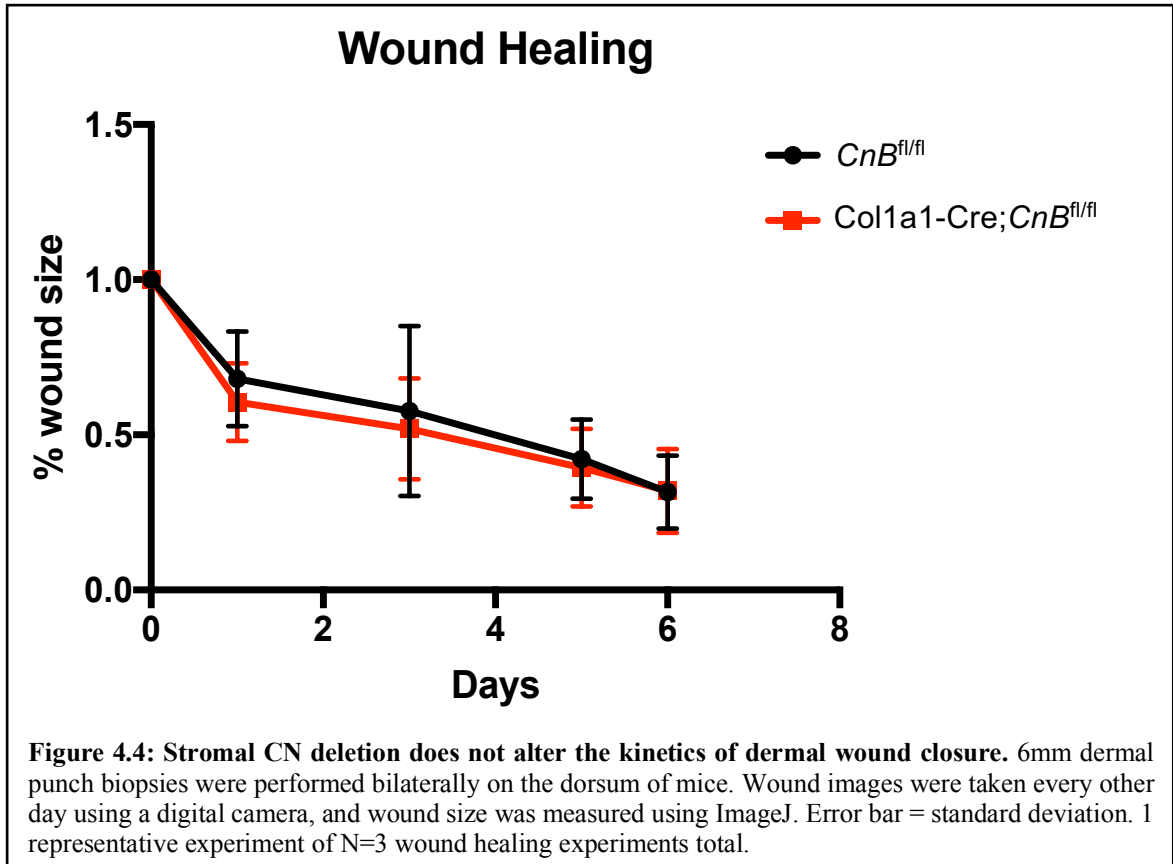
Prior studies suggest that CN signaling may modulate fibrosis, and chronic calcineurin inhibition is associated with fibrotic disease. Therefore, we examined the role of stromal CN deletion in a bleomycin-induced model of lung fibrosis using Masson's trichrome staining of lung sections and quantification of total collagen (blue) signal. Col1a1-Cre mice in the absence of bleomycin demonstrated a trend toward higher amounts of collagen in the lung compared to WT; however, there was no difference in collagen content between WT and Col1a1-Cre mice treated with bleomycin (**Figure 4.3**). This

suggests that stromal CN deletion may lead to baseline differences in collagen content in the lung but does not affect the fibrotic response to bleomycin in this model.



*Stromal calcineurin deletion does not alter kinetics of dermal wound closure*

Previous literature has identified a potential role for calcineurin signaling in dermal wound healing<sup>66</sup>; therefore, we elected to study the kinetics of wound healing in mice with stromal CN deletion using bilateral punch biopsies on the dorsal skin. We observed no difference in wound closure kinetics between *CnB<sup>fl/fl</sup>* and *Col1a1-Cre;CnB<sup>fl/fl</sup>* mice (**Figure 4.4**), suggesting that stromal CN is not required for timely wound closure.



## Discussion

We demonstrated that stromal CN deletion using the  $Col1a1-Cre-ER(T);CnB^{fl/fl}$  mouse did not affect outcomes in models of lung tumor cell colonization, lung fibrosis, and dermal wound healing. However, study of fibroblast morphology and activation marker expression using a physiologically relevant 3D culture demonstrated that stiffness-dependent modulation of FAP, but not  $\alpha$ SMA, on fibronectin-coated substrata may require calcineurin signaling.

Our data suggest that deletion of calcineurin in lung fibroblasts alters cell morphology when cultured on fibronectin-coated hydrogels tuned to physiologically relevant stiffness. Consistent with our previous studies, we showed that on soft (2 kPa)

fibronectin-coated hydrogels, WT fibroblasts expressed FAP at higher levels compared to when they are cultured on stiff (20-25 kPa) fibronectin-coated hydrogels. In comparison, *Cn*<sup>-/-</sup> fibroblasts did not upregulate their expression of FAP when they are cultured on soft hydrogels. Calcineurin deletion did not affect stiffness-dependent regulation of  $\alpha$ SMA expression. Similarly, *Cn*<sup>-/-</sup> fibroblasts exhibited increased cell spreading compared to WT on soft, but not stiff, hydrogels, suggesting that CN deletion may specifically affect the FAP<sup>+</sup> population of fibroblasts. These results are not consistent with the literature findings mentioned in **Chapter 1**, which suggest that calcineurin is required for the  $\alpha$ SMA<sup>+</sup> myofibroblast phenotype. However, it is likely that the CN-mediated regulation of activation marker expression is substratum-dependent; for example, preliminary data suggests that FAP is upregulated in *Cn*<sup>-/-</sup> fibroblasts compared to WT when they are cultured on type I collagen gels (data not shown). At the same time, analysis of the promoter regions of FAP and  $\alpha$ SMA show that FAP contains multiple consensus binding sequences for NFAT, whereas  $\alpha$ SMA does not (see **Conclusions and Future Directions**). It may be that NFAT directly regulates FAP expression but not  $\alpha$ SMA, but that CN/NFAT modulates the myofibroblast phenotype and  $\alpha$ SMA expression indirectly by affecting transduction through other signaling pathways.

One possibility that might explain these negative results *in vivo* is that calcineurin deletion in lung fibroblasts at the protein level was only partial (~60% deletion) despite observing high levels of Col1a1-Cre expression via qPCR. Residual CN-expressing fibroblasts may have been sufficient to mask subtle differences in disease progression in these models. There are several possibilities as to why CN was not completely deleted from fibroblasts *in vivo*. First, Col1a1-Cre expression may vary significantly in various

subpopulations of lung fibroblasts. Expression of the 2.3kb fragment of the *Colla1* promoter had not previously been assessed in adult lung fibroblasts, and we demonstrated its expression via qPCR. However, while the complete *Colla1* promoter is expressed in all fibroblasts, the 2.3kb fragment may only be expressed in certain fibroblast subpopulations, leading to incomplete deletion of CN in all lung fibroblasts. Second, despite continually administering tamoxifen, stromal precursors that do not yet express Cre via the *Colla1* promoter may still be actively recruited from the bone marrow and escape deletion in this manner. A third possibility is that the process of isolation via selection for adherent fibroblasts artificially selects for those fibroblasts that did not undergo CN deletion due to differences in adhesion and/or proliferation of *Cn<sup>-/-</sup>* fibroblasts.

However, it may be that stromal CN deletion is sufficient to cause phenotypic differences in these lung fibroblasts, but that we did not observe differences in these disease models for other reasons. First, while intravenous tumor cell injections are a commonly utilized experimental model of tumor cell colonization in the lung, this approach is not the most physiologically relevant or accurate model of lung metastasis. Primary tumors are known to secrete circulating factors, including cytokines and exosomes, that prime the lung for metastasis. In the absence of primary tumor conditioning, there may be no significant differences in lung colonization at baseline. Additionally, our intravenous tumor colonization assays utilized sarcoma tumor cells; unlike the Lewis lung carcinoma and PDAC cells used in our injection-resection assays, these tumor cells are of mesenchymal origin. Because of this, their interactions with the microenvironment are likely different compared to epithelial tumor cell lines. Indeed, the majority of studies examining the role of fibroblasts in cancer have been performed in epithelial tumor cell lines, and the role of

activated fibroblasts in mesenchymal tumors is less well defined. Therefore, it may be that SKPY42.1 colonization and outgrowth are unaffected by stromal CN deletion, whereas LLC or PDAC would demonstrate significant differences in one or both of these metrics. Future studies will specifically examine the effects of stromal CN deletion on PDAC colonization and outgrowth.

Next, the bleomycin lung fibrosis assays are complicated by the fact that the lung fibrosis we observed was not statistically significant in WT mice. That having been said, the increase in collagen content in the lungs of untreated *Colla1-Cre* mice is consistent with our *in vitro* findings that *Cn<sup>-/-</sup>* fibroblasts are more activated in the absence of activating stimuli compared to WT. By increasing the bleomycin dosage, number of doses, or by administering the bleomycin intratracheally instead of intraperitoneally, the amount of fibrosis induced would be significantly greater, possibly amplifying any differences in lung fibrosis between WT and stromal CN-null mice. Even if stromal CN deletion is shown to increase lung fibrosis, this difference may instead be due to the increase in collagen content seen at baseline; therefore, a more relevant metric might be to compare the increase in collagen content between untreated and bleomycin-treated conditions. This would specifically assess whether stromal CN leads to more or less robust induction of fibrosis upon exposure to bleomycin.

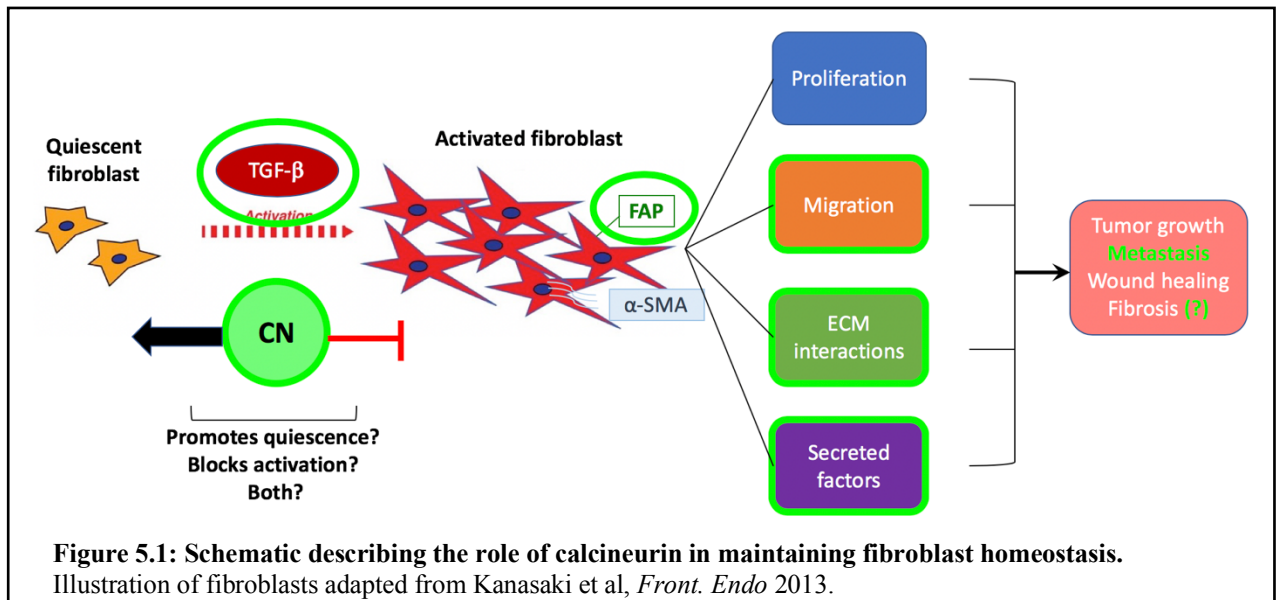
Finally, in the case of dermal wound healing, wound closure kinetics may not be the most relevant measurement by which to analyze the mechanism of wound healing in stromal CN knockout mice. Our lab has previously shown that CD44 deletion in mice does not affect the time it takes for a dermal wound to close; however, the kinetics of fibroblast activation and ECM reorganization in the healing wound are significantly altered<sup>162</sup>. Thus,

future studies should focus on the fibroblast activation and ECM dynamics in the developing dermal wound in order to determine whether or not stromal CN deletion affects these particular readouts.

Taken together, these results highlight the importance of selecting physiologically and experimentally relevant biological assays. While the negative results seen may represent the fact that stromal CN deletion indeed has no effect on lung colonization, bleomycin-induced fibrosis, or dermal wound healing, it is important to further optimize experimental conditions to ensure maximal likelihood that any true differences are detected. Additionally, the functional assays *in vitro* identified a specific role for CN in maintenance of the quiescent, homeostatic state. It may be of greater interest to further assess these mice in non-disease-stimulated settings and profile their tissues at baseline, as stromal CN may lead to greater amounts of activation and fibrosis in the absence of disease compared to WT.

## CONCLUSIONS AND FUTURE DIRECTIONS

Taken together, my work demonstrates that calcineurin plays an important role in fibroblast homeostasis and activation, the response to TGF- $\beta$  stimulation, and tumor growth *in vitro* and *in vivo*. I showed that calcineurin deletion leads to a baseline phenotype consistent with an activated, pro-tumorigenic, CAF-like state in lung fibroblasts, and that this phenotype promotes metastatic outgrowth *in vivo*. Then, I outlined preliminary work that shows that calcineurin is required for fibroblasts to functionally respond to TGF- $\beta$  stimulation. Finally, I further examined the role of stromal CN deletion in a number of *in vivo* assays. This work has identified an important regulator of fibroblast homeostasis that may also mediate their ability to respond to activating stimuli such as TGF- $\beta$ . Future studies should seek to further define the disruption of homeostasis by CN deletion, delve into the specific transcriptional mechanisms behind the functional phenotype of CN-null fibroblasts, and investigate other aspects of the effects of stromal CN deletion *in vivo*.



## **Calcineurin regulates functional fibroblast homeostasis**

Collectively, my data demonstrate that calcineurin deletion from fibroblasts leads to a phenotype that is overall consistent with greater activation “at baseline.” First, it is important to recognize that the “baseline” at which fibroblasts are studied is still far from the quiescent conditions that would be observed *in vivo*. Tissue culture plastic has an elastic modulus in the gigapascal range, several orders of magnitude stiffer than the majority of tissues in the body; therefore, when fibroblasts are cultured on traditional tissue culture dishes, they are activated by this significant increase in mechanical stiffness. While my experiments were often performed on soft (<1kPa) type I collagen gels or tuned polyacrylamide hydrogels, all primary fibroblasts were still isolated by selecting for adherent cells on tissue culture plastic, and they were cultured on either uncoated or gelatin-coated tissue culture dishes prior to use in experiments. We and others have shown significant plasticity of the fibroblast phenotype, with fibroblasts able to downregulate  $\alpha$ SMA expression when they are moved from a stiff to a soft substratum<sup>60,85</sup>. While passaging cells onto a softer substrate may partially “deactivate” these primary fibroblasts, there is evidence that activation of fibroblasts can induce long-term epigenetic modifications<sup>57</sup>, and the effects of even transient culture on substrata of supraphysiologic mechanical stiffness cannot be discounted.

My data identify a role for CN signaling in several functional readouts of fibroblast activation, especially those related to the deposition and remodeling of extracellular matrix. The functional changes upon deletion of CN in fibroblasts lead to an activated, pro-tumorigenic, more CAF-like phenotype. Deletion of CN leads to the formation of fibroblast-derived matrices that have a greater amount of, more linearized, and parallel-

oriented collagen fibers; the architecture of *Cn*<sup>-/-</sup> FDMs is consistent with a TACS-2 to TACS-3 collagen signal, whereas WT FDMs more closely resemble TACS-1. The differences between WT and *Cn*<sup>-/-</sup> FDMs parallel the changes in collagen architecture during tumor progression. When PDAC tumor cells are cultured on *Cn*<sup>-/-</sup> FDMs, they become more migratory and adopt a more elongated morphology, two behaviors that are often consistent with greater tumor cell invasion. Whether the changes in morphology and motility observed in PDAC cells are associated with greater epithelial-mesenchymal transition (EMT) on *Cn*<sup>-/-</sup> FDMs compared to WT FDMs is an interesting question that should be addressed in the future.

Another important, still unanswered question is whether the phenotype of CN-null fibroblasts we have observed relies on NFAT signaling, and if so, which activation-associated genes are regulated by NFAT. While there is not yet evidence of calcineurin-mediated regulation of the expression of many activation-associated genes, we have shown that many of these genes contain at least one NFAT binding site, suggesting that NFAT is at least capable of either activating or repressing their transcription. Using ConTra V3, an online resource that allows for the identification and visualization of primer binding sites in genes from a variety of organisms<sup>163</sup>, we identified a number of activation-associated murine genes that contained at least one NFAT binding consensus sequence, including fibroblast activation protein (FAP) and several collagen genes, suggesting that NFAT signaling may specifically be able to modulate the phenotypes we observed (data not shown). It is important to note that because NFAT requires a transcriptional co-factor for optimal DNA binding, a gene does not necessarily need to contain an NFAT consensus sequence in order for it to be regulated by NFAT. Because NFAT has weak DNA-binding

capabilities that often require co-activation by another transcription factor, the presence of an NFAT binding site in a gene's promoter is not sufficient evidence that it is regulated by NFAT *in vivo*.

More recently, the general philosophy surrounding activated fibroblasts has shifted to define a cell state of “activation” rather than the cell type of “activated fibroblast<sup>57</sup>.” Similarly, quiescence is now thought of as a state requiring active maintenance as opposed to a default cellular state. My data suggest that calcineurin is required to maintain the quiescent state, restrain the activated state, or, possibly, both. One complication with many of the studies that claim to “deprogram” activated fibroblasts into a quiescent state is that they often introduce genetic alterations or drug treatment prior to exposure to the activating stimulus, thus instead showing that these perturbations block activation. Thus, it will be critical to assess the role of calcineurin both in maintaining homeostasis in quiescent fibroblasts as well as potentially deprogramming or “deactivating” activated fibroblasts.

While my work is the first to identify a role for CN specifically in fibroblast homeostasis, CN deletion or inhibition has been shown to disrupt homeostasis in many other cell types and disease models. One of the main methods through which calcineurin inhibitors prevent transplant rejection is by promoting the recruitment and activity of myeloid-derived suppressor cells (MDSCs); further, evidence suggests that CN/NFAT may control homeostasis of many innate immune cell populations<sup>137,138</sup>. Additionally, inhibition of calcineurin has been shown to induce tumor-promoting effects in keratinocytes, which may partially account for the increase in cutaneous squamous cell carcinomas seen in patients treated long-term with calcineurin inhibitors<sup>139</sup>. In neurons, calcineurin modulates retinoic acid synthesis, and prolonged calcineurin inhibition leads to an increase in

excitatory neuron activity and a loss of homeostatic synaptic plasticity<sup>140</sup>. Therefore, there is a precedent for CN playing a role in homeostasis.

Further, despite their activation at baseline, my data show that *Cn*<sup>-/-</sup> fibroblasts are unable to respond to specific activating stimuli. Unlike WT fibroblasts, they do not significantly remodel their secreted matrix when treated with tumor cell-conditioned media compared to control media. Tumor-conditioned media consists of a large number of different growth factors, cytokines, chemokines, and exosomes secreted by tumor cells, and it is unclear which of these factors are responsible for the remodeling of FDMs observed in WT fibroblasts, or which of these factors requires CN for their secretion. Given that my data identified an impaired functional response to TGF- $\beta$  in *Cn*<sup>-/-</sup> fibroblasts, and because many tumors secrete TGF- $\beta$ , it may be that the inability of *Cn*<sup>-/-</sup> fibroblasts to respond to tumor-conditioned media is at least partially mediated by TGF- $\beta$ . In order to test this hypothesis, fibroblast-derived matrices could be generated in the presence and absence of TGF- $\beta$  to determine whether TGF- $\beta$  treatment alone is sufficient to induce these changes in FDM architecture in WT fibroblasts. TGF- $\beta$  neutralizing antibodies could also be added to tumor-conditioned media to determine whether TGF- $\beta$  signaling is required for tumor cell-induced changes in WT FDMs.

### **Future directions to further characterize the role of CN in fibroblast homeostasis**

In order to complement the current genetic deletion studies, pharmacologic inhibition of CN should be performed to determine whether inhibition of phosphatase activity of CN is sufficient to recapitulate the phenotype observed in CN-null fibroblasts. Additionally, specifically inhibiting NFAT would help to determine whether the activation

of fibroblasts upon deletion of CN is dependent on NFAT-mediated transcription. Initial studies comparing CsA and FK506/tacrolimus treatment in WT fibroblast-derived matrices demonstrated that CsA treatment of WT fibroblasts leads to thinner matrices than vehicle treatment; conversely, FK506 treatment leads to an increase in matrix content and alignment very similar to that seen in *Cn*<sup>-/-</sup> fibroblasts (data not shown). Consistent with previous literature showing that CsA has anti-fibrotic effects independent of calcineurin inhibition<sup>117</sup>, this suggests that the differences in *Cn*<sup>-/-</sup> FDMs observed are in fact due to a reduction in calcineurin activity as opposed to Cre or adenoviral treatment. However, preliminary data suggests that FK506 increases fibroblast proliferation, which we did not observe in CN-null fibroblasts. As with any drug, FK506 likely has off-target effects independent of calcineurin inhibition that may also be affecting these assays. Future experiments would assess the effects of FK506 or the NFAT inhibitor VIVIT on functional assays in order to determine whether the CN-null phenotype requires calcineurin phosphatase activity and/or NFAT-mediated transcription.

One of the most important next steps in the study of calcineurin and fibroblast homeostasis is to determine the exact transcriptional changes that mediate the functional differences we have observed upon deletion of CN. First, the NFAT isoforms primarily responsible for fibroblast activation must be identified. Initial immunofluorescence for NFAT isoforms has been performed but requires optimization. In this experiment, fibroblasts treated with various activating stimuli would be probed for nuclear localization of all four NFAT isoforms in order to determine which translocate to the nucleus upon activation. Once the predominant NFAT isoforms have been identified, loss- and gain-of-function experiments using deletion or overexpression of specific isoforms could be

performed to determine whether this phenocopies the results seen in *Cn<sup>-/-</sup>* fibroblasts. Additionally, ChIP for activation-associated genes would determine whether NFAT occupancy of these genes is altered upon fibroblast activation; ChIP-seq analysis would identify global changes in NFAT occupancy in the presence of an activating stimulus such as TGF- $\beta$  or an increase in substratum stiffness.

While my work has identified how CN deletion affects several functions of activated fibroblasts, it is still unclear how CN regulates their transdifferentiation into specific subtypes of activated fibroblasts. One aspect of fibroblast activation that is incompletely studied in my work is the heterogeneous nature of activated fibroblasts, and indeed, fibroblasts in general. Beyond FAP and  $\alpha$ SMA, a large number of other activated fibroblast markers define a large number of subsets of activated fibroblasts. While these markers often overlap, completely profiling the activation markers expressed by *Cn<sup>-/-</sup>* fibroblasts at baseline and in the presence of activating stimuli such as TGF- $\beta$  or mechanical stiffness would help to define how exactly calcineurin modulates fibroblast activation, and in which populations. Better knowledge of how CN informs fibroblast heterogeneity will identify which specific subsets of activated fibroblasts are targeted by calcineurin inhibitor therapy, thus better defining the specific effects on the stroma as well as the tumor microenvironment in general.

Future experiments should also characterize the role of CN in fibroblast-mediated remodeling of the ECM and subsequent cytoskeletal reorganization of fibroblasts cultured on WT vs *Cn<sup>-/-</sup>* FDMs. The effects of CN deletion on expression and activity of MMPs as well as lysyl oxidase (LOX) and other collagen cross-linking enzymes should be investigated, as these remodeling enzymes are known to contribute to the linearization of

collagen fibers during matrix remodeling. While my studies have focused on the role of CN in fibroblast-mediated collagen deposition and remodeling, the effects of CN deletion on other ECM proteins should be studied as well. As mentioned in **Chapter 1**, the ECM consists of significant amounts of fibronectin and hyaluronic acid, among other proteins, whose secretion and structure can be altered by activated fibroblasts. Expression analysis of a wide variety of ECM proteins and matrix remodeling enzymes at both the mRNA and protein levels would determine whether the increase in fibrillar collagen signal induced by *Cn*<sup>-/-</sup> fibroblasts in type I collagen gels and FDMs is due to increased ECM expression, increased matrix remodeling, or both.

The immediate next steps to identify the specific role that calcineurin plays in TGF- $\beta$ -mediated activation are, as previously discussed in **Chapter 3**, to examine the canonical and noncanonical TGF- $\beta$  signaling pathways downstream of receptor binding and Smad phosphorylation to better examine where the specific block in signaling is located. Further studies with a large variety of activating stimuli should be performed to specifically identify the role of CN in each of these settings. This will determine whether CN signaling is required for the response to specific stimuli or more generally restrains fibroblast activation in response to all activating stimuli.

While we have shown that deletion of calcineurin leads to a phenotype consistent with fibroblast activation, it is also important to determine whether the converse is true, i.e. if increased activation of the calcineurin/NFAT pathway induces a quiescent fibroblast phenotype. This will identify whether calcineurin maintains homeostasis, suppresses activation, or both. This can be accomplished either by expressing a constitutively active mutant of CN or NFAT, or by deleting an endogenous calcineurin inhibitor such as Dscr1.

However, our work using the *Dscr1*-null mouse demonstrates that the response to calcineurin signaling often follows a bell-shaped curve; either too little or too much calcineurin signaling can have similar effects<sup>105</sup>. It may be that excessive activation of calcineurin signaling also has an activating effect in lung fibroblasts, as was observed by Davis et al<sup>164</sup>.

### **Stromal CN deletion restrains metastatic outgrowth**

The studies examining stromal CN deletion in mice I have performed show that stromal CN in the lung serves to restrain lung metastasis growth; deletion of CN from lung fibroblasts encourages outgrowth of lung metastases, leading to larger tumor sizes. This could be through a variety of mechanisms. First, Finally, the alterations in secretion and remodeling of extracellular matrix could create a pro-tumorigenic collagen signature in both the lung and the metastases; as the FDMs represented a shift from TACS 1-2 to TACS 2-3 upon calcineurin deletion, the effects on matrix *in vivo* could similarly remove collagen-induced restraints on tumor growth. However, picrosirius red staining reveals that fibrillar collagen content in PDAC lung metastases is minimal, and there is not a noticeable capsule around these tumors. Therefore, the effects of stromal CN deletion could also include other components of the ECM that also affect tumor outgrowth, such as fibronectin.

In addition, my work broadens the understanding of the expression pattern 2.3kb fragment of the *Coll1a1* promoter. Previous work had suggested that this fragment of the promoter was specific only to osteoblasts and osteoclasts and expressed at lower levels in dermal fibroblasts. However, the previous studies only examined expression in lung fibroblasts of embryonic mice whose mothers had been given tamoxifen, and expression

in adult lung fibroblasts had not yet been assessed. I have shown that the 2.3kb-Coll1a1-Cre-ER(T) is expressed in lung fibroblasts by qPCR and by demonstrating CN deletion in isolated lung fibroblasts. This underlines the importance of examining tissue-specific promoter expression in adult as well as embryonic mice.

As was discussed previously, one of the difficulties inherent in studying the effects of tissue-specific gene deletion *in vivo* is that the correct disease model, time points, and variables must be chosen in order for the results to be physiologically relevant, or in our case, even detected in the first place. It is important to consider that *in vivo* models featuring activated fibroblasts may not in fact be the best method of studying stromal CN deletion. Given that our major *in vitro* phenotypes exist in the absence of activating stimuli, it may be that stromal CN deletion has long-term effects on normal tissues due to the constant activation of fibroblasts.

### **Future directions to characterize the effects of stromal CN deletion *in vivo***

There remains a significant amount of phenotypic profiling of the stromal CN-null mouse that needs to be performed. First, given that calcineurin deletion *in vitro* led to significant phenotypic differences in baseline states as opposed to activated states, the lungs and skin of these mice should be analyzed for baseline collagen content and architecture, as well as fibroblast activation marker expression. In addition, aging-related organ fibrosis (e.g. renal, dermal, pulmonary, and cardiac fibrosis) should be compared between WT and stromal CN-null mice; while aging is a process that involves inflammation and fibroblast activation, increased amounts of baseline stromal activation may shift the kinetics and/or increase the severity of aging-related fibrosis. By lowering

the “activation threshold” of fibroblasts, aging-related changes such as fibrosis and senescence may be more dramatic in the setting of stromal CN deletion.

As previously discussed, future experiments should also continue and expand on the investigation of the role of stromal CN deletion in various disease models. Bleomycin lung fibrosis and dermal wound healing assays could be modified in a way that maximizes the differences between WT and stromal CN-null mice. There are also many aspects of both primary tumors and lung metastases that could be investigated, such as the effects of CN deletion on immune surveillance, tumor angiogenesis, and collagen architecture/remodeling over the course of tumor growth and progression. The tumors that were resected in our models of metastasis were sufficiently large to have already surpassed the angiogenic and stromagenic switches, and analyzing large tumors may not detect differences in a model in which activation and homeostasis are affected in baseline conditions. This may explain why preliminary studies examining the vasculature in these resected tumors did not demonstrate large differences in vessel density. Our data suggest that stromal deletion of CN may alter very early stages of micrometastatic outgrowth in a lung colonization model of tumor growth. Thus, analysis of primary tumors and metastases should be performed at multiple time points starting at very early stages to determine the effects of stromal CN deletion on the kinetics of stromal activation in tumorigenesis and metastasis. It may be that lowering the activation threshold by deleting calcineurin leads to earlier triggering of the angiogenic and/or stromagenic switch.

Finally, to complement the current model, deletion of CN from the stroma could be performed using a variety of other methods. First, I have obtained a mouse expressing Cre-ER(T) driven by the *Col1a2* promoter, a promoter that is known for being more

broadly expressed across all fibroblasts and connective tissue in the body, and am in the process of crossing this mouse to *CnB<sup>fl/fl</sup>* mice in order to potentially achieve higher proportions of CN deletion in lung fibroblasts, as well as to compare the effects of CN deletion in fibroblasts expressing the *Coll1a1* vs *Coll1a2* promoter. Additionally, use of other fibroblast or activated fibroblast promoters in the deletion of CN would complement the *in vitro* phenotypic profiling experiments mentioned above; by deleting calcineurin specifically from  $\alpha$ SMA, FAP, or PDGFR-expressing fibroblasts, for example, we would be able to better understand the ways in which CN expression is required for the homeostasis or activation of those specific fibroblast sub-populations.

### **Clinical implications**

This work identifies another possible mechanism through which chronic calcineurin inhibition may lead to increased malignancy in transplant patients. Previously, the pathophysiology of calcineurin inhibitor-induced malignancy had been mainly suggested to be via its immune suppressive properties<sup>101</sup>. However, our data suggest that another mechanism through which these drugs may lead to an increase in tumor formation is through their effects on the stroma. Some of the pro-tumorigenic effects of calcineurin inhibition on the stroma may in fact have effects on the immune system through decreased immune surveillance of tumors or increase in overall inflammation. However, we showed that calcineurin deletion leads to pro-tumorigenic changes in collagen deposition, remodeling, and contractility, thus it is very likely that chronic calcineurin inhibitor treatment also leads to the formation of pro-tumorigenic ECM in tissues, thus facilitating the formation of malignancies. By understanding the mechanism through which chronic

calcineurin inhibition might create a tumor-permissive stroma, we can potentially develop drugs that prevent this baseline stromal activation and at least partially mitigate the increase in malignancy and fibrotic disease observed in transplant patients.

It is important to note that our work furthers the biological understanding of CN-mediated fibroblast homeostasis, but there is still a significant amount of work that remains in order for this to translate to specific therapies in the future. Given that calcineurin plays such important and vastly differing roles in different tissues, any modality that broadly targets calcineurin/NFAT will likely have significant on- and off-target effects that will complicate or likely render these therapies ineffective. Because of this, further work needs to be performed in order to determine more specific downstream targets of CN/NFAT signaling as previously described. Given its role as a homeostatic regulator, there are two potential methods of targeting CN/NFAT signaling in a way that abrogates fibroblast activation. First, certain pro-activation genes can be negatively targeted to block stromal activation, a modality that is currently being studied to varying degrees of success as discussed in **Chapter 1**. Second, and more novel, specific homeostatic regulators could be positively targeted to increase their function and maintain fibroblast homeostasis in the face of activating stimuli such as cancer or inflammation. Before clinical therapies can be developed, further work needs to be done to identify the specific molecular mechanisms through which calcineurin maintains the quiescent fibroblast phenotype.

There are several potential clinical-translational applications of this data. Increased understanding of the ways in which CN regulates specific fibroblast activation-associated genes could be used to better target the activation of stromal cells in both the primary tumor and distant metastatic sites. However, just as targeting angiogenesis alone resulted in

limited efficacy, so too will stroma-targeting therapies likely need to be used in adjunctively with other methods of treatment. Ideally, inducing homeostasis or blocking activation through CN-mediated processes would increase the efficacy of other cancer therapies, such as traditional chemotherapy or immunotherapy. That having been said, as early cancer screening and detection continues to improve, we may be able to use these modalities to target the stroma at the distant site in a way that prevents the colonization and/or outgrowth of metastases, so that patients with early-stage cancer may receive these treatments in order to ensure that their disease does not progress.

In conclusion, my work has identified CN as a novel regulator of fibroblast homeostasis. While further studies will be required in order to translate these findings into clinical therapies, these data raise interesting questions regarding the maintenance of the quiescent and activated states in fibroblasts, and they provide potential alternate mechanisms for the increase in tumorigenesis observed in transplant patients receiving long-term calcineurin inhibition therapy.

## MATERIALS AND METHODS

### Primary lung fibroblast isolation and culture

Fibroblasts were cultured in DMEM-F12 + L-glutamine (Gibco) with 10% heat-inactivated FBS, L-glutamine, and penicillin-streptomycin. To isolate primary lung fibroblasts, lungs from male and female 3-5-week-old mice were dissociated in Hank's buffered saline solution (HBSS) containing 5 mg/ml type II collagenase and 0.5 mg/ml deoxyribonuclease I (Worthington, #LS004176 and #LS002139) in the Miltenyi GentleMACS Octo. Dissociated lungs were passed through 100 $\mu$ m and 40 $\mu$ m filters to obtain a single cell suspension before resuspending in culture media and plating; fibroblasts were allowed to adhere for 1-2 hours at 37° C before non-adherent cells were washed off. Fibroblast identity was confirmed by immunostaining cultured cells for vimentin (goat, Santa Cruz #sc-7557, 1:100), CD45.2 (biotinylated mouse, BD Pharmingen #553771, 1:100), and CD31 (rat, BD Pharmingen #553370, 1:100), followed by secondary antibody and streptavidin (Alexa Fluor 647 anti-goat IgG, Alexa Fluor 488 anti-rat IgG, Alexa Fluor 555 streptavidin, all 1:100; Invitrogen #A-21447, A-11006, Thermo Fisher #S-21381 respectively); fibroblasts were >99% vimentin-positive, with <5% CD45<sup>+</sup> contaminants and no CD31<sup>+</sup> cells present.

For soft collagen gel cultures, fibroblasts were plated on thick 1 mg/ml type I collagen gels; type I rat tail collagen (Corning #354236) was diluted in 10X PBS and sterile ddH<sub>2</sub>O at 1 mg/ml and neutralized using 1 N NaOH per manufacturer's instructions. Collagen gels were allowed to solidify for 1-3 hours prior to plating. Fibroblasts were plated onto collagen gels and cultured for 48 hours prior to phase contrast and multiphoton second harmonic generation (2P-SHG) imaging.

### **Acute deletion of calcineurin *in vitro***

To acutely delete calcineurin B (*CnB*) *in vitro*, P1 *CnB*<sup>fl/fl</sup> fibroblasts were treated with 300 MOI AdCMV-Cre (U Iowa Viral Vector Core Facility) overnight in 10% serum media; culture media was washed out and cells were washed with PBS before replacing with fresh culture media and allowing the cells to recover for a day. Fibroblasts were passaged once prior to use in experiments; all fibroblasts were passage 3 at the time of use in experiments. Controls were either WT fibroblasts treated with AdCre, *CnB*<sup>fl/fl</sup> fibroblasts from the same isolation treated with AdGFP, or *CnB*<sup>fl/fl</sup> fibroblasts from the same isolation without viral transduction. *CnB* deletion was confirmed by Western blot for calcineurin A as described below.

### **Proliferation assays**

For proliferation assays, fibroblasts were plated in gelatin-coated 24-well plates and serum-starved overnight. Day 0 counts were measured, then media was exchanged for either 1% or 10% FBS + DMEM-F12 culture media. On each measurement day, 3 wells per condition were trypsinized, and dead cells were stained with trypan blue before counting using a hemocytometer. EdU proliferation assays were performed on gelatin-coated chamber slides using the Click-iT EdU Alexa Fluor 594 Imaging Kit (Invitrogen) according to manufacturer's instructions; fibroblasts were pulsed with 10  $\mu$ M EdU for 16-18 hours prior to fixation and staining.

### ***In vitro* scratch wound healing assays and live-cell imaging**

Scratch assays were performed as described previously<sup>156</sup>. Briefly, cells were plated at 100% confluence in 12 well plates and allowed to adhere overnight. Cell layers were wounded using a P200 pipet tip, washed once with PBS, and replaced with DMEM-F12 1% FBS culture media. 2 experimental replicates were imaged at 0, 2, 6, 12, 24, and 48 hours post-wounding using an inverted microscope, and 2 replicates were imaged every 15 minutes using a Nikon inverted microscope with a stage incubator for live cell imaging. Live cell imaging replicates were stained using the SiR-Hoechst far-red kit (Spirochrome #CY-SC007), and cell tracking was analyzed using Nikon NIS-Elements software. Each experimental condition was performed in triplicate.

### **Transwell migration and invasion assays**

For migration and invasion assays, 6.5mm (24 well) and 12mm (12 well) Transwell inserts with a pore size of 8  $\mu\text{m}$  (Corning) were used respectively.  $5 \times 10^4$  (6.5mm) or  $7.5 \times 10^4$  (12mm) WT or *Cn*<sup>-/-</sup> fibroblasts were plated into each transwell insert containing serum-free DMEM-F12 media in the upper chamber and 10% serum containing media in the lower chamber. For migration assays, inserts were uncoated; for invasion assays, inserts were coated with 75 $\mu\text{l}$  1mg/ml neutralized type I rat tail collagen and allowed to gel for 1 hour prior to cell seeding. For invasion assays, uncoated transwells were used as a positive control; for both migration and invasion assays, serum-free media was placed in the lower chamber as a negative control. 24 hours following plating, the upper chamber was wiped with a cotton swab to remove any un migrated cells and washed with PBS; inserts were fixed and stained in fresh wells containing 0.5% crystal violet in 25% methanol solution for 15 minutes, washed by dipping in deionized water and allowed to dry completely before

imaging. Images were taken by inverting the insert onto a glass slide and tile-scanning using a Zeiss Axio Imager M2 upright microscope with Zen Pro software. The percentage of crystal violet-positive area on each insert was measured using ImageJ. Each assay was performed in triplicate, and experiments were repeated at least three times.

### **2P-SHG imaging and analysis**

Images of fibroblasts cultured on collagen and FDMs were acquired using the Leica SP8 multiphoton upright confocal microscope available through the Penn Vet Imaging Core. Forward SHG signal was collected, and in non-cell-extracted cultures, autofluorescence in an adjacent channel was collected to identify cells and differentiate between SHG and non-SHG signal. 3-5 images per sample were taken for analysis, and Z-stacks were performed to obtain maximum intensity projections through the thickness of the sample. Images were processed using LAS AF software. Where appropriate, collagen fiber analysis was performed using CT-FIRE and CurveAlign software; fiber alignment scores were generated in CurveAlign.

### **Collagen contraction/remodeling assays**

Collagen gel contraction assays were performed as previously described<sup>127</sup>. Briefly,  $5 \times 10^5$  fibroblasts were embedded in 500  $\mu$ l of 1 mg/ml rat tail type I collagen solution (Corning) in a 24 well plate. Collagen gels were allowed to solidify for 1 hour before the gels were detached and 500  $\mu$ l of DMEM-F12 1% FBS culture media was added. Images were taken at 0, 6, 12, 24, 48, and 72 hours post-detachment using a gel documentation

system. Collagen gel areas were measured using ImageJ software; each time point was normalized to the area of an empty well. Assays were performed in triplicate.

### **Measurement of collagenase activity using Type I DQ™ Collagen**

To visualize collagenase activity, fibroblasts were cultured in chamber slides that were either coated with gelatin or a thick type I collagen gel as described previously (200 µl/well). DQ™ type I collagen from bovine skin conjugated to fluorescein (Invitrogen, #D12060) or DQ™ gelatin from pig skin (Invitrogen, #D12054) was overlaid on cultures by adding to fresh culture media at 25 µg/ml. After 24 hours of incubation, cultures were fixed using Prefer glyoxal fixative (Anatech Ltd) or 4% paraformaldehyde (PFA) in PBS (Affymetrix/USB) and mounted/cover slipped using Fluorogel II with DAPI. Images were acquired using a Zeiss Axio Imager M2 upright fluorescent microscope and processed with Zen Pro software.

### **Fibroblast-derived matrix (FDM) generation, extraction, and analysis**

FDMs were generated as per Cukierman et al.<sup>128</sup>. Briefly,  $5 \times 10^5$  (35mm dish),  $2 \times 10^5$  (12 well plate), or  $5 \times 10^4$  (35mm glass bottom dish) fibroblasts were plated onto gelatin-crosslinked dishes to 100% confluency. 75 µg/ml L-ascorbic acid (Sigma-Aldrich #A4544) was added to complete culture media and changed every other day for 8-10 days (35mm dish). Matrices were decellularized using 0.5% Triton X-100 and 20 mM NH<sub>4</sub>OH in PBS and stabilized at 4° C overnight before use. For analysis of earlier time points, FDMs were generated in triplicate in 12 well plates, and matrices were decellularized, extracted and solubilized following 3 and 5 days of ascorbic acid treatment.

To generate tumor cell-conditioned media, SR0144 lung tumor cells (generously provided by Dr. Carla Kim, Harvard University) were grown to 80% confluence, and culture media was replaced with serum-free DMEM for 24 hours. Conditioned media was centrifugated to remove all cells and insoluble material prior to use. Media for unstimulated and tumor-conditioned FDMs had a final serum concentration of 2.5% and consisted of a 1:1 dilution of either tumor-conditioned media or serum-free DMEM with 5% FBS DMEM-F12, with a total concentration of 75 µg/ml L-ascorbic acid as above.

### **Western blotting of cell lysates and FDMs**

Cells were lysed in radioimmunoprecipitation assay buffer (RIPA, 50 mmol/L Tris-HCl pH 8, 150 mmol/L NaCl, 1% Triton-X, 0.5% sodium deoxycholate, and 0.1% SDS), centrifuged at 16,000 x g for 10 minutes, and supernatant was collected. Total protein content was quantified using BCA assay (Pierce). FDMs were solubilized in Protein Extraction Reagent Type 4 (Sigma-Aldrich C0356) and stored at -80 C until use. Protein loading of FDMs was normalized using the Bio-Rad Protein Assay Kit on samples diluted 1:10. Total protein of FDMs was analyzed by running samples in 4x Laemmli sample buffer (Bio-Rad) on a 4-12% gradient gel (Invitrogen) and silver staining using a kit (Pierce). SDS-PAGE of lysates was performed using 3-10 µg per sample at 120-150 V on 8, 10, or 12% gels depending on the size of the protein in question using the Bio-Rad Mini Protean Tetra Cell system. Proteins were transferred onto nitrocellulose or PVDF membranes at 90 V for 2 hours using the Bio-Rad Mini Trans-Blot system. Blots were blocked in 5% non-fat dry milk (LabScientific M-0841) in TBS-T (TBS + 0.1% Tween 20) and incubated with primary antibody diluted in blocking buffer at 4° C overnight

(calcineurin A: 1:2000, Abcam #ab3673; actin: 1:5000, Sigma #A2668). Blots were washed in TBS-T, and secondary antibody (anti-rabbit IgG HRP conjugate, Cell Signaling CST7074, 1:1000-1:5000) was incubated in blocking buffer for 1 h at room temperature then washed with TBS-T. Bands were visualized using enhanced chemiluminescence reagent (100 mM Tris pH 8.6, 0.2 mM p-coumaric acid, 1.25 mM luminol, 2.6 mM).

### **Imaging analysis of cell behavior on FDMs**

$10^4$  WT or *Cn*<sup>-/-</sup> fibroblasts or MH6449 PDAC cells were plated in 35mm wells containing either WT or *Cn*<sup>-/-</sup> FDMs and allowed to adhere for 16 h before fixing with 4% PFA in PBS. Wells were blocked with 5% normal goat serum, 1% BSA, and 0.001% thimerosal in PBS, followed by Fc receptor blocking for 20 minutes (1:200, BD Pharmingen #553141). Primary antibodies were incubated in blocking buffer at 4° C overnight (paxillin: 1:100, BD Biosciences #612405), and secondary antibodies were incubated in 1% BSA in PBS for 1 h at RT. Following secondary antibody incubation (1:1000, Invitrogen #A-11032) cells were incubated with Alexa Fluor 488-conjugated phalloidin (1:40, Cell Signaling Technologies, #8878S) prior to mounting and coverslipping with Fluorogel II with DAPI. Confocal imaging was performed on a Leica TCS SP5 laser scanning confocal microscope and processed using LAS AF software.

For live cell imaging studies, WT and *Cn*<sup>-/-</sup> FDMs were generated and decellularized in 12 well plates.  $5 \times 10^4$  YFP<sup>+</sup> MH6449 PDAC cells or  $1 \times 10^5$  GFP<sup>+</sup> primary lung ECs were plated onto decellularized matrices, and cell movement was tracked for 24 hours following plating using a Nikon inverted microscope with stage incubator for

live cell imaging. Individual cell tracking and velocity/direction analysis was performed using Nikon NIS-Elements software.

### **Endothelial cell co-culture assays and angiogenic secretome analysis**

Primary GFP<sup>+</sup> lung endothelial cells (ECs) were isolated as described previously<sup>165</sup> using CD31 MicroBeads (Miltenyi Biotec #130-097-148) and cultured in Advanced DMEM (Gibco) + 15% FBS, 25 mM HEPES, 0.1 mg/ml heparin, 100 µg/ml bovine endothelial growth supplement (Alfa Aesar #J64516), L-glutamine, and penicillin/streptomycin. On day 0 of the experiment,  $2.5 \times 10^5$  each of fibroblasts and ECs were mixed 1:1 and embedded in growth factor reduced basement membrane extract (BME, Trevigen #3533-001-02) in 35mm glass bottom dishes. After 1 hour, organoid media (DMEM-F12, 10% KnockOut Serum Replacement (Gibco), 1x Insulin-Transferrin-Selenium (Gibco), L-glutamine, penicillin/streptomycin) was added, and 3-5 phase-contrast and fluorescence images per sample were taken at 0, 12, 24, 48, and 72 hours using an inverted tissue culture microscope with GFP filter. Tube formation was quantified by counting the number of tubes per high power field. Conditioned media for angiogenic secretome analysis was generated by culturing fibroblasts on BME in serum-free media for 24 hours prior to collection. Conditioned media was analyzed using the Proteome Profiler Mouse Angiogenesis Array (R&D #ARY015). Conditioned media (750 µl/sample) was hybridized to membranes, and chemiluminescent signal was normalized to total protein content using lysate from fibroblast cultures.

### ***In vivo* model of stromal-specific calcineurin deletion**

The University of Pennsylvania Animal Care and Use Committee approved all studies. Mice with inducible stromal-specific deletion of calcineurin B were obtained by cross-breeding C57Bl/6 *Cnβ1<sup>fl/fl</sup>* mice<sup>126</sup> with C57Bl/6 *Col1a1-Cre-ER(T)* mice (JAX #016241)<sup>133</sup>. Breeding cages were maintained using *Col1a1-Cre;CnB<sup>fl/fl</sup>* crossed to *CnB<sup>fl/fl</sup>* in order to ensure hemizyosity of the Cre transgene. In order to acutely delete *CnB in vivo*, mice were given 1 mg tamoxifen in 100 μl corn or peanut oil (Sigma-Aldrich) intraperitoneally daily for 5 days, followed by 2 days without treatment. During tumor experiments, mice received 1-2 additional doses of tamoxifen per week to account for recruitment of bone marrow-derived stromal cells. Calcineurin deletion was confirmed by Western blot of isolated lung fibroblasts; lungs were dissociated and plated as described above, and after 30-60 minutes, non-adherent cells were removed and the adherent cell layer washed with PBS and collected in lysis buffer.

To confirm *Col1a1-Cre-ER(T)* mRNA expression in lung fibroblasts, a portion of isolated lung fibroblasts were taken in Trizol, RNA extracted using the Dymo Direct-ZOL kit with on-column DNase digestion, and reverse transcription performed using the Applied Biosciences High Capacity cDNA Reverse Transcription Kit. A total of 200ng of cDNAs per qPCR reaction were added to 2x SYBR Green qPCR Master Mix (Bimake), and reactions were run and measured using the ViiA 7 Real-Time PCR System. Primers: GAPDH: forward 5'-AGGTCGGTGTGAACGGATTTG-3' and reverse 5'-TGTAGACCATGTAGTTGAGGTCA-3' and *Col1a1-Cre*: forward 5'-CCAGCCGCAAAGAGTCTACA-3' and reverse 5'-ACAATCAAGGGTCCCCAAAC-3'.

### **Injection-resection model of lung metastasis**

Lewis lung carcinoma (LLC) cells were obtained from ATCC; MH6449 KPY PDAC cells were a generous gift from Dr. Ben Stanger at the University of Pennsylvania. Tumor cells were cultured in DMEM + 4 g/L glucose (Gibco), 10% heat-inactivated FBS (Gemini), L-glutamine (Gibco), and penicillin-streptomycin (Lonza). Tumor cells were passaged to be 70-80% confluent on the day of injection. Mice were 8-12 weeks at the time of tumor injection with the exception of one PDAC injection-resection experiment, in which mice were approximately 52 weeks of age and had been receiving tamoxifen weekly. Tumors were established by injecting  $1 \times 10^6$  (PDAC) or  $5 \times 10^6$  (LLC) tumor cells in 100  $\mu$ l serum free DMEM subcutaneously into the right hind flank under isoflurane anesthesia. Tumors were measured using digital calipers, and volume was estimated using the ellipsoid volume equation  $V = \frac{1}{2} * \text{width}^2 * \text{length}$ . Once tumors reached a volume of 400-600  $\text{mm}^3$ , they were resected under sterile conditions, and surgical sites were closed using nonabsorbable monofilament suture (Covidien). Tumors were flash-frozen in OCT immediately following resection. Mice received 5mg/kg Metacam (Boehringer Ingelheim) for 3 days following resection, and any dehiscenced surgical sites were re-sutured if necessary. 14 days after resection, mice were euthanized and lungs were perfused with saline prior to dissection; lungs were dissected and either formalin-fixed for paraffin embedding or fixed in 4% PFA followed by incubation in 30% sucrose before freezing in OCT. FFPE samples were sectioned at 5  $\mu$ M, and frozen samples were sectioned at 9-10  $\mu$ M. Lung tumors were measured and normalized to total lung area using ImageJ software.

### **Statistical analysis**

Statistical analysis was performed using GraphPad Prism 7. P values were calculated using Student's t-test (two-tailed, unpaired) or ANOVA where appropriate.

### **Materials and Methods: Chapter 3**

#### *TGF- $\beta$ treatment of fibroblasts*

Fibroblasts were treated with 0.5-10 ng/ml of pre-activated human TGF- $\beta$ 1 (R&D Systems). For the majority of activation studies, TGF- $\beta$  was used at 2ng/ml. Because fetal bovine serum itself contains TGF- $\beta$ , unless otherwise specified, studies were conducted in 1% serum containing media to minimize the activating effects of the culture media in unstimulated conditions.

#### *Cytokine secretome array*

Fibroblast-conditioned media was collected from fibroblasts cultured on soft 1mg/ml type I collagen gels by replacing media with serum free culture media +/- 2 ng/ml TGF- $\beta$ 1 and collecting 24 hours later. Media was centrifuged to remove cells and particulate matter, and aliquots were flash-frozen and stored at -80 C until use. Secretome array analysis was performed using 750  $\mu$ l of conditioned media according to kit instructions (R&D Systems).

#### *Analysis of TGF- $\beta$ secretion/activation in scratch assays*

In order to assess total TGF- $\beta$  secretion and latent TGF- $\beta$  activation, confluent fibroblast monolayers were either left unwounded or scratched in a cross-hatch pattern with a sterile plastic comb before being washed with PBS, and media was replaced with serum free culture media containing 30 ng/ml latent TGF- $\beta$ 1 (R&D Systems). Media was collected 24 hours later, centrifuged to remove cells and debris, flash-frozen on dry ice,

and stored at -80 C until use. Cell layers were lysed in RIPA buffer, and lysate protein concentration was determined by BCA for sample normalization. A sandwich ELISA kit for TGF- $\beta$ 1 (Enzo Biosciences) was used to determine both activated and total TGF content in conditioned media. For activated TGF, samples were used undiluted; for total TGF, samples were pre-activated with 1 N HCl according to kit instructions and diluted 1:10 in sample dilution buffer prior to use.

#### *Western blot of Smad2 phosphorylation*

Western blots were performed as previously described. pSmad2: 1:1000, Cell Signaling; tSmad2/3: 1:1000, Cell Signaling. pSmad signal was assessed first, then blots were stripped by washing 3 x 15min in TBS-T before re-blocking in 5% milk and incubating with tSmad2/3 antibody. pSmad signal was visualized using Femto ECL reagent (Thermo Fisher); tSmad signal was visualized using previously described homemade ECL reagent.

## **Materials and Methods: Chapter 4**

### *Polyacrylamide hydrogel assays and flow cytometry*

Polyacrylamide hydrogels were generated according to the protocols created by Dr. Richard Assoian's group.<sup>160</sup> They were either acquired from the University of Pennsylvania ITMAT Core Facility or generated by myself according to their protocol. Hydrogels were coated with fibronectin solution at least overnight prior to use. Prior to plating, hydrogels were transferred with sterile forceps to tissue culture wells coated with 1% agarose to prevent cell adhesion to the well. 40mm hydrogels were plated with  $1.5 \times 10^5$  (20-25 kPa) or  $3.5 \times 10^5$  (2 kPa) fibroblasts depending on their stiffness; cells were cultured

for 48 hours in full serum media prior to use in downstream assays. For phalloidin imaging, 12mm hydrogels were used, and cell numbers scaled down accordingly. Phalloidin staining was performed as described previously.

For flow cytometry experiments, cells were collected via trypsinization and pelleted in a 96 well plate for all staining steps. Fibroblasts plated on plastic were used for single stain compensation controls and isotype antibody controls. All staining steps were performed in FACS buffer (2% FBS in PBS). Following 15 minutes of Fc block (1:200), primary antibody (biotinylated mouse anti-FAP, 1:124; isotype biotinylated mouse IgGK1, 1:100, BD #550615) was incubated for 30 minutes at room temperature, followed by incubation with APC-conjugated streptavidin for 15 minutes (1:200). Live-dead staining was performed using the Fixable Violet Dead Cell Stain Kit (Molecular Probes). Cells were fixed and permeabilized using the Cytotfix/Cytoperm kit (BD Biosciences) prior to staining with FITC-aSMA antibody (1:270, Sigma #F3777; isotype FITC-IgG2a, 1:50). Samples were analyzed on an Attune NxT flow cytometer (Thermo Fisher).

#### *Intravenous tumor cell colonization assays*

SKPY42.1 tumor cells were obtained by isolating tumor cells from the sarcoma of a KPY (Kras<sup>G12D</sup>;p53<sup>fl/fl</sup>;Rosa26-LSL-YFP) mouse that had received AdCre injection in the hindlimb<sup>161</sup>; tumors were dissociated using the gentleMACS Octo with heating element, and cell suspensions were plated in 10% FBS DMEM and allowed to adhere overnight before washing the cell layer. Single cell clones of these tumor cell lines were obtained by serial dilution, and the subclones with the greatest invasive capability in *in vitro* Matrigel-coated Transwell assays were identified. Cells were cultured in 10% FBS

DMEM + 4 g/L glucose + L-glutamine + pen/strep and passaged to 70-80% confluence prior to use in experiments.

*CnB<sup>fl/fl</sup>* and *Coll1a1-Cre;CnB<sup>fl/fl</sup>* mice were treated with tamoxifen as described prior to use in tail vein injection assays. On the day of injection,  $3 \times 10^5$  cells in 100  $\mu$ l serum free DMEM were injected into the lateral tail vein of each mouse using a restrainer. Starting the day after tail vein injection, tamoxifen was continuously administered 2-3 times per week where noted. Mice were euthanized and lungs harvested at the indicated time points. Lung analysis was performed using H&E stained paraffin sections as described previously, and images were analyzed using ImageJ software.

#### *Bleomycin model of lung fibrosis*

Mice were treated with tamoxifen as described previously prior to the start of the assay. For bleomycin lung fibrosis assays, a total of 5 doses of bleomycin (1 U per mouse in 400ul PBS for a dosage of 50 U/kg) were administered intraperitoneally every 5 days; mice were sacrificed 5 days after the final bleomycin injection. PBS was used as a vehicle for untreated controls. Lung analysis was performed using Masson's trichrome stained paraffin sections, and images were analyzed using ImageJ software.

#### *Assessment of cutaneous wound healing*

Mice were treated with tamoxifen as described previously prior to the start of the assay. Dermal wounds were generated on the dorsum of the mouse using bilateral 6mm punch biopsies under isoflurane anesthesia. Every other day, mice were briefly placed under isoflurane anesthesia, and wounds were imaged using a digital camera with a ruler for reference. Wounds were covered using non-adhesive gauze pads to prevent scabbing and interference with wound healing. This experiment was repeated a total of three times,

once without covering the wound and twice covering the wounds. Wound area was measured using ImageJ.

## REFERENCES

1. Chaffer, C. L. & Weinberg, R. A. A Perspective on Cancer Cell Metastasis. *Science* (80-). **331**, 1559–1564 (2011).
2. Siegel, R. L., Miller, K. D. & Jemal, A. Cancer statistics, 2019. *CA. Cancer J. Clin.* **69**, 7–34 (2019).
3. Klein, C. A. Parallel progression of primary tumours and metastases. *Nat. Rev. Cancer* **9**, 302–312 (2009).
4. Puré, E. The road to integrative cancer therapies: emergence of a tumor-associated fibroblast protease as a potential therapeutic target in cancer. *Expert Opin. Ther. Targets* **13**, 967–73 (2009).
5. Paget, S. The distribution of secondary growths in cancer of the breast. 1889. *Cancer Metastasis Rev.* **8**, 98–101 (1989).
6. Kaplan, R. N. *et al.* VEGFR1-positive haematopoietic bone marrow progenitors initiate the pre-metastatic niche. *Nature* **438**, 820–827 (2010).
7. Bergers, G. & Benjamin, L. E. Tumorigenesis and the angiogenic switch. *Nat. Rev. Cancer* **3**, 401–10 (2003).
8. Chung, A. S., Lee, J. & Ferrara, N. Targeting the tumour vasculature: Insights from physiological angiogenesis. *Nat. Rev. Cancer* **10**, 505–514 (2010).
9. Vasudev, N. S. & Reynolds, A. R. Anti-angiogenic therapy for cancer: Current progress, unresolved questions and future directions. *Angiogenesis* **17**, 471–494 (2014).
10. Ebos, J. M. L., Lee, C. R. & Kerbel, R. S. Tumor and host-mediated pathways of resistance and disease progression in response to antiangiogenic therapy. *Clin. Cancer Res.* **15**, 5020–5025 (2009).
11. Yu, J. *et al.* Efficacy and safety of angiogenesis inhibitors in advanced gastric cancer: A systematic review and meta-analysis. *J. Hematol. Oncol.* **9**, 1–15 (2016).
12. Yang, Y. Cancer immunotherapy: harnessing the immune system to battle cancer. *J. Clin. Invest.* **125**, 3335–3337 (2015).
13. Wei, S. C., Duffy, C. R. & Allison, J. P. Fundamental mechanisms of immune checkpoint blockade therapy. *Cancer Discov.* **8**, 1069–1086 (2018).
14. Brentjens, R. J. *et al.* CD19-Targeted T Cells Rapidly Induce Molecular Remissions in Adults with Chemotherapy-Refractory Acute Lymphoblastic Leukemia. *Sci. Transl. Med.* **5**, 177ra38-177ra38 (2013).
15. Wilkins, O., Keeler, A. M. & Flotte, T. R. CAR T-Cell Therapy: Progress and Prospects. *Hum. Gene Ther. Methods* **28**, 61–66 (2017).
16. Valkenburg, K. C., De Groot, A. E. & Pienta, K. J. Targeting the tumour stroma to

- improve cancer therapy. *Nat. Rev. Clin. Oncol.* **15**, 366–381 (2018).
17. Harper, J. & Sainson, R. C. A. Regulation of the anti-tumour immune response by cancer-associated fibroblasts. *Semin. Cancer Biol.* **25**, 69–77 (2014).
  18. Ozdemir, B. C. *et al.* Depletion of carcinoma-associated fibroblasts and fibrosis induces immunosuppression and accelerates pancreas cancer with reduced survival. *Cancer Cell* **25**, 719–34 (2014).
  19. Costa, A. *et al.* Fibroblast Heterogeneity and Immunosuppressive Environment in Human Breast Cancer. *Cancer Cell* **33**, 463–479.e10 (2018).
  20. Hetheridge, C., Mavria, G. & Mellor, H. Uses of the in vitro endothelial-fibroblast organotypic co-culture assay in angiogenesis research. *Biochem. Soc. Trans.* **39**, 1597–600 (2011).
  21. Ito, T., Ishii, G., Chiba, H. & Ochiai, A. The VEGF angiogenic switch of fibroblasts is regulated by MMP-7 from cancer cells. *Oncogene* **26**, 7194–7203 (2007).
  22. Newman, A. C. *et al.* Analysis of stromal cell secretomes reveals a critical role for stromal cell-derived hepatocyte growth factor and fibronectin in angiogenesis. *Arterioscler. Thromb. Vasc. Biol.* **33**, 513–22 (2013).
  23. Martin, T. A., Harding, K. G. & Jiang, W. G. Regulation of angiogenesis and endothelial cell motility by matrix-bound fibroblasts. *Angiogenesis* **3**, 69–76 (1999).
  24. Kalas, W. *et al.* Oncogenes and Angiogenesis: Down-regulation of Thrombospondin-1 in Normal Fibroblasts Exposed to Factors from Cancer Cells Harboring Mutant Ras. *Cancer Res.* **65**, 8878–8886 (2005).
  25. Watnick, R. S. *et al.* Thrombospondin-1 repression is mediated via distinct mechanisms in fibroblasts and epithelial cells. *Oncogene* 1–13 (2014). doi:10.1038/onc.2014.228
  26. Limoge, M. *et al.* Tumor-fibroblast interactions stimulate tumor vascularization by enhancing cytokine-driven production of MMP9 by tumor cells. **8**, 35592–35608 (2017).
  27. Du, P. *et al.* Human lung fibroblast-derived matrix facilitates vascular morphogenesis in 3D environment and enhances skin wound healing. *Acta Biomater.* **54**, 333–344 (2017).
  28. Pollina, E. A. *et al.* Regulating the angiogenic balance in tissues: A potential role for the proliferative state of fibroblasts. *Cell Cycle* **7**, 2056–2070 (2008).
  29. Feig, C. *et al.* Targeting CXCL12 from FAP-expressing carcinoma-associated fibroblasts synergizes with anti-PD-L1 immunotherapy in pancreatic cancer. *Proc. Natl. Acad. Sci.* **110**, 20212–20217 (2013).
  30. Keklikoglou, I. *et al.* Periostin Limits Tumor Response to VEGFA Inhibition. *Cell Rep.* **22**, 2530–2540 (2018).
  31. De Palma, M., Biziato, D. & Petrova, T. V. Microenvironmental regulation of tumour angiogenesis. *Nat. Rev. Cancer* **17**, 457–474 (2017).
  32. Narra, K. *et al.* Phase II trial of single agent Val-boroPro (Talabostat) inhibiting fibroblast activation protein in patients with metastatic colorectal cancer. *Cancer Biol. Ther.* **6**,

- 1691–1699 (2007).
33. Konstantinopoulos, P. A., Karamouzis, M. V., Papatsoris, A. G. & Papavassiliou, A. G. Matrix metalloproteinase inhibitors as anticancer agents. *Int. J. Biochem. Cell Biol.* **40**, 1156–1168 (2008).
  34. Lo, A. *et al.* Tumor-promoting desmoplasia is disrupted by depleting FAP-expressing stromal cells. *Cancer Res.* **75**, 2800–2810 (2015).
  35. Cremasco, V. *et al.* FAP delineates heterogeneous and functionally divergent stromal cells in immune-excluded breast tumors. *Cancer Immunol. Res.* canimm.0098.2018 (2018). doi:10.1158/2326-6066.CIR-18-0098
  36. Fang, J. *et al.* A potent immunotoxin targeting fibroblast activation protein for treatment of breast cancer in mice. *Int. J. Cancer* **138**, 1013–1023 (2016).
  37. Wang, L.-C. S. *et al.* Targeting Fibroblast Activation Protein in Tumor Stroma with Chimeric Antigen Receptor T Cells Can Inhibit Tumor Growth and Augment Host Immunity without Severe Toxicity. *Cancer Immunol. Res.* **2**, 154–166 (2014).
  38. Roberts, E. W. *et al.* Depletion of stromal cells expressing fibroblast activation protein- $\alpha$  from skeletal muscle and bone marrow results in cachexia and anemia. *J. Exp. Med.* **210**, 1137–1151 (2013).
  39. Desmouliere, A., Darby, I. A., Laverdet, B. & Bonté, F. Fibroblasts and myofibroblasts in wound healing. *Clin. Cosmet. Investig. Dermatol.* **5**, 301 (2014).
  40. Tracy, L. E., Minasian, R. A. & Caterson, E. J. Extracellular Matrix and Dermal Fibroblast Function in the Healing Wound. *Adv. Wound Care* **5**, 119–136 (2016).
  41. Provenzano, P. P. *et al.* Enzymatic Targeting of the Stroma Ablates Physical Barriers to Treatment of Pancreatic Ductal Adenocarcinoma. *Cancer Cell* **21**, 418–429 (2012).
  42. Hingorani, S. R. *et al.* HALO 202: Randomized phase II Study of PEGPH20 Plus Nab-Paclitaxel/Gemcitabine Versus Nab-Paclitaxel/Gemcitabine in Patients With Untreated, Metastatic Pancreatic Ductal Adenocarcinoma. *J. Clin. Oncol.* **36**, 359–366 (2018).
  43. Poltavets, V., Kochetkova, M., Pitson, S. M. & Samuel, M. S. The Role of the Extracellular Matrix and Its Molecular and Cellular Regulators in Cancer Cell Plasticity. *Front. Oncol.* **8**, 1–19 (2018).
  44. Egeblad, M., Rasch, M. G. & Weaver, V. M. Dynamic interplay between the collagen scaffold and tumor evolution. *Curr. Opin. Cell Biol.* **22**, 697–706 (2010).
  45. Exposito, J. Y., Valcourt, U., Cluzel, C. & Lethias, C. The fibrillar collagen family. *Int. J. Mol. Sci.* **11**, 407–426 (2010).
  46. Page-McCaw, A., Ewald, A. J. & Werb, Z. Matrix metalloproteinases and the regulation of tissue remodelling. *Nat. Rev. Mol. Cell Biol.* **8**, 221–233 (2007).
  47. Acharya, P. S., Zukas, A., Chandan, V., Katzenstein, A. A. & Pure, E. Fibroblast activation protein : a serine protease expressed at the remodeling interface in idiopathic pulmonary fibrosis B. 352–360 (2006). doi:10.1016/j.humpath.2005.11.020

48. Huang, X. *et al.* Matrix Stiffness–Induced Myofibroblast Differentiation Is Mediated by Intrinsic Mechanotransduction. *Am. J. Respir. Cell Mol. Biol.* **47**, 340–348 (2012).
49. Jokinen, J. *et al.* Integrin-mediated cell adhesion to type I collagen fibrils. *J. Biol. Chem.* **279**, 31956–31963 (2004).
50. Barczyk, M., Carracedo, S. & Gullberg, D. Integrins. *Cell Tissue Res.* **339**, 269–280 (2010).
51. Schultz, G. S. & Wysocki, A. Interactions between extracellular matrix and growth factors in wound healing. *Wound Repair Regen.* **17**, 153–162 (2009).
52. O'Reilly, M. S. *et al.* Endostatin: An Endogenous Inhibitor of Angiogenesis and Tumor Growth. *Cell* **88**, 277–285 (1997).
53. Flier, J., Underhill, L. & Dvorak, H. Tumors: wounds that do not heal. *New Engl. J. ...* **315**, 1650–1659 (1986).
54. Provenzano, P. P. *et al.* Collagen density promotes mammary tumor initiation and progression. *BMC Med.* **6**, 1–15 (2008).
55. Alexander, S., Koehl, G. E., Hirschberg, M., Geissler, E. K. & Friedl, P. Dynamic imaging of cancer growth and invasion: A modified skin-fold chamber model. *Histochem. Cell Biol.* **130**, 1147–1154 (2008).
56. Kong, P., Christia, P., Saxena, A., Su, Y. & Frangogiannis, N. G. Lack of specificity of fibroblast-specific protein 1 in cardiac remodeling and fibrosis. *AJP Hear. Circ. Physiol.* **305**, H1363–H1372 (2013).
57. Kalluri, R. The biology and function of fibroblasts in cancer. *Nat. Rev. Cancer* **16**, 582–598 (2016).
58. Shiga, K. *et al.* Cancer-associated fibroblasts: Their characteristics and their roles in tumor growth. *Cancers (Basel)*. **7**, 2443–2458 (2015).
59. Xie, T. *et al.* Single-Cell Deconvolution of Fibroblast Heterogeneity in Mouse Pulmonary Fibrosis. *Cell Rep.* **22**, 3625–3640 (2018).
60. Avery, D., Govindaraju, P., Jacob, M. & Todd, L. Extracellular matrix directs phenotypic heterogeneity of activated fibroblasts. *Matrix Biol.* (2017). doi:10.1016/j.matbio.2017.12.003
61. Öhlund, D., Elyada, E. & Tuveson, D. Fibroblast heterogeneity in the cancer wound. *J. Exp. Med.* **211**, 1503–1523 (2014).
62. Sugimoto, H., Mundel, T., Kieran, M. & Kalluri, R. Identification of fibroblast heterogeneity in the tumor microenvironment. *Cancer Biol. ...* 1640–1646 (2006).
63. Bartoschek, M. *et al.* Spatially and functionally distinct subclasses of breast cancer-associated fibroblasts revealed by single cell RNA sequencing. *Nat. Commun.* **9**, 5150 (2018).
64. Liberato, T., Pessotti, D. S., Fukushima, I. & Kitano, E. S. Signatures of protein expression revealed by secretome analyses of cancer associated fibroblasts and melanoma

- cell lines. *J. Proteomics* **174**, 1–8 (2018).
65. Koeck, S. *et al.* The influence of stromal cells and tumor- microenvironment-derived cytokines and chemokines on CD3 CD8 tumor infiltrating lymphocyte subpopulations. *Oncoimmunology* **6**, 1–15 (2017).
  66. Davis, J., Burr, A. R., Davis, G. F., Birnbaumer, L. & Molkenin, J. D. A TRPC6-Dependent Pathway for Myofibroblast Transdifferentiation and Wound Healing In Vivo. *Dev. Cell* **23**, 705–715 (2012).
  67. Dienus, K., Bayat, A., Gilmore, B. F. & Seifert, O. Increased expression of fibroblast activation protein-alpha in keloid fibroblasts: Implications for development of a novel treatment option. *Arch. Dermatol. Res.* **302**, 725–731 (2010).
  68. Flaberg, E. *et al.* High-throughput live-cell imaging reveals differential inhibition of tumor cell proliferation by human fibroblasts. *Int. J. Cancer* **128**, 2793–2802 (2011).
  69. Stoker, M. G., Shearer, M. & O'Neill, C. Growth inhibition of polyoma-transformed cells by contact with static normal fibroblasts. *J. Cell Sci.* **1**, 297–310 (1966).
  70. Lee, K. W., Yeo, S. Y., Sung, C. O. & Kim, S. H. Twist1 is a key regulator of cancer-associated fibroblasts. *Cancer Res.* **75**, 73–85 (2015).
  71. Kotas, M. E. & Medzhitov, R. Homeostasis, Inflammation, and Disease Susceptibility. *Cell* **160**, 816–827 (2015).
  72. Yao, G. Modelling mammalian cellular quiescence. *Interface Focus* **4**, 20130074–20130074 (2014).
  73. Baba, M. *et al.* Loss of Folliculin Disrupts Hematopoietic Stem Cell Quiescence and Homeostasis Resulting in Bone Marrow Failure. *Stem Cells* **34**, 1068–1082 (2016).
  74. De Wever, O., Van Bockstal, M., Mareel, M., Hendrix, A. & Bracke, M. Carcinoma-associated fibroblasts provide operational flexibility in metastasis. *Semin. Cancer Biol.* **25**, 33–46 (2014).
  75. Webster, K. D., Ng, W. P. & Fletcher, D. A. Tensional homeostasis in single fibroblasts. *Biophys. J.* **107**, 146–155 (2014).
  76. Lemons, J. M. S. *et al.* Quiescent Fibroblasts Exhibit High Metabolic Activity. *PLoS Biol.* **8**, e1000514 (2010).
  77. GILROY, D. W., SAUNDERS, M. A., SANSORES-GARCIA, L., MATIJEVIC-ALEKSIC, N. & WU, K. K. Cell cycle-dependent expression of cyclooxygenase-2 in human fibroblasts. *FASEB J.* **15**, 288–290 (2001).
  78. Heinzemann, K. *et al.* Cell-surface phenotyping identifies CD36 and CD97 as novel markers of fibroblast quiescence in lung fibrosis. *Am. J. Physiol. Cell. Mol. Physiol.* [ajplung.00439.2017](https://doi.org/10.1152/ajplung.00439.2017) (2018). doi:10.1152/ajplung.00439.2017
  79. Kolodsick, J. E. *et al.* Prostaglandin E2 Inhibits Fibroblast to Myofibroblast Transition via E. Prostanoid Receptor 2 Signaling and Cyclic Adenosine Monophosphate Elevation. *Am. J. Respir. Cell Mol. Biol.* **29**, 537–544 (2003).

80. Keerthisingam, C. B. *et al.* Cyclooxygenase-2 deficiency results in a loss of the anti-proliferative response to transforming growth factor- $\beta$  in human fibrotic lung fibroblasts and promotes bleomycin-induced pulmonary fibrosis in mice. *Am. J. Pathol.* **158**, 1411–1422 (2001).
81. Sandulache, V. C., Parekh, A., Li-Korotky, H., Dohar, J. E. & Hebda, P. A. Prostaglandin E2 inhibition of keloid fibroblast migration, contraction, and transforming growth factor (TGF)- $\beta$ 1-induced collagen synthesis. *Wound Repair Regen.* **15**, 122–133 (2007).
82. Chlenski, A. *et al.* SPARC enhances tumor stroma formation and prevents fibroblast activation. *Oncogene* **26**, 4513–4522 (2007).
83. Sangaletti, S. *et al.* SPARC oppositely regulates inflammation and fibrosis in bleomycin-induced lung damage. *Am. J. Pathol.* **179**, 3000–3010 (2011).
84. Strandjord, T. P., Madtes, D. K., Weiss, D. J. & Sage, E. H. Collagen accumulation is decreased in SPARC-null mice with bleomycin-induced pulmonary fibrosis. *Am. J. Physiol.* **277**, L628-35 (1999).
85. Wang, H., Haeger, S. M., Kloxin, A. M., Leinwand, L. A. & Anseth, K. S. Redirecting valvular myofibroblasts into dormant fibroblasts through light-mediated reduction in substrate modulus. *PLoS One* **7**, (2012).
86. Lehtonen, S. T., Veijola, A., Karvonen, H., Lappi-blanco, E. & Sormunen, R. Pirfenidone and nintedanib modulate properties of fibroblasts and myofibroblasts in idiopathic pulmonary fibrosis. *Respir. Res.* 1–12 (2016). doi:10.1186/s12931-016-0328-5
87. Gabasa, M., Ikemori, R., Hilberg, F., Reguart, N. & Alcaraz, J. Nintedanib selectively inhibits the activation and tumour-promoting effects of fibroblasts from lung adenocarcinoma patients. **117**, 1128–1138 (2017).
88. Dauer, P. *et al.* Inactivation of Cancer-Associated-Fibroblasts Disrupts Oncogenic Signaling in Pancreatic Cancer Cells and Promotes Its Regression. 1321–1334 (2018). doi:10.1158/0008-5472.CAN-17-2320
89. Arandkar, S., Furth, N., Elisha, Y., Belugali, N. & Kuip, H. Van Der. Altered p53 functionality in cancer-associated fibroblasts contributes to their cancer- supporting features. (2018). doi:10.1073/pnas.1719076115
90. Procopio, M. G. *et al.* Combined CSL and p53 downregulation promotes cancer-associated fibroblast activation. *Nat. Cell Biol.* **17**, 1193–1204 (2015).
91. Clocchiatti, A. *et al.* Androgen receptor functions as transcriptional repressor of cancer-associated fibroblast activation Find the latest version : Androgen receptor functions as transcriptional repressor of cancer-associated fibroblast activation. (2018).
92. Borok, Z. *et al.* Cell Plasticity in Lung Injury and Repair: Report from an NHLBI Workshop, April 19-20, 2010. *Proc. Am. Thorac. Soc.* **8**, 215–222 (2011).
93. Rusnak, F. & Mertz, P. Calcineurin: form and function. *Physiol. Rev.* **80**, 1483–521 (2000).
94. Mancini, M. & Toker, A. NFAT proteins: emerging roles in cancer progression. *Nat. Rev. Cancer* **9**, 810–820 (2009).

95. Baek, K.-H. *et al.* Down Syndrome Suppression of Tumor Growth and the Role of the Calcineurin Inhibitor DSCR1. *Nature* **459**, 1126–1130 (2009).
96. Hasle, H., Friedman, J. M., Olsen, J. H. & Rasmussen, S. A. Low risk of solid tumors in persons with Down syndrome. *Genet. Med.* **18**, 1151–1157 (2016).
97. Xavier, A. C., Ge, Y. & Taub, J. W. Down syndrome and malignancies: A unique clinical relationship - A paper from the 2008 William Beaumont Hospital symposium on molecular pathology. *J. Mol. Diagnostics* **11**, 371–380 (2009).
98. Baek, K. H. *et al.* Down's syndrome suppression of tumour growth and the role of the calcineurin inhibitor DSCR1. *Nature* **459**, 1126–1130 (2009).
99. Robbs, B. K., Cruz, A. L. S., Werneck, M. B. F., Mognol, G. P. & Viola, J. P. B. Dual Roles for NFAT Transcription Factor Genes as Oncogenes and Tumor Suppressors. *Mol. Cell. Biol.* **28**, 7168–7181 (2008).
100. Qin, J.-J. *et al.* NFAT as cancer target: Mission possible? *Biochim. Biophys. Acta - Rev. Cancer* **1846**, 297–311 (2014).
101. Durnian, J. M., Stewart, R. M. K., Tatham, R., Batterbury, M. & Kaye, S. B. Cyclosporin-A associated malignancy. *Clin. Ophthalmol.* **1**, 421–30 (2007).
102. Buchholz, M. & Ellenrieder, V. An emerging role for Ca<sup>2+</sup>/calcineurin/NFAT signaling in cancerogenesis. *Cell Cycle* **6**, 16–19 (2007).
103. Medyouf, H. & Ghysdael, J. The calcineurin/NFAT signaling pathway: A novel therapeutic target in leukemia and solid tumors. *Cell Cycle* **7**, 297–303 (2008).
104. Minami, T. *et al.* The calcineurin-NFAT-angiopoietin-2 signaling axis in lung endothelium is critical for the establishment of lung metastases. *Cell Rep.* **4**, 709–23 (2013).
105. Ryeom, S. *et al.* Targeted deletion of the calcineurin inhibitor DSCR1 suppresses tumor growth. *Cancer Cell* **13**, 420–31 (2008).
106. Fellström, B. Cyclosporine nephrotoxicity. *Transplant. Proc.* **36**, S220–S223 (2004).
107. Rush, D. The impact of calcineurin inhibitors on graft survival. *Transplantation Reviews* **27**, 93–95 (2013).
108. Moreno, J. . *et al.* Chronic renal dysfunction after liver transplantation in adult patients: prevalence, risk factors, and impact on mortality. *Transplant. Proc.* **35**, 1907–1908 (2003).
109. Johnson, D. W. *et al.* Cyclosporin exerts a direct fibrogenic effect on human tubulointerstitial cells: roles of insulin-like growth factor I, transforming growth factor beta1, and platelet-derived growth factor. *J Pharmacol Exp Ther* **289**, 535–542 (1999).
110. Gooch, J. L., Roberts, B. R., Cobbs, S. L. & Tumlin, J. A. Loss of the  $\alpha$ -isoform of calcineurin is sufficient to induce nephrotoxicity and altered expression of transforming growth factor- $\beta$ . *Transplantation* **83**, 439–447 (2007).
111. Herum, K. M. *et al.* Syndecan-4 signaling via NFAT regulates extracellular matrix

- production and cardiac myofibroblast differentiation in response to mechanical stress. *J. Mol. Cell. Cardiol.* **54**, 73–81 (2013).
112. Wilkins, B. J. & Molkentin, J. D. Calcium-calcineurin signaling in the regulation of cardiac hypertrophy. *Biochem. Biophys. Res. Commun.* **322**, 1178–1191 (2004).
  113. Davis, J., Burr, A. R., Davis, G. F., Birnbaumer, L. & Molkentin, J. D. A TRPC6-Dependent Pathway for Myofibroblast Transdifferentiation and Wound Healing In Vivo. *Dev. Cell* **23**, 705–715 (2012).
  114. Hirota, N., Ito, T., Miyazaki, S., Ebina, M. & Homma, S. Gene Expression Profiling of Lung Myofibroblasts Reveals the Anti-Fibrotic Effects of Cyclosporine. 283–293 (2014). doi:10.1620/tjem.233.283.Correspondence
  115. Zhou, A. Y. & Ryeom, S. Cyclosporin a promotes tumor angiogenesis in a calcineurin-independent manner by increasing mitochondrial reactive oxygen species. *Mol. Cancer Res.* **12**, 1663–76 (2014).
  116. Hu, G. *et al.* Human structural proteome-wide characterization of Cyclosporine a targets. *Bioinformatics* **30**, 3561–3566 (2014).
  117. Yamazaki, R. *et al.* Antifibrotic effects of cyclosporine A on TGF- b 1 – treated lung fibroblasts and lungs from bleomycin-treated mice : role of hypoxia-inducible factor-1 a. (2018). doi:10.1096/fj.201601357R
  118. Balkwill, F. R., Capasso, M. & Hagemann, T. The tumor microenvironment at a glance. *J. Cell Sci.* **125**, 5591–5596 (2012).
  119. Pure, E. & Lo, A. Can Targeting Stroma Pave the Way to Enhanced Antitumor Immunity and Immunotherapy of Solid Tumors? *Cancer Immunol. Res.* **4**, 269–278 (2016).
  120. Olumi, A. F. *et al.* Carcinoma-associated Fibroblasts Direct Tumor Progression of Initiated Human Prostatic Epithelium. *Cancer Res.* **59**, 5002–5011 (1999).
  121. Jacob, M., Chang, L. & Puré, E. Fibroblast activation protein in remodeling tissues. *Curr. Mol. Med.* **12**, 1220–43 (2012).
  122. Puré, E. & Blomberg, R. Pro-tumorigenic roles of fibroblast activation protein in cancer: back to the basics. *Oncogene* **37**, 4343–4357 (2018).
  123. Hinz, B., Celetta, G., Tomasek, J. J., Gabbiani, G. & Chaponnier, C. Alpha-Smooth Muscle Actin Expression Upregulates Fibroblast Contractile Activity. *Mol. Biol. Cell* **12**, 2730–2741 (2001).
  124. Chang, H. Y. *et al.* Diversity, topographic differentiation, and positional memory in human fibroblasts. *Proc. Natl. Acad. Sci.* **99**, 12877–12882 (2002).
  125. Kalluri, R. & Zeisberg, M. Fibroblasts in cancer. *Nat. Rev. Cancer* **6**, 392–401 (2006).
  126. Neilson, J. R., Winslow, M. M., Hur, E. M. & Crabtree, G. R. Calcineurin B1 is essential for positive but not negative selection during thymocyte development. *Immunity* **20**, 255–66 (2004).
  127. Grinnell, F., Ho, C. H., Lin, Y. C. & Skuta, G. Differences in the regulation of fibroblast

- contraction of floating versus stressed collagen matrices. *J. Biol. Chem.* **274**, 918–923 (1999).
128. Castelló-cros, R. & Cukierman, E. *Extracellular Matrix Protocols*. **522**, (Humana Press, 2009).
  129. Orimo, A. *et al.* Stromal fibroblasts present in invasive human breast carcinomas promote tumor growth and angiogenesis through elevated SDF-1/CXCL12 secretion. *Cell* **121**, 335–48 (2005).
  130. Kojima, Y. *et al.* Autocrine TGF-beta and stromal cell-derived factor-1 (SDF-1) signaling drives the evolution of tumor-promoting mammary stromal myofibroblasts. *Proc Natl Acad Sci U S A* **107**, 20009–20014 (2010).
  131. Xu, J. *et al.* Role of the SDF-1 / CXCR4 Axis in the Pathogenesis of Lung Injury and Fibrosis. (2007). doi:10.1165/rcmb.2006-0187OC
  132. Jackson, E. K. *et al.* SDF-1 $\alpha$  (stromal cell-derived factor 1 $\alpha$ ) induces cardiac fibroblasts, renal microvascular smooth muscle cells, and glomerular mesangial cells to proliferate, cause hypertrophy, and produce collagen. *J. Am. Heart Assoc.* **6**, 1–20 (2017).
  133. Kim, J.-E., Nakashima, K. & de Crombrughe, B. Transgenic Mice Expressing a Ligand-Inducible Cre Recombinase in Osteoblasts and Odontoblasts. *Am. J. Pathol.* **165**, 1875–1882 (2004).
  134. Rossert, J., Eberspaecher, H. & Crombrughe, B. De. Separate cis-acting DNA elements of the mouse pro-alpha1(I) collagen promoter direct expression of reporter genes to different type I collagen-producing cells in transgenic mice. **129**, 1421–1432 (1995).
  135. Malik, R., Lelkes, P. I. & Cukierman, E. Biomechanical and biochemical remodeling of stromal extracellular matrix in cancer. *Trends Biotechnol.* **33**, 230–236 (2015).
  136. Han, W. *et al.* Oriented collagen fibers direct tumor cell intravasation. *Proc. Natl. Acad. Sci.* **113**, 11208–11213 (2016).
  137. Wang, X. *et al.* Calcineurin-NFAT axis controls allograft immunity in myeloid-derived suppressor cells through reprogramming T cell differentiation. *Mol. Cell. Biol.* **35**, 598–609 (2014).
  138. Fric, J. *et al.* NFAT control of innate immunity. *Blood* **120**, 1380–1389 (2012).
  139. Dotto, G. P. Calcineurin Signaling as a Negative Determinant of Keratinocyte Cancer Stem Cell Potential and Carcinogenesis. *Cancer Res.* **71**, 2029–2033 (2011).
  140. Arendt, K. L. *et al.* Calcineurin mediates homeostatic synaptic plasticity by regulating retinoic acid synthesis. *Proc. Natl. Acad. Sci.* **112**, E5744–E5752 (2015).
  141. Li, H., Rao, A. & Hogan, P. G. Interaction of calcineurin with substrates and targeting proteins. *Trends Cell Biol.* **21**, 91–103 (2011).
  142. Gooch, J. L., Gorin, Y., Zhang, B.-X. & Abboud, H. E. Involvement of calcineurin in transforming growth factor-beta-mediated regulation of extracellular matrix accumulation. *J. Biol. Chem.* **279**, 15561–70 (2004).

143. Nishida, M. *et al.* Gα12/13-mediated up-regulation of TRPC6 negatively regulates endothelin-1-induced cardiac myofibroblast formation and collagen synthesis through nuclear factor of activated T cells activation. *J. Biol. Chem.* **282**, 23117–23128 (2007).
144. Sesler, C. L. & Zayzafoon, M. NFAT signaling in osteoblasts regulates the hematopoietic niche in the bone microenvironment. *Clin. Dev. Immunol.* **2013**, (2013).
145. Du, M. R. *et al.* Cyclosporin A promotes crosstalk between human cytotrophoblast and decidual stromal cell through up-regulating CXCL12/CXCR4 interaction. *Hum. Reprod.* **27**, 1955–1965 (2012).
146. Hinck, A. P. Structural studies of the TGF-βs and their receptors - Insights into evolution of the TGF-β superfamily. *FEBS Lett.* **586**, 1860–1870 (2012).
147. Stewart, A. G., Thomas, B. & Koff, J. TGF-β: Master regulator of inflammation and fibrosis. *Respirology* (2018). doi:10.1111/resp.13415
148. Hinz, B. The extracellular matrix and transforming growth factor-β1: Tale of a strained relationship. *Matrix Biol.* **47**, 54–65 (2015).
149. Cordeiro, M. F., Bhattacharya, S. S., Schultz, G. S. & Khaw, P. T. TGF-β1, -β2, and -β3 in vitro: Biphasic effects on Tenon's fibroblast contraction, proliferation, and migration. *Investig. Ophthalmol. Vis. Sci.* **41**, 756–763 (2000).
150. Zi, Z., Chapnick, D. A. & Liu, X. Dynamics of TGF-β/Smad signaling. *FEBS Letters* **586**, 1921–1928 (2012).
151. Massagué, J. How cells read TGF-β signals. *Nat. Rev. Mol. Cell Biol.* **1**, 169–178 (2000).
152. Wu, D. T., Bitzer, M., Ju, W., Mundel, P. & Böttinger, E. P. TGF-β Concentration Specifies Differential Signaling Profiles of Growth Arrest/Differentiation and Apoptosis in Podocytes. *J. Am. Soc. Nephrol.* **16**, 3211–3221 (2005).
153. Massagué, J. TGFβ signalling in context. *Nat. Rev. Mol. Cell Biol.* **13**, 616–630 (2012).
154. Tone, Y. *et al.* Smad3 and NFAT cooperate to induce Foxp3 expression through its enhancer. **9**, (2008).
155. Bismuth, G. & Mami-chouaib, F. Smad and NFAT Pathways Cooperate To Induce CD103 Expression in Human CD8 T Lymphocytes. (2017). doi:10.4049/jimmunol.1302192
156. Acharya, P. S. *et al.* Fibroblast migration is mediated by CD44-dependent TGF β activation. (2008). doi:10.1242/jcs.021683
157. Eickelberg, O. *et al.* Transforming growth factor-β1 induces interleukin-6 expression via activating protein-1 consisting of JunD homodimers in primary human lung fibroblasts. *J. Biol. Chem.* **274**, 12933–12938 (1999).
158. Maltman, J., Pragnell, I. B. & Graham, G. J. Transforming growth factor beta: is it a downregulator of stem cell inhibition by macrophage inflammatory protein 1 alpha? *J Exp Med* **178**, 925–932 (1993).
159. Saito, F. *et al.* Role of interleukin-6 in bleomycin-induced lung inflammatory changes in mice. *Am. J. Respir. Cell Mol. Biol.* **38**, 566–571 (2008).

160. Cretu, A., Castagnino, P. & Assoian, R. Studying the Effects of Matrix Stiffness on Cellular Function using Acrylamide-based Hydrogels. 7–11 (2010). doi:10.3791/2089
161. Kirsch, D. G. *et al.* A spatially and temporally restricted mouse model of soft tissue sarcoma. *Nat. Med.* **13**, 992–997 (2007).
162. Govindaraju, P., Todd, L., Shetye, S., Monslow, J. & Puré, E. CD44-dependent inflammation, fibrogenesis, and collagenolysis regulates extracellular matrix remodeling and tensile strength during cutaneous wound healing. *Matrix Biol.* **75–76**, 314–330 (2019).
163. Kreft, L. *et al.* ConTra v3: A tool to identify transcription factor binding sites across species, update 2017. *Nucleic Acids Res.* **45**, W490–W494 (2017).
164. Davis, J., Burr, A. R., Davis, G. F., Birnbaumer, L. & Molkentin, J. D. A TRPC6-Dependent Pathway for Myofibroblast Transdifferentiation and Wound Healing In Vivo. *Dev. Cell* **23**, 705–715 (2012).
165. Lee, J.-H. *et al.* Lung stem cell differentiation in mice directed by endothelial cells via a BMP4-NFATc1-thrombospondin-1 axis. *Cell* **156**, 440–55 (2014).